# THE IMPACT OF INSTABILITY ON THE CARRYING CAPACITY OF STEEL SLENDER SECTIONS

**Master Academic Dissertation**

**Speciality: Structural Engineering**

**Academic year: 2021/2022**

**Presented by DAHLOUZ MANEL**

Submitted publically on June the 12th 2022

Dr.SOLTANI Mohammed Redha      Grade MCB      President

Dr.LABED Abderrahim      Grade MCB      Supervisor

Dr.Boulaares Said      Grade MAA      Examiner

بِسْمِ اللَّهِ الرَّحْمَٰنِ الرَّحِيمِ

# شكر وعرفان

سبحانك اللهم لا علم لنا إلا ما علمتنا، نشكر الله ونحمده فضل نعمه علينا، نعمة العقل التي أنار بها دربنا وفكرنا ونعمة الذاكرة التي حفظنا بها سرنا وجهرنا.

والصلاة والسلام على قدوة المربين نبينا محمد وعلى آله و صحبه أجمعين.

إن من تمام شكر الله، شكر أهل الفضل والبر، وعملا بقول نبيه محمد ﷺ: « من لم يشكر القليل لم يشكر الكثير ومن لم يشكر الناس لم يشكر الله » رواه " أحمد و الترمذي " .

و نخص بالشكر الجزيل لأساتذة الخير الذين علموا بلا شك أن العلم من أجمل العبادات وأفضلها،

وإن من آمالنا وتطلعاتنا في هذا الصرح أن نتقدم بجزيل الشكر إلى كل من ساعدنا وساهم في تكويننا طيلة مشوارنا الدراسي من أساتذة التعليم الابتدائي،

وصولا إلى أساتذة التعليم العالي والبحث العلمي في قسم الهندسة المدنية و نخص بالذكر الأستاذ المشرف المحترم " العابد عبد الرحيم"على كل ما قدمه لنا من معلومات و توجيهات قيمة ساهمت في إثراء بحثنا العلمي،

فهو برهان للذين بذلوا شاق الجهد و يسروا العسير بقدرة الصمد القدير .

كما نشكر كافة أعضاء لجنة المناقشة التي شرفتنا بقبولها مناقشة مذكرتنا، كل من الأستاذ " سلطاني محمد رضا" رئيسا و الأستاذ

" بولعراس السعيد" ممتحنا الذين لاشك أنهم سيفيضون علينا بتوجيهاتهم القيمة وملاحظاتهم السديدة.

ثم الشكر موصول للزميلين " أبو طير بكر وائل" و" بوجاجة مروى"

دون أن نغض الطرف بالشكر والثناء عن إخواننا الطلبة المقربين بصلة العلم في فيحاء الأخوة والسند.

وخاصة طلبة ماستر 2 دفعة 2022 راجين من المولى العليّ القدير كل التوفيق والفلاح .

و في الأخير نشكر كل من قدم لنا يد العون والمساعدة من قريب أو بعيد ولو بكلمة طيبة أو بتوجيه أو حتى بدعوة في ظهر الغيب لهم جزيل الشكر والعرفان.

ولكم منا فائق التقدير و الاحترام.

# إهـــداء

الحمد لله على منه وامتنانه والشكر له على نعمه و إنعامه حمدا كثيرا طيبا، الذي أنعم علي بنعمة العلم وسهل لي طريقا

أبغي فيه علما ووفقني في إنهاء عملي المتواضع هذا.

إلى من بلغ الرسالة وأدى الأمانة ونصح الأمة، إلى نبي الرحمة ونور العالمين، سيدنا محمد عليه الصلاة وأزكى التسليم .

إلى التي بالأماني حملتني، وبالتهاني استقبلتني، وبالحنان رعتني، إلى من لم يعرف دعائها حدود ولا عطاءها قيود، إلى

بسمة الحياة وسر الوجود، إلى ينبوع الصبر والتفاؤل والأمل: أمي الغالية .

إلى من جرع الكأس فارغا ليسقيني قطرة حب، إلى من كلت أنامله ليقدم لنا لحظة سعادة، إلى من حصد الأشواك عن

دربي ليمهد لي طريق العلم، إلى القلب الكبير الذي أحمل اسمه بكل فخر وأعتز به في كل مكان: أبي العزيز.

إلى سندي وقوتي وملاذي، إلى من آثروني على أنفسهم، إلى من علموني علم الحياة، إلى القلوب الطاهرة: إخوتي

وأخواتي .

إلى التي يأنس بها قلبي و تقر بها عيني برعم العائلة: " نسرين ".

إلى نفسي و نفسيتي.

إلى من جمعني بهم دم واحد وقلب واحد وبيت واحد: كل الأهل والأقارب.

إلى كل الأصدقاء الأوفياء والزملاء الأعزاء التي جمعتني بهم الحياة خصوصا حبيبات قلبي " توامي اسيا "،

" هبيبي صفاء "،  " دوايدي أميرة ".

إلى كل من تصفح هذه المذكرة وانتفع بها وتذكرنا بدعائه.

إلى كل هؤلاء أهدي ثمرة جهدي

** دهلوز منال **

# LIST OF SYMBOLS

## LATIN CHARACTERS

| | |
|---|---|
| $h_w$ | Clear web depth between flanges |
| $t_w$ | Thickness of web |
| $b$ | Distance between mid-planes of flanges |
| $t_f$ | Thickness of flange |
| $f_y$ | Material yield stress |
| $A$ | Cross-sectional area |
| $I_y$ | Moment of inertia |
| $I_Z$ | Moment of inertia |
| $W_{el.y}$ | Elastic resistance modulus |
| $q$ | Loading |
| $M_{el.y}$ | Elastic moment |
| $I_t$ | Inertia of torsion |
| $I_w$ | Factor of warping |
| $G$ | Shear modulus |
| $E$ | Elastic modulus of steel |
| $K_\sigma$ | The buckling factor |
| $b_{eff}$ | The effective depth |
| $b_{e1}$ | The depth of web left at the top |
| $b_{e2}$ | The depth of web left at the bottom |
| $l_w$ | The ineffective portion of web has a length |
| $A_w$ | The net loss of area of the web |
| $A_{eff}$ | Effective area of section |
| $Z_{eff}$ | Position of effective centroid |
| $I_{eff}$ | Effective second moment of area |
| $W_{eff}$ | The lesser elastic section modulus |
| $M_{eff}$ | Effective moment |
| $M_{cr}$ | The critical moment |
| $q_{cr}$ | Critical load |

## GREEK CHARACTERS

$\mathbf{E}$          Strain used for section classification

$\mathbf{\Psi}$          The stress ratio

$\mathbf{\lambda_p}$          The normalized slenderness ratio

$\mathbf{\lambda_p}$          The reduction factor

$\mathbf{\mu_{cr}}$          Buckling mode coefficient

# LIST OF TABLES

# LIST OF FIGURES

# CONTENTS

x

**CONCLUSIONS AND SUGGESTIONS FOR FUTURE WORKS**

1. Conclusions

2. Recommendations and suggestions for future work

**Bibliography**

# *ABSTRACT*

This thesis deals with the impact of buckling on the carrying capacity of slender sections (class 4) considering the elastic and inelastic analyses. Steel sections can be regarded as a combination of individual plate elements connected together to form the required shape. Two instabilities are being investigated: Local buckling (LB), Lateral Torsional Buckling (LTB) and most often their interactions. LB influences the behaviour of slender sections by preventing them to attain their full capacity, greatly diminishes their load bearing capability. While LTB makes the overall behaviour of steel member changing from initially in-plane bending to combined a large lateral displacement and twist angle with a partial failure or whole failure element. The classification of steel sections with regard to local buckling is presented as per EC3 and AISC provisions. In order to accomplish the objectives of this research work, the author has followed the procedure: First of all, an extensive literature overview has been made covering the different instability phenomenon susceptible to occur in slender beams: LB and LTB with the code's provisions. The necessary theoretical background of advanced analysis of the Effective Length Approach (ELA) of slender sections has been reviewed with application to the studied cases. The essential understanding of basic theory of the elastic (eigen modes) and inelastic behaviours of steel slender sections was also performed. The parametric comparative study undertaken in this investigation considers some parameters that are believed to influence the bending strength of slender sections of three sections S1, S2 and S3. These parameters are the slenderness (class) of flanges and load locations in the cross section. The study covers both elastic linear and inelastic buckling behaviour. Analytical elastic buckling study as per EC3 of the prediction of $M_{cr}$ taking into account of the elastic and effective properties respectively was performed. Another buckling analysis based on the eigen modes, taking into account the same parameters, is carried out by mean of FE modelling using LTBEAM and ABAQUS software. Very good agreement was found when comparing the outcomes of the three studies were compared. Then a true, more sophisticated inelastic analysis to describe the nonlinear behaviour of slender sections has been carried out throughout 3D models built-up in ABAQUS. The inelastic analysis was done using RIKS approach implanted in ABAQUS. The results have shown the particular importance of the flange class in an inelastic behaviour of slender section with regard to LTB which is mainly bending behaviour. According to the obtained results, it seems that, in the elastic range, the class of flange does not have any significant impact on the general resistance to LTB of slender sections. However, as far as the inelastic behaviour is concerned, sections S1, S2 and S3, despite that all sections are classified in class 4, have shown different behaviours according to their flange class in the prediction of $P_{cr}$ and the post-buckling behaviour of the section. Better performance has been found in S1 and lesser in S2 and the worst was S3 (web and flanges being class 4). The load positions of have shown their importance in both elastic and inelastic behaviours. It

has been found that situations when the load is applied in the compressive flange. Some very interesting conclusions have been drawn this parametric comparative investigation with some suggestions for future work.

**Key words**: Instability, classification, LB, LTB, ELA, FEA, elastic and inelastic behaviour, load location, flange class.

E

# ملخص

تتناول هذه الأطروحة تأثير الالتواء على القدرة الاستيعابية للأقسام النحيلة (الفئة 4) مع مراعاة التحليلات المرنة وغير المرنة. يمكن اعتبار المقاطع الفولاذية مزيجًا من عناصر اللوحة الفردية المتصلة معًا لتشكيل الشكل المطلوب. يتم التحقيق في اثنين من حالات عدم الاستقرار: الانبعاج المحلي (LB) ، والإلتواء الجانبي (LTB) وفي أغلب الأحيان تفاعلاتهما. يؤثر LB على سلوك الأقسام النحيلة من خلال منعها من بلوغ سعتها الكاملة ، مما يقلل بشكل كبير من قدرتها على تحمل الأحمال. بينما تقوم LTB بتغيير السلوك الكلي للعضو الفولاذي من الانحناء الأولي في المستوى إلى الجمع بين إزاحة جانبية كبيرة وزاوية التواء مع فشل جزئي أو عنصر فشل كامل. يتم تقديم تصنيف أقسام الصلب فيما يتعلق بالتشابك المحلي وفقًا لبنود EC3 و AISC. من أجل تحقيق أهداف هذا العمل البحثي، اتبع المؤلف الإجراء: أولاً وقبل كل شيء، تم عمل نظرة عامة شاملة للأدبيات التي تغطي ظاهرة عدم الاستقرار المختلفة التي يمكن أن تحدث في حزم رفيعة LB و LTB: مع أحكام الكود. تمت مراجعة الخلفية النظرية اللازمة للتحليل المتقدم لنهج الطول الفعال (ELA) للأقسام النحيلة مع التطبيق على الحالات المدروسة. تم أيضًا إجراء الفهم الأساسي للنظرية الأساسية للأشكال المرنة (أنماط eigen والسلوكيات غير المرنة للأقسام النحيلة الفولاذية. الدراسة المقارنة التي أجريت في هذا التحقيق تأخذ بعين الاعتبار بعض المتغيرات التي يعتقد أنها تؤثر على مقاومة الانحناء للأقسام النحيلة لثلاثة أقسام S1 و S2 و S3. هذه المعلمات هي رقة (فئة) الشفاه ومواقع التحميل في المقطع العرضي. تغطي الدراسة كلاً من سلوك الانثناء الخطي المرن وغير المرن. تم إجراء دراسة تحليلية للالتواء المرن حسب EC3 لتنبؤ $M_{cr}$ مع مراعاة الخصائص المرنة والفعالة على التوالي. يتم إجراء تحليل التواء آخر يعتمد على أوضاع eigen ، مع مراعاة نفس المعلمات ، عن طريق نمذجة FE باستخدام برنامجي LTBEAM و ABAQUS. تم العثور على اتفاق جيد للغاية عند مقارنة نتائج الدراسات الثلاث. ثم تم إجراء تحليل غير مرن حقيقي وأكثر تعقيدًا لوصف السلوك غير الخطي للأقسام النحيلة عبر النماذج ثلاثية الأبعاد التي تم إنشاؤها في ABAQUS. تم إجراء التحليل غير المرن باستخدام طريقة RIKS المزروعة في ABAQUS. أظهرت النتائج الأهمية الخاصة لفئة الفلنجات في السلوك غير المرن للقسم النحيف فيما يتعلق بـ LTB الذي يعد سلوك الانحناء بشكل أساسي. وفقًا للنتائج التي تم الحصول عليها، يبدو أنه في النطاق المرن، لا يكون لفئة تأثير كبير على المقاومة العامة للأقسام الرفيعة LTB. ومع ذلك ، فيما يتعلق بالسلوك غير المرن ، فإن الأقسام S1 و S2 وS3 ، على الرغم من أن جميع الأقسام مصنفة في الفئة 4 ، أظهرت سلوكيات مختلفة وفقًا لفئة الحافة الخاصة بها في التنبؤ بـ $P_{cr}$ وسلوك ما بعد الانحناء لـ الجزء. تم العثور على أداء أفضل في S1 وأقل في S2 والأسوأ كان) S3 الويب والشفاه من الدرجة 4). أظهرت مواضع الحمل أهميتها في كل من السلوكيات المرنة وغير المرنة. لقد وجد أن الحالات التي يتم فيها تطبيق الحمل في شفة الانضغاط. تم استخلاص بعض الاستنتاجات المهمة للغاية في هذا البحث المقارن البارومتري مع بعض الاقتراحات للعمل المستقبلي الكلمات. الرئيسية: عدم الاستقرار، التصنيف، LB، LTB، ELA، FEA، السلوك المرن وغير المرن، موقع التحميل و الطبقة الوحيدة.

F

# *Résumé*

Cette thèse traite de l'impact de l'instabilité sur la capacité portante des sections élancées (classe 4) en utilisant les analyses élastiques et inélastiques. Les profilés en acier peuvent être considérés comme une combinaison d'éléments individuels de plaque reliés entre eux pour former la forme requise. Deux instabilités sont étudiées : le voilement local (LB), le déversement (LTB) et éventuellement leurs interactions. LB influence le comportement des sections élancées en les empêchant d'atteindre leur pleine capacité, diminue considérablement leur capacité de résistance. Alors que LTB balance le comportement global de l'élément d'une flexion initiale dans le plan de forte inertie à la combinaison d'un grand déplacement latéral et d'un angle de torsion avec une défaillance partielle ou totale de l'élément. La classification des profilés en acier dépend du voilement local est présentée selon les dispositions des codes EC3 et AISC. Afin d'accomplir les objectifs de ce travail de recherche, l'auteur a suivi la démarche suivante : Tout d'abord, une revue bibliographique abondante a été faite couvrant les différents phénomènes d'instabilité susceptibles de se produire dans les poutres élancées : LB et LTB avec les recommandations des codes. Le contexte théorique nécessaire à l'analyse avancée de l'approche de la longueur efficace (ELA) avec des applications aux sections élancées considérées dans cette étude. La compréhension essentielle de l'analyse modale des comportements élastiques (modes propres) et inélastiques des sections élancées en acier a également été effectuée. L'étude comparative paramétrique entreprise dans cette enquête considère certains paramètres qui sont censés influencer la résistance à la flexion des sections minces de trois sections S1, S2 et S3. Ces paramètres sont l'élancement (classe) des semelles et les emplacements des charges dans la section transversale. L'étude couvre à la fois le comportement de flambement linéaire élastique et inélastique. Une étude analytique du flambement élastique selon EC3 de la prédiction de $M_{cr}$ tenant compte respectivement des propriétés élastiques et effectives a été réalisée. Une autre analyse de flambement basée sur les modes propres, prenant en compte les mêmes paramètres, est réalisée au moyen d'une modélisation EF à l'aide des logiciels LTBEAM et ABAQUS. Un très bon accord a été trouvé lors de la comparaison des résultats des trois études. Ensuite, une véritable analyse inélastique plus sophistiquée pour décrire le comportement non linéaire des sections élancées a été réalisée à travers des modèles 3D construits dans ABAQUS. L'analyse inélastique a été réalisée à l'aide de l'approche RIKS implantée dans ABAQUS. Les résultats ont montré l'importance particulière de la classe de semelle dans un comportement inélastique de section élancée vis-à-vis du LTB qui est principalement un comportement en flexion. D'après les résultats obtenus, il semble que, dans le domaine élastique, la classe de semelle n'ait pas d'impact significatif sur la résistance générale au LTB des sections élancées. Cependant, en ce qui concerne le comportement inélastique, les sections S1, S2 et S3, bien que toutes les sections soient classées en classe 4, ont montré des comportements différents

G

selon leur classe de semelle dans la prédiction de $P_{cr}$ et le comportement post-voilement de la section. De meilleures performances ont été trouvées en S1 et moins en S2 et les pires étaient en S3 (l'âme et les semelles étant de classe 4). Les positions de charge appliquée par rapport au centre de torsion ont montré leur importance aussi bien dans les comportements élastiques qu'inélastiques. Notamment, des situations défavorables lorsque la charge est appliquée dans la semelle en compression. Des conclusions très intéressantes ont été tirées de cette étude comparative paramétrique avec quelques suggestions pour des travaux futurs.

**Mots clés** : Instabilité, classification, LB, LTB, ELA, FEA, comportement élastique et inélastique, localisation de la charge, classe de la semelle.

H

# GENERAL INTRODUCTION

### 1.  Slender steel beams

The main objective of this thesis is the investigation of the impact of buckling behaviour of class 4 slender steel cross section on their carrying capacity of these beams. The term 'slender section' should not be confused with 'slender beam'. Where the slenderness of any plate element is more than the yield limit, the section is classified as slender. Normally it is best to avoid using slender sections, but it is sometimes necessary to check a section of this type. When the aspect ratio is relatively high, then local buckling may prevent any part of the cross-section from reaching the design strength. Such sections are called slender sections and are classified as Class 4 sections; their capacity is based on a reduced design strength as specified in Clause 3. The limiting aspect ratios for elements of the most commonly used cross-sections subject to pure bending, pure axial load or combined bending and axial loads. A parametric investigation is made a numerical elastic and inelastic modelling along with a theoretical background of such sections. For class 4 cross-sections it is assumed that parts of the area under compression due to local instability phenomena do not have any resistance (lost area): typically, the compressed portions of the cross-sections, which have to be neglected for the resistance checks, are the parts close to the free end of an outstand flange or the central part of an internal compressed element. Currently, EC8-1 does not account for structures with class 4 members.

In general, the properties of the effective section in cross-sections of class 4 (slender) are obtained by defining certain effective widths in the compressed areas of the parts, in accordance with the criteria.

Recent research on the behaviour of slender sections have been reported namely  [Taras and Greiner 2010; Couto et al 2015; João Ferreira et al 2017; Lee and Chiew 2019; Couto et al 2019, and Seres and Fejes 2020]. These and others have investigated the inelastic behavior to LTB of slender steel sections of class 4 as per EC3 with some interesting conclusions.

### 2.  General considerations

Flexural members built up of plates that form horizontal flanges at top and bottom and joined to vertical or near vertical webs are called plate girders. They differ from beams primarily in that their web depth-to-thickness ratio is larger flange. The webs generally are braced by perpendicular plates called stiffeners, to control local buckling or withstand excessive web shear. Plate girders are most often used to carry heavy loads or for long spans for which rolled shapes are not available

Steel members with thin-walled cross-sections are commonly used in steel structures due to its lightness and long span capacity. Beams are members subjected to bending are also generally affected

by shear forces, which have to be adequately considered in all the safety checks. Furthermore, the design of beams has to take into account both serviceability (mainly, check on deflections and dynamic effects) and ultimate limit states, including, in addition to resistance, stability verifications when relevant.

Slender steel I- girder sections are commonly used for long-span beams of industrial halls, composite bridges, where mainly flanges provide the bending resistance and web has a relatively small thickness providing only hinged support to the flanges and resistance to shear stresses. To maximize their load-carrying capacity, steel beams are often oriented in such a way that the strong axis of the cross-section is perpendicular to the loading plane. When a beam is loaded in this manner, several failure modes are possible depending on its lateral unsupported length L. For a doubly symmetric I-shaped compact section, if L is less than a reference length referred to by the AISC (2011).

The buckling resistance assessment is usually based on appropriate buckling curves and requires the computation of the elastic critical moment, which is strongly dependent on several factors such as, the bending moment distribution, the restraints at the end supports and in correspondence of the load points, the beam cross-section, the distance between the load application point and the shear centre. The high strength and stiffness-to-weight ratios of structural steel often results in relatively slender members and systems in which stability is a primary design consideration.

### Steel mode failures

According to [Chen and Duan 2014] there are four fundamental failure modes for steel members; yielding, rupture, buckling, and fatigue. Buckling failures can be characterized by an instability of a member as a whole (global buckling) or as instability of one or more of the elements of a cross section (local buckling). In this context, the word "element" is meant to describe a plate component that makes up part of a cross section. For instance, the web of an I-shaped girder or the flanges of a channel are cross-sectional "elements." With respect to local buckling, classification of the cross-sectional elements as slender, non-slender, compact, or noncombat aids greatly in determining which of the four fundamental failure modes may govern and how they are addressed. This section provides the background needed to understand the classification of the sections for local buckling.

### Buckling of steel thin-walled members

The steel material is characterized by a symmetrical mono axial stress-strain (σ–ε) constitutive law, which can be determined by monotonic tension tests on samples taken from the base material before the working process or from the products in correspondence of appropriate locations. The response of steel members can, however, be significantly different in tension or compression, owing to the relevant influence of the buckling phenomena.

In case of thin-walled members, that is member which has a cross-section components with high values of ratio width over thickness, the local instability phenomena might occur in the elastic range, hence preventing the spread of plasticity in the cross-section, that is, the achievement not only of the plastic moment but also of the elastic moment. These kinds of cross-sections are sensitive for local web buck-ling; however, the dominant failure mode of the entire girder is lateral-torsional buckling (LTB). Therefore, these girders should be designed for coupled instabilities, for the interaction of local plate buckling of the web and global LTB of the entire girder.

Individual members may be combined in a quite great variety of ways to produce a more efficient compound cross-section member. The resistance can significantly be limited by instability phenomenon in the range of standard products.

The instability of compressed steel members as well as of all the members realized with other materials can be distinguished in:

• An overall buckling or Euler buckling, which affects the element throughout its length (or a relevant portion of it).

• Local buckling, already which affects the compressed plates forming the cross-section, characterized by relatively short wavelength buckling.

**N.B.** Also, there is a third type of instability, the so-called distortional buckling, distortional buckling is characterized by relative displacements of the fold-line of the cross-section and the associated wave-length is generally in the range delimited by one of local buckling and one of global buckling.

### Local buckling

A very important phenomenon affecting steel slender member behaviour and, as a consequence, the whole structural performance, is the local buckling that typically affects thin-walled members. Local buckling is a phenomenon that influences the behaviour of thin-walled structural steel elements in a major way and it can be the determining factor for their design in contemporary construction. Its occurrence prevents slender sections from attaining their full capacity, greatly diminishes their load bearing capability and should be completely avoided to ensure the safety and serviceability of steel structures.

### Lateral torsional buckling

Lateral-torsional buckling is a kind of failure that occurs when the in-plane bending capacity of a member exceeds its resistance to out-of-plane lateral buckling and twisting. Physically, the phenomenon of LTB in which the overall behaviour of steel member changes from initially in-plane

bending to combined a large lateral displacement and twist angle due to an application of load on an unsupported beam. The LTB can cause partial failure or whole failure in the structure. The stress at which buckling occurs depends on a variety of factors ranging from the dimensions of the member to the boundary conditions to the properties of the material of the member. The resistance of a steel beam in bending depends on the cross-section resistance or the occurrence of lateral instability.

**Classification of sections**

The local buckling of cross sections affects their resistance and rotation capacity and must be considered in design. The evaluation of the influence of local buckling of a cross section on the resistance or ductility of a steel member is complex. Consequently, a deemed-to-satisfy approach was developed in the form of cross section classes that greatly simplify the problem.

AISC cross-section classification criteria are based, as in Eurocode 3, on the steel grade and on the width-to-thickness ratios distinguished for stiffened elements (elements supported along two edges parallel to the direction of the compression force) and unstiffened elements (elements supported along only one edge parallel to the direction of the compression force).

More details will be provided in Chapter 4.

- Classification in Accordance with European Standards

Eurocode 3 proposes a criterion for the classification of cross-sections based on the slenderness ratio (width over thickness ratio) of each compressed component of the cross-section, as well as on other factors. It should be noted that, in case of compressed member, no distinctions can be observed in the performance of the elements of the first three classes, owing to the stress distribution in axially loaded cross-sections limited to yielding strength. The cross-section resistance to axial compression should be based on the plastic capacity (plastic axial force) in compact sections (class 1, 2 or 3), but taking into account the local buckling resistance through an effective elastic capacity in class 4 sections. The buckling resistance should be evaluated according to the relevant buckling mode and relevant imperfections of real members, as described in the following sections.

- Classification in Accordance with US Standards

AISC 360-10 addresses classification of cross-sections in Chapter B, Section B4; the code deals with members subjected to axial load and members subjected to bending in a different way. The classification of cross-sections is classified on the basis of type of load acting on the element (i.e. compression and bending).

N.B. Contrary to the European approach, which assumes the same classification criteria for both static and seismic design, it must be remarked that AISC Seismic provisions propose a different classification criterion when profiles are used in seismic areas.

**Resistance of cross sections to EC3**

According to [Simões da Silva et al 2010], the resistance of cross sections depends on their class (clause 6.2.1(3)) in EC3. According to the definition of the four cross section classes (see 2.4), cross section classes 1 and 2 reach their full plastic resistance, while class 3 cross sections only reach their elastic resistance. Class 4 cross sections are not able to reach their elastic resistance because of local buckling. Nevertheless, using the concept of effective section [EC3 2006], they are effectively treated as class 3 cross sections and their resistance is evaluated as an elastic resistance.

The design value of an action effect, at each cross section, should not exceed the corresponding design resistance, and if several action effects act simultaneously, the combined effect should not exceed the resistance for that combination (clause 6.2.1(1)). Shear lag effects and local buckling effects should be included according to the concept of effective section of EC3-1-5 (CEN, 2006c). Shear buckling effects **should also be considered according to EC3-1-5 (clause 6.2.1(2)).**

### 3. Motivation and aim of the present work

Exploring the impact of different buckling phenomenon on the elastic and inelastic behaviour of slender steel beam under static loadings is quite interesting, consideration several parameters that are believed to greatly influence the elastic and inelastic buckling. These parameters are: variation of flange's slender ratio, from class 1, class 3 and class4, load localisation in the cross section. The numerical modelling of the beams has been developed through well-known software: LTBeam for elastic buckling analysis and ABAQUS for both elastic and inelastic buckling behaviours of slender steel beams. By performing this task, the author of this dissertation has learned how to deal with complex analyses in 3D models.

### 4. Methodology

To be able to meet the aim of the thesis the following steps were performed with tasks that need to be executed:

- Understanding the different instability phenomenon susceptible to occur in beams under transverse static loadings.
- Detecting the buckling interaction: local and torsional buckling.
- Understanding the theoretical background of the effective length approach used for effective geometric properties.
- Hand-calculations of some cases using effective length approach.
- Explore the methods and assumptions used in LTBEAM and ABAQUS software
- Understand the elastic and inelastic instability behaviour of steel slender sections and the theory behind lateral-torsional buckling.

M

- Built-up 3D models of beams with slender sections for linear and nonlinear buckling analyses in ABAQUS software.
- Extract and discuss the obtain results.
- Compare the performance of different beams
- Draw some conclusions and suggestions for future wok.

## 5.      Organisation of the dissertation

The present thesis has been partitioned in six chapters as follows:

- A general introduction on steel beams summarises some concepts used in this work along with important definitions.  Also, a description of the scope and objective of the present research work and the way to attain the planned objectives is given.

- **Chapter 1**: A concisely presentation and discussion on the local buckling and classification criteria of steel beams sections along with the parameters influencing this classification. A special attention has  been  paid  to components under compression  and bending.

- **Chapter 2**:  A concisely presentation of the theory of stability of thin-walled steel structures is given. Introduces a theoretical insight of LTB with an overview of LTB in standards and guides and background of the European standards (EC3) with some details, EC3 and ANSI/AISC 360-16 (June 2018) provisions.

- **Chapter 3**: Dealing with the effective length approach. A detailed hand calculation of the designed beams of class 4 used in this study is given.

- **Chapter 4**:  Displays an overview of the use the finite element method in structural analysis. LTBeam and ABAQUS are introduced. Technics and capabilities of assessing the lateral torsional buckling of laterally of unrestrained beams.

- **Chapter 5**: In this chapter, presents and discusses the results of the elastic linear buckling analysis. Some concluding remarks are given.

- **Chapter 6**:  This chapter is devoted to a presentation of results of the inelastic buckling analysis with a full discussion and the comparison of obtained results.

- **Conclusions and recommendations for future works**: provides the essential the conclusions coming up from this research work on the key parameters governing the elastic and inelastic behaviours of slender beams, and followed some recommendations for future works

# $\mathcal{C}$HAPTER 1:

# LOCAL BUCKLING AND SECTION CLASSIFICATIONS IN STEEL DESIGN CODES

## 1.1 Introduction

Sections normally used in steel structures are I-sections, Channels or angles etc. which are called open sections, or rectangular or circular tubes which are called closed sections. These sections can be regarded as a combination of individual plate elements connected together to form the required shape. The strength of compression members made of such sections depends on their slenderness ratio. Higher strengths can be obtained by reducing the slenderness ratio *i.e.* by increasing the moment of inertia of the cross-section. Similarly, the strengths of beams can be increased, by increasing the moment of inertia of the cross-section. For a given cross-sectional area, higher moment of inertia can be obtained by making the sections thin-walled. As discussed earlier, plate elements laterally supported along edges and subjected to membrane compression or shear may buckle prematurely. Therefore, the buckling of the plate elements of the cross section under compression/shear may take place before the overall column buckling or overall beam failure by lateral buckling or yielding. This phenomenon is called *local buckling*. Thus, local buckling imposes a limit to the extent to which sections can be made thin-walled.

## 1.2 Local buckling

### 1.2.1 General definition

Local buckling is a phenomenon that influences the behaviour of thin-walled structural steel elements in a major way and it can be the determining factor for their design in contemporary construction. Its occurrence prevents slender sections from attaining their full capacity, greatly diminishes their load bearing capability and should be completely avoided to ensure the safety and serviceability of steel structures. Also, local buckling has the effect of reducing the load carrying capacity of columns and beams due to the reduction in stiffness and strength of the locally buckled plate elements. Therefore, it is desirable to avoid local buckling before yielding of the member. It is important to point out that most of the hot rolled steel sections have enough wall thickness to eliminate local buckling before yielding. However, fabricated sections and thin-walled cold-formed steel members usually experience local buckling of plate elements before the yield stress is reached.

### 1.2.2 Effect of local buckling on structures

Local buckling prevents the development of plastic hinges with such rotation capacity for cross-sections of higher classes and, unless computationally demanding shell elements are used, elastic analysis is required. For cross-sections liable to buckle locally, special precautions need to be taken in design. However, it should be remembered that local buckling does not always spell disaster. Local buckling involves distortion of the cross-section.

### 1.2.3 Types of local buckling

Some kinds of local buckling can be mention as follows:

- Local buckling exhibit local deformation of outstand e.g. a flange of I beam
- Local buckling occurs when the flange outstands to thickness ratio ($b/t_f$) is high Called flange buckling
- The web is also subjected to compressive stresses from bending with a limiting to $d/t_w$ ratio beyond which web will buckle even though the axis of the axis remains straight called web buckling

Consider an I-section column, subjected to uniform compression. The plates supported on three sides (outstands) have a buckling coefficient $k$ roughly one-tenth that for plates supported on all four sides (internal elements). Therefore, in open sections such as I- sections, the flanges which are outstands tend to buckle before the webs which are supported along all edges. Further, the entire length of the flanges is likely to buckle in the case of the axially compressed member under consideration, in the form of waves. On the other hand, in closed sections such as the hollow rectangular section, both flanges and webs behave as internal elements and the local buckling of the flanges and webs depends on their respective width-thickness ratios. In this case also, local buckling occurs along the entire length of the member and the member develops a 'chequer board' wave pattern Figure. 1.2 (*b*) and Figure 1.2.
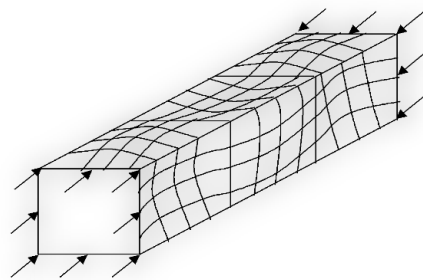


(a)
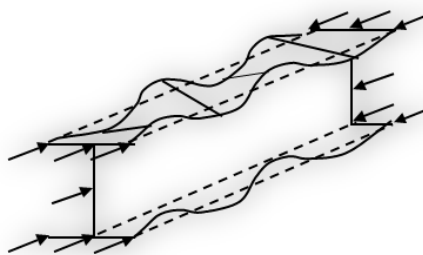


**(b)**

**Figure 1.1 Local buckling of compression members**

**Figure 1.2 Experimental local buckling in flanges and web of steel member**

Normally, the bending moment varies over the length of the beam and so local buckling may occur only in the region of maximum bending moment. Local buckling has the effect of reducing the load carrying capacity of columns and beams due to the reduction in stiffness and strength of the locally buckled plate elements. Therefore, it is desirable to avoid local buckling before yielding of the member. Most of the hot rolled steel sections have enough wall thickness to eliminate local buckling before yielding. However, fabricated sections and thin-walled cold-formed steel members usually experience local buckling of plate elements before the yield stress is reached.

**1.3 Section classifications**

**1.3.1 General**

Structural analysis of steel frames is typically performed using beam elements. Since these elements are unable to explicitly capture the local buckling behaviour of steel cross-sections, traditional steel design specifications use the concept of cross-section classification to determine the extent to which the strength and deformation capacity of a cross-section are affected by local buckling. In the case of beams, the compression flange behaves as a plate element subjected to uniform compression and, depending on whether it is an outstand or an internal element, undergoes local buckling at the corresponding critical buckling stress. However, the web is partially under compression and partially under tension. Even the part in compression is not under uniform compression. Therefore, the web buckles as a plate subjected to in- plane bending compression.

**1.3.2 Objectives of the classification**

- To **determine strength** of the structural steel component, it requires the designer to **consider the cross-sectional behaviour** and the overall member behaviour.

- Purpose of classification: to identify the extent to which **the resistance and rotation capacity of cross sections is limited** by its local buckling resistance.

- Clause 5.5.1 and 6.2 cover the cross-sectional aspects of the design process.

### 1.4 Classification of cross sections to codes

### 1.4.1 Principles

It is useful to classify sections based on their tendency to buckle locally before overall failure of the member takes place. There is no shift in the position of the cross-section as a whole as in global or overall buckling. In some cases, local buckling of one of the elements of the cross- section may be allowed since it does not adversely affect the performance of the member as a whole. In the context of plate bucking, it was pointed out that substantial reserve strength exists in plates beyond the point of elastic buckling. Utilization of this reserve capacity may also be the objective of design. Therefore, local buckling may be allowed in some cases, provided due care is taken to estimate the reduction in the capacity of the section due to it and the consequences are clearly understood.

### 1.4.2 Classification process

The classification process of a cross section depends on the following parameters:

1  width to thickness ratio c/t of the parts subjected to compression (clause 5.5.2(3)),

2  type of element (internal part or an outstand part),

3  the applied internal forces,

4  the steel grade.

As the plate elements in structural sections are relatively thin compared with their width, when loaded in compression (as a result of axial loads and/or from bending) they may buckle locally.

The disposition of any plate element within the cross section to buckle may limit the axial load carrying capacity, or the bending resistance of the section, by preventing the attainment of yield.

Avoidance of premature failure arising from the effects of local buckling may be achieved by limiting the width-to-thickness ratio for individual elements within the cross section.
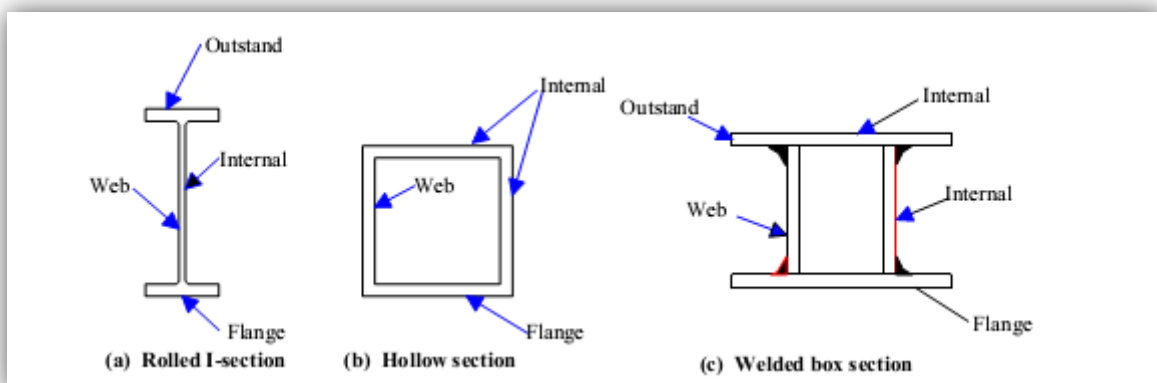


**Figure 1.3 Internal or outstand elements EC3**

### 1.4.3 Parameters affecting the classification

In the design of steel structures, classification of steel section is fundamentally important as it

determines many basic properties of the section as well as how the section resistances are calculated in many design guidelines.

The cross-section of most structural members is considered as an assemblage of individual parts. As these parts are plate elements and are relatively thin, they may buckle locally when subjected to compression (local buckling). In turn, this may limit the compression resistance and the bending resistance. This phenomenon is independent of the length of the member and hence is termed local buckling. It is dependent upon a number of parameters:

The following are of particular importance:

- **Width to thickness ratio of the individual compression elements**. This is often termed the aspect ratio. Wide, thin compression elements are more prone to buckling.

- **Support conditions:** This is dependent upon the edge restraint to the individual compression element. If the compression element is supported by other elements along both edges parallel to the direction of the member, then it is called an internal part as both edges are prevented from deflecting out of plane. If this condition only occurs along one edge, it is said to be an outstand part as the free edge is able to deflect out of plane. Each half of the flange of an I section is an outstand part; the web is an internal compression part.

- **Yield strength of the material:** The higher the yield strength of the material, the greater is the likelihood of local buckling before yielding is reached.

- **Stress distribution across the width of the plate element**: The most severe form of stress distribution is uniform compression, which will occur throughout a cross-section under axial compression or in the compression flange of an I section in bending. The web of an I section under flexure will be under a varying stress, which is a less severe condition. This is because the maximum compressive stress will only occur at one location and the stress level will reduce across the width of the element, possibly even changing to a tensile value.

### 1.4.4 Classification to Eurocode 3

In EC3 code, cross-sections are placed into one of four behavioural classes depending upon the material yield strength, the width to thickness ratios ($b/t_f$ or $d/t_w$) of the individual compression parts (e.g. web and flanges) within the cross-section and the loading arrangement. In the Eurocode 3 (EC3), four classes of section are defined namely: class 1 (Plastic); class 2 (compact), class 3 (semi-compact) and class 4 (slender). The use of plastic design methods is restricted to Class 1 cross-sections, which possess sufficient rotation capacity for plastic hinges to develop and a collapse mechanism to form. According to clause 5.5.2(1), four classes of cross sections are defined, depending on their rotation capacity and ability to form rotational plastic hinges:

 **Class 1 cross sections** are those which can form a plastic hinge with the rotation capacity required from plastic analysis without reduction of the resistance;

 **Class 2 cross sections** are those which can develop their plastic resistance moment, but have limited rotation capacity because of local buckling;

 **Class 3 cross sections** are those in which the stress in the extreme compression fibre of the steel member, assuming an elastic distribution of stresses, can reach the yield strength. However, local buckling is liable to prevent development of the plastic resistance moment;

 **Class 4 cross sections** are those in which local buckling will occur before the attainment of yield stress in one or more parts of the cross section.

 The bending behaviour of members with cross sections of classes 1 to 4 is illustrated in Figure 1.2, where Mel and $M_{pl}$ are, respectively, the elastic moment and the plastic moment of the cross section.

 The classification of a cross section depends on the width to thickness ratio t c of the parts subjected to compression (clause 5.5.2(3)), the applied internal forces and the steel grade. Parts subject to compression include every part of a cross section which is either totally or partially in compression under the load combination considered (clause 5.5.2(4)).
According to EC3, the classification of a cross section is based on its maximum resistance to the type of applied internal forces, independent from their values. This procedure is straightforward to apply for cross sections subject to compression forces or bending moment, acting separately. However, in the case of bending and axial force, there is a range of M-N values that correspond to the ultimate resistance of the cross section. Consequently, there are several values of the parameter (limit for classes 1 and 2) or the parameter (limit for class 3), both being dependent on the position of the neutral axis.
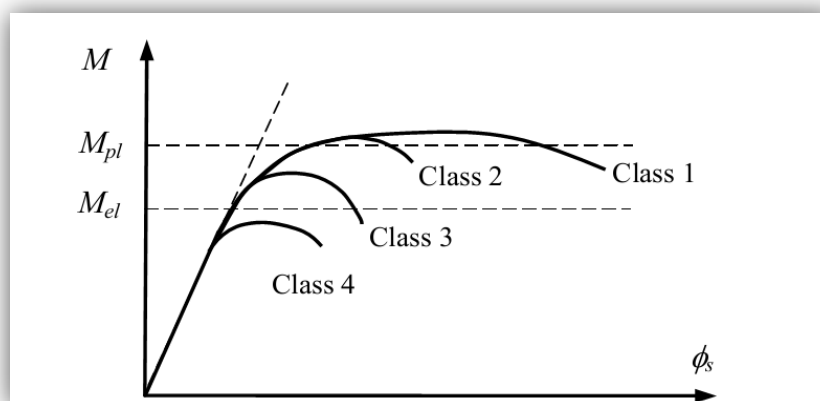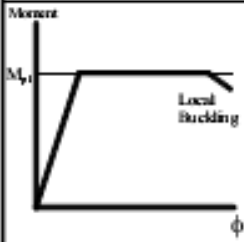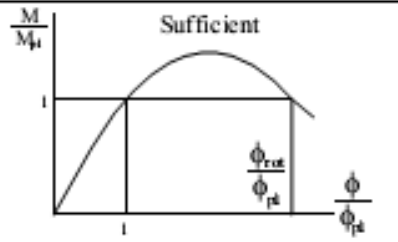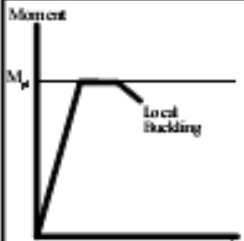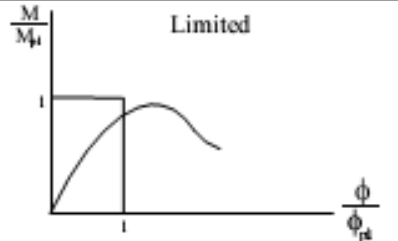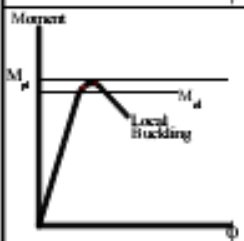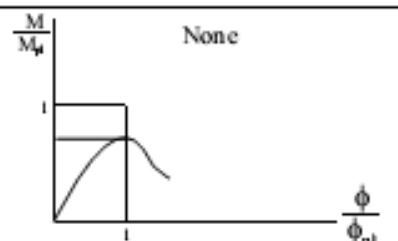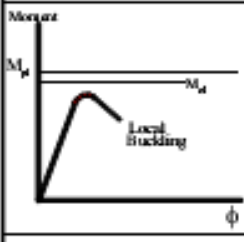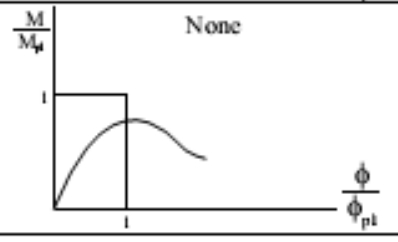


Figure 1.4 Cross section behaviour in bending EC3.

**Table 1.1 summarises the classes in terms of behaviour, moment capacity and rotational capacity.**

| Model of Behaviour | Moment Resistance | Rotation Capacity | Class |
|---|---|---|---|
| Moment, $M_{pl}$, Local Buckling, $\phi$ | Plastic moment on gross section, $f_y$ | $\frac{M}{M_{pl}}$ Sufficient, $\frac{\phi_{rot}}{\phi_{pl}}$, $\frac{\phi}{\phi_{pl}}$ | 1 |
| Moment, $M_{pl}$, Local Buckling, $\phi$ | Plastic moment on gross section, $f_y$ | $\frac{M}{M_{pl}}$ Limited, $\frac{\phi}{\phi_{pl}}$ | 2 |
| Moment, $M_{pl}$, $M_{el}$, Local Buckling, $\phi$ | Elastic moment on gross section, $f_y$ | $\frac{M}{M_{pl}}$ None, $\frac{\phi}{\phi_{pl}}$ | 3 |
| Moment, $M_{pl}$, $M_o$, Local Buckling, $\phi$ | Plastic moment on effective section, $f_y$ | $\frac{M}{M_{pl}}$ None, $\frac{\phi}{\phi_{pl}}$ | 4 |

$M_{el}$ elastic moment resistance of cross-section
$M_{pl}$ plastic moment resistance of cross-section
$M$ applied moment
$\phi$ rotation (curvature) of section
$\phi_{pl}$ rotation (curvature) of section required to generate fully plastic stress distribution across section

The moment resistances for the four classes defined above are:
- ❖ for Classes 1 and 2: the plastic moment ($M_{pl}= W_{pl}. f_y$) ,
- ❖ for Class 3: the elastic moment ($M_{el}= W_{el}. f_y$) ,
- ❖ for Class 4: the local buckling moment ($M_o< M_{el}$).

### Table 1.2 Maximun width –to-thickness rations for internal comprassion parts as per EC3

Table 2.21 – Maximum width-to-thickness ratios for internal compression parts

**Internal compression parts**

| Class | Part subjected to bending | Part subjected to compression | Part subjected to bending and compression |
|---|---|---|---|
| Stress distribution (compression +ve) | | | |
| 1 | $c/t \leq 72\varepsilon$ | $c/t \leq 33\varepsilon$ | if $\alpha > 0.5$, $c/t \leq \dfrac{396\varepsilon}{13\alpha-1}$<br><br>if $\alpha \leq 0.5$, $c/t \leq \dfrac{36\varepsilon}{\alpha}$ |
| 2 | $c/t \leq 83\varepsilon$ | $c/t \leq 38\varepsilon$ | if $\alpha > 0.5$, $c/t \leq \dfrac{456\varepsilon}{13\alpha-1}$<br><br>if $\alpha \leq 0.5$, $c/t \leq \dfrac{41.5\varepsilon}{\alpha}$ |
| Stress distribution (compression +ve) | | | |
| 3 | $c/t \leq 124\varepsilon$ | $c/t \leq 42\varepsilon$ | if $\Psi > -1$,<br>$c/t \leq \dfrac{42\varepsilon}{0.67+0.33\Psi}$<br><br>if $\Psi \leq -1$ [*),<br>$c/t \leq 62\varepsilon(1-\Psi)\sqrt{(-\Psi)}$ |

| $\varepsilon = \sqrt{235/f_y}$ | $f_y$ (N/mm$^2$) | 235 | 275 | 355 | 420 | 460 |
|---|---|---|---|---|---|---|
| | $\varepsilon$ | 1.00 | 0.92 | 0.81 | 0.75 | 0.71 |

*) $\Psi \leq -1$ applies where either the compression stress $\sigma < f_y$ or the tensile strain $\varepsilon_y > f_y/E$.

## Table 1.3 Maximun width –to-thickness rations of flanges as per EC3

Table 2.22 – Maximum width-to-thickness ratios of outstand flanges
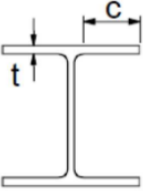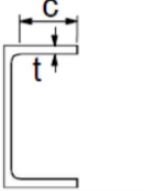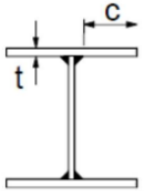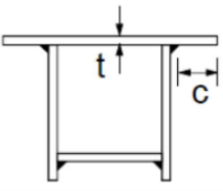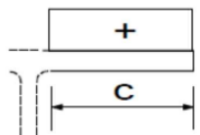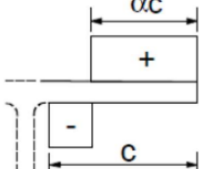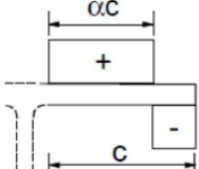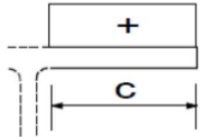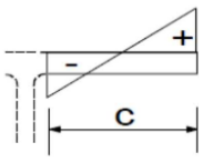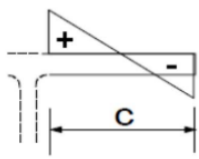
**Outstand flanges**



| Class | Rolled sections | Welded sections | |
|---|---|---|---|
| | Part subjected to compression | Part subjected to bending and compression | |
| | | Tip in compression | Tip in tension |
| Stress distribution (compression +ve) |  |  |  |
| 1 | $c/t \le 9\varepsilon$ | $c/t \le \dfrac{9\varepsilon}{\alpha}$ | $c/t \le \dfrac{9\varepsilon}{\alpha\sqrt{\alpha}}$ |
| 2 | $c/t \le 10\varepsilon$ | $c/t \le \dfrac{10\varepsilon}{\alpha}$ | $c/t \le \dfrac{10\varepsilon}{\alpha\sqrt{\alpha}}$ |
| Stress distribution (compression +ve) |  |  |  |
| 3 | $c/t \le 14\varepsilon$ | $c/t \le 21\varepsilon\sqrt{k_\sigma}$ For $k_\sigma$ see EN 1993-1-5 | |

| $\varepsilon = \sqrt{235/f_y}$ | $f_y$ (N/mm$^2$) | 235 | 275 | 355 | 420 | 460 |
|---|---|---|---|---|---|---|
| | $\varepsilon$ | 1.00 | 0.92 | 0.81 | 0.75 | 0.71 |

**Table 1.4 Maximun width –to-thickness angles and tubular sections as per EC3**
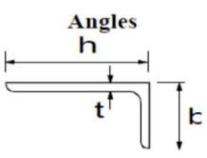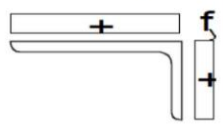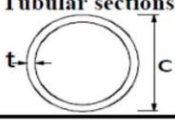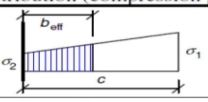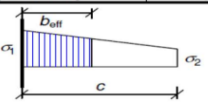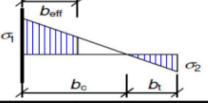
Table 2.23 – Maximum width-to-thickness ratios of angles and tubular sections

| | Angles | |
|---|---|---|
| See also Table 2.22 | h, t, b | Does not apply to angles in continuous contact with other components |

| Class | Section in compression |
|---|---|
| Stress distribution (compression +ve) | + , f , + |
| 3 | $h/t \leq 15\varepsilon$ : $\dfrac{b+h}{2t} \leq 11.5\varepsilon$ |

**Tubular sections**

t, c

| Class | Section in bending and/or compression |
|---|---|
| 1 | $d/t \leq 50\varepsilon^2$ |
| 2 | $d/t \leq 70\varepsilon^2$ |
| 3 | $d/t \leq 90\varepsilon^2$ <br> **NOTE:** For $d/t > 90\,\varepsilon^2$ see EN 1993-1-6 |

| $\varepsilon = \sqrt{235/f_y}$ | $f_y$ (N/mm²) | 235 | 275 | 355 | 420 | 460 |
|---|---|---|---|---|---|---|
| | $\varepsilon$ | 1.00 | 0.92 | 0.81 | 0.75 | 0.71 |
| | $\varepsilon^2$ | 1.00 | 0.85 | 0.66 | 0.56 | 0.51 |

**Table 1.5 Outstand compression elements as per EC3**

Table 4.2: Outstand compression elements

| Stress distribution (compression positive) | | | Effectiveᵖ width $b_{eff}$ | |
|---|---|---|---|---|
| $b_{eff}$, $\sigma_2$, $\sigma_1$, c | | | $1 > \psi \geq 0$: <br> $b_{eff} = \rho\, c$ | |
| $b_t$, $b_c$, $\sigma_1$, $\sigma_2$, $b_{eff}$ | | | $\psi < 0$: <br> $b_{eff} = \rho\, b_c = \rho\, c\,/\,(1-\psi)$ | |
| $\psi = \sigma_2/\sigma_1$ | 1 | 0 | -1 | $1 \geq \psi \geq -3$ |
| Buckling factor $k_\sigma$ | 0,43 | 0,57 | 0,85 | $0,57 - 0,21\psi + 0,07\psi^2$ |
| $b_{eff}$, $\sigma_1$, $\sigma_2$, c | | | $1 > \psi \geq 0$: <br> $b_{eff} = \rho\, c$ | |
| $b_{eff}$, $\sigma_1$, $\sigma_2$, $b_c$, $b_t$ | | | $\psi < 0$: <br> $b_{eff} = \rho\, b_c = \rho\, c\,/\,(1-\psi)$ | |

| $\psi = \sigma_2/\sigma_1$ | 1 | $1 > \psi > 0$ | 0 | $0 > \psi > -1$ | -1 |
|---|---|---|---|---|---|
| Buckling factor $k_\sigma$ | 0,43 | $0,578\,/\,(\psi + 0,34)$ | 1,70 | $1,7 - 5\psi + 17,1\psi^2$ | 23,8 |

### 1.4.5 Features of class 4 sections

In calculating the effective geometrical properties for Class 4 sections, and as already mentioned, it is assumed that parts of the area under compression due to local instability phenomena do not have any resistance (lost area): typically, the compressed portions of the cross-sections, which have to be neglected for the resistance checks, are the parts close to the free end of an outstand flange or the central part of an internal compressed element.

Furthermore, the effects of local plate buckling usually control the load carrying capacity of thin-walled sections, denominated as class 4 sections in EC3. Local plate buckling is taken into account by effective cross-section properties. The values $A_{eff}$ and $W_{eff}$ are calculated each for the relevant loading case only. For example, $A_{eff}$ is calculated under the assumption that an axial force N is present only.

#### United States Provisions for Steel Design

The main specification to apply for the design of steel structures in United States is ANSI/AISC 360-10 'Specification for Structural Steel Buildings' that addresses steel constructions as well as composite constructions: steel acting compositely with reinforced concrete. This specification states design requirements (stability and strength) for steel members and composite constructions, design of connections, fabrication and erection, Quality Control and Quality Assurance.

Differently from Eurocodes, AISC 360-10 allows use of the semi-probabilistic limit state method as well as the working stress (allowable stress) design method. The first method is called Load and Resistance Factor Design (LRFD) and the second one ASD. The two methods are specified as alternatives and the ASD method is maintained for those who have been using it in the past (senior engineers), before LRFD method was introduced.

Very useful tools for the designer are the AISC manuals: mainly the AISC 325 Steel Construction Manual and AISC 327 Seismic Design Manual, which discuss very interesting design examples to help in design activity.
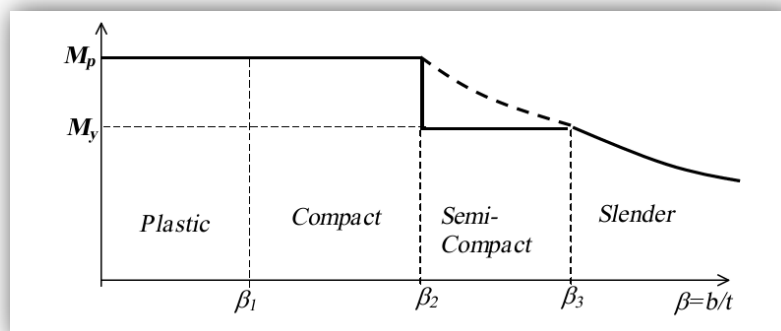


**Figure 1.5 Moment Capacities of Sections AISC as per 2016**

As already mentioned, AISC 360-10 addresses classification of cross-sections in Chapter B, Section B4; the code deals with members subjected to axial load and members subjected to bending in a different way:

- Members subjected to axial load are distinguished as non-slender or slender;
- Members subjected to flexure are distinguished as compact, non-compact or slender.

The classification for members subjected to axial load and bending is absent in the US approach.

Classifications criteria are listed in Table B4.1.a of AISC specifications (reproduced in Table 4.4a) for compressed members and in Table B4.1b (reproduced in Table 4.4b) for members in bending.

Classification criteria are based, as in the EC3 code, on steel grade and on width-to-thickness ratios for stiffened elements (elements supported along two edges parallel to the direction of the compression force, typically webs of I- or C-shaped sections) and unstiffened elements (elements supported along only one edge parallel to the direction of the compression force, typically flanges of I- or C-shaped sections).

AISC code defines:

**(a)** for members subjected to axial load:

$\lambda_r$, that is width-to-thickness ratio that defines non-slender/slender limit;

**(b)** for members subject to flexure:
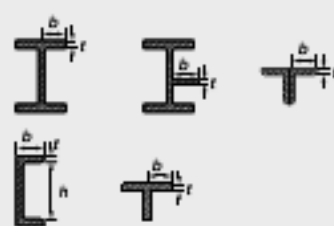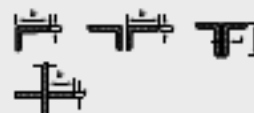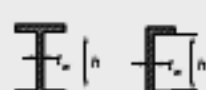
$\lambda_p$, that is width-to-thickness ratio that defines compact/non-compact limit;

$\lambda_r$, that is width-to-thickness ratio that defines non-compact/slender limit.

It should be noted that:
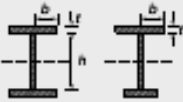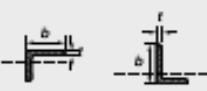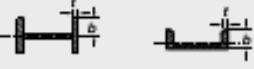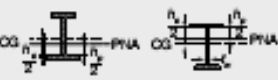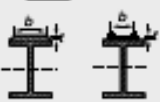
- US flange width is one-half of full flange width, while in EC3 it is the outstanding part of the flange (one-half of full flange width less one-half of web thickness less the fillet or corner radius);
- US web width of rolled sections, as in EC3 code, is the clear distance between flanges less the fillet or corner radius at both flanges;

**Table 1.6 Width-to-thickness ratios for members subject to axial compression (from Table B4.1a of AISC 360-10)**

| Case | Description of element | Width to thickness ratio | Limiting width-to-thickness ratio $\lambda_r$ (non-slender/slender) | Examples |
|---|---|---|---|---|
| | | **Unstiffened elements** | | |
| 1 | Flanges of rolled I-shaped sections, plates projecting from rolled I-shaped sections; outstanding legs of pairs of angles connected with continuous contact, flanges of channels and flanges of tees | $b/t$ | $0.56\sqrt{\dfrac{E}{F_y}}$ | |
| 2 | Flanges of built-up I-shaped sections and plates or angle legs projecting from built-up I-shaped sections | $b/t$ | $0.64\sqrt{\dfrac{k_c E}{F_y}}$ | |
| 3 | Legs of single angles, legs of double angles with separators and all other unstiffened elements | $b/t$ | $0.45\sqrt{\dfrac{E}{F_y}}$ | |
| 4 | Stems of tees | $d/t$ | $0.75\sqrt{\dfrac{E}{F_y}}$ | |
| | | **Stiffened elements** | | |
| 5 | Webs of doubly-symmetric I-shaped sections and channels | $h/t_w$ | $1.49\sqrt{\dfrac{E}{F_y}}$ | |
| 6 | Walls of rectangular HSS and boxes of uniform thickness | $b/t$ | $1.40\sqrt{\dfrac{E}{F_y}}$ | |
| 7 | Flange cover plates and diaphragm plates between lines of fasteners or welds | $b/t$ | $1.40\sqrt{\dfrac{E}{F_y}}$ | |
| 8 | All other stiffened elements | $b/t$ | $1.49\sqrt{\dfrac{E}{F_y}}$ | |
| 9 | Round HSS | $D/t$ | $0.11\dfrac{E}{F_y}$ | |

HSS, hollow square section.

**Table 1.7 Width-to-thickness ratios for members subject to flexure (from Table B4.1b of AISC 360-10).**

| Case | Description of element | Width-to-thickness ratio | $\lambda_p$ (compact/non-compact) | $\lambda_r$ (non-compact/slender) | Examples |
|------|------------------------|--------------------------|-----------------------------------|-----------------------------------|----------|
| 10 | Flanges of rolled I-shaped sections, channels and tees | $b/t$ | $0.38\sqrt{\dfrac{E}{F_y}}$ | $1.00\sqrt{\dfrac{E}{F_y}}$ |  |
| 11 | Flanges of doubly and singly symmetric I-shaped built-up sections | $b/t$ | $0.38\sqrt{\dfrac{E}{F_y}}$ | $0.95\sqrt{\dfrac{k_c E}{F_L}}$ |  |
| 12 | Legs of single angles | $b/t$ | $0.54\sqrt{\dfrac{E}{F_y}}$ | $0.91\sqrt{\dfrac{E}{F_y}}$ |  |
| 13 | Flanges of all I-shaped sections and channels in flexure about the weak axis | $b/t$ | $0.38\sqrt{\dfrac{E}{F_y}}$ | $1.00\sqrt{\dfrac{E}{F_y}}$ |  |
| 14 | Stems of tees | $d/t$ | $0.84\sqrt{\dfrac{E}{F_y}}$ | $1.03\sqrt{\dfrac{E}{F_y}}$ |  |
| 15 | Webs of doubly symmetric I-shaped sections and channels | $h/t_w$ | $3.76\sqrt{\dfrac{E}{F_y}}$ | $5.70\sqrt{\dfrac{E}{F_y}}$ |  |
| 16 | Webs of singly symmetric I-shaped sections | $h_c/t_w$ | $\dfrac{\dfrac{h_c}{h_p}\sqrt{\dfrac{E}{F_y}}}{\left(0.54\dfrac{M_p}{M_y}-0.09\right)^2}\le\lambda_r$ | $5.70\sqrt{\dfrac{E}{F_y}}$ |  |
| 17 | Flanges of rectangular HSS and boxes of uniform thickness | $b/t$ | $1.12\sqrt{\dfrac{E}{F_y}}$ | $1.40\sqrt{\dfrac{E}{F_y}}$ |  |
| 18 | Flange cover plates and diaphragm plates between lines of fasteners or welds | $b/t$ | $1.12\sqrt{\dfrac{E}{F_y}}$ | $1.40\sqrt{\dfrac{E}{F_y}}$ |  |
| 19 | Webs of rectangular HSS and boxes | $h/t$ | $2.42\sqrt{\dfrac{E}{F_y}}$ | $5.70\sqrt{\dfrac{E}{F_y}}$ |  |
| 20 | Round HSS | $D/t$ | $0.07\dfrac{E}{F_y}$ | $0.31\dfrac{E}{F_y}$ |  |

# CHAPTER 2:

# BACKGROUND FOR LATERAL TORSIONAL BUCKLING AND CODE PROVISIONS

## 2.1 General

Historically, buckling of structural members have long been recognized as a potentially dangerous failure mode. Buckling of columns was first brought to attention by Euler (1744) more than two hundred years ago. Bryan (1891) first introduced the theoretical work on the elastic buckling of plates. He presented how the elastic buckling of plates could be applied to the sides of a ship. It was quickly realized that the buckling behaviour of a plate was quite different from that of a column. For a column, buckling terminates the ability of a member to resist axial load, and the buckling load is thus the failure load of the member. However, this might not be the behaviour for plate elements. Most of the structural plate elements can, subsequent to reaching the buckling load, continue to resist increasing axial loads.  These structural plate elements do not fail until a load considerably in excess of the buckling load. In essence plate elements possess substantial post-buckling strength. The buckling load of a plate is therefore not the failure load.  Also, the failure load of a structural member made up with these plate elements may not correspond to the local buckling of its plate elements. Thus, one must determine the load-carrying capacity of a plate or a structural member made of plate elements by considering the post-buckling behaviour.

### 2.2 Concept of stability

The Stability is one of the most critical ultimate states for steel structures during the construction and during their lifetime. The main objective and the most difficult challenges of structural stability is to determine the critical load under which a structure loses its stability. Due to their high strength, steel beams are characterized by small thicknesses of section walls, which leads to various forms of stability losses. Structural stability problems have substantial effects on the design steps of steel structures. Stability is a potent issue in the design of steel structures which may cause serious structural failure. The stress at which buckling occurs depends on a variety of factors ranging from the dimensions of the member to the boundary conditions to the properties of the material of the member. Determining the buckling stress is a fairly complex undertaking [Erath, S. (2020)].

### 2.3 Stability analysis

In a broad sense, the purpose of analysis of stability of a structure is to determine the loads on a structure, which leads to the appearance of new forms of equilibrium. These forms of equilibrium usually lead to collapse of a structure and corresponding loads are referred as critical ones. The stability of a structure will be provided if acting loads are less than the critical ones. While, the buckling analysis is to determine the critical load (or critical loads factor) and corresponding buckling mode shapes.

A study of the stability of structures is aimed at calculating the elastic critical load and deducing appropriate design loads for the compression elements, to ensure that buckling does not

occur. This is generally a complex procedure although the techniques can be built up from the matrix analysis methods presented in later chapters. Fortunately, the stability analysis of a structure can be considered subsequent to the linear elastic analysis. Further, in many cases Codes of Practice offer sufficient guidance for a stability analysis not to be necessary. Nevertheless, important structures are subjected to stability analysis and the computational effort required is continually being reduced by developments in computer applications [Erath, S. (2020)].

### 2.4 General definition of stability

Broadly speaking, stability can be defined as the ability of a physical system to return to equilibrium when disturbed slightly. For a mechanical system, Dirichlet stated: "the equilibrium of a mechanical system is considered stable if, when moving the points of the system from their equilibrium position with an infinitesimal quantity with a low initial speed, the displacement of different points of the system remain, during the displacement, contained within the limits imposed [Erath, S. (2020)].

### 2.5 Stability theories of thin-walled steel structures

By approaching thin-walled structures, the consideration of inherent stability phenomenon is imperative. Over the past century, compressive research works have been invested to help predict the critical buckling load limits for different types of structures. The theoretical and experimental research indicated the effect of geometric imperfections and boundary conditions can altered limits of the value of the buckling load.

Stability theories have been developed in order to determine the conditions via which a structure, in equilibrium, ceases to be stable. Stability is essentially an extreme geometrical property of structures, which can be found for large slenderness, flat thin plates or cylindrical thin shells. Normally, systems are considered with a variable parameter which typically represents the external load (mechanical), but which can also be temperature (thermal buckling) or other types of loadings. For each limit load value, there is only one non-buckling configuration [A.Labed].

It is possible that systems undergo large deformations before even the elastic limit of the material is reached, especially in the case of structures with Class 4 sections as a result of the local buckling. However, this situation is not dangerous for the system when the deformations do not contribute to the increase of mechanical stresses. The system is still elastically stable. On the other hand, and despite the fact that the elastic limit is not yet reached, it does exist a situation where large deformations contribute to the increase of internal stresses, which generally leads to the ruin of the system and then elastically unstable.

Critical stability loads can be determined using:

-    The classical resolution of differential equations of equilibrium.

- Approaches based on energy methods.

It is worth to remind that the resolution of differential equations of equilibrium can only be accomplished for simple buckling problems. For more complicated structures situations, it is common to use the alternative energy methods, iterative methods can also be utilized to solve stability problems. Hypotheses on the nature of the deformation, the elastic system can be approached using suitable and modifiable parameters or generalized coordinates, determined in such a way as to meet the equilibrium conditions.

### 2.6 General on the instability Modes in steel structures

As explained in the resistance of a steel member subjected to axial compression depends on the cross-section resistance or the occurrence of instability phenomena. As steel members usually have high slenderness the design for compression is governed by the instability phenomena such as:

• Flexural buckling

• Torsional buckling

• Flexural torsional buckling

• Lateral torsional buckling

The buckling resistance should be evaluated according to the relevant buckling mode and relevant imperfections of real members, as described in the following sections.

Flexural Buckling

Flexural buckling is a phenomenon that occurs about the axis of the highest slenderness ratio and the smallest radius of gyration. It can happen in any member subjected to compression, which in the end will lead to deflection of the member. An illustration of the flexural buckling can be seen in Figure1.3.

Torsional Buckling

Torsional buckling is a form of buckling occurring about the longitudinal axis of a member, where the centre of the member remains straight while the rest of the section rotates. Flexural Torsional Buckling

According to [da Silva et al., 2010], flexural torsional buckling consists of the simultaneous occurrence of torsional and bending deformations along the axis of the member.

### 2.7 Lateral torsional buckling

### 2.7.1 General

Open section beams bent in their stiffer principle plane are susceptible to a type of buckling deflecting sideways and twisting, the so-called lateral instability, lateral-torsional or flexural-torsional instability. In particular, this form of instability is due to the compression force acting on a part of the

profile causing instability with lateral deflection partially prevented by the tension part of the profile, which generates twist.

Design standards consider lateral–torsional buckling as one of the ultimate limit states that must be checked for steel members in bending, when relevant. The buckling resistance assessment is usually based on appropriate buckling curves and requires the computation of the elastic critical moment, which is strongly dependent on several factors such as, the bending moment distribution, the restraints at the end supports and in correspondence of the load points, the beam cross-section, the distance between the load application point and the shear centre

### 2.7.2 Definition

Lateral Torsional Buckling (LTB), is a mode of buckling that occurs when a flexural member undergoes both lateral deflection and twisting as illustrated in Fig. 1. However, the complex nature of the LTB phenomenon makes it difficult to embrace all the affecting factors and assumptions responsible for that phenomenon. In fact, the LTB resistance capacity of a slender section depends upon a number of factors. These several factors which are believed to influence the resistance to LTB such as : the distance between lateral and /or torsional braces, the type and position of the applied loads, the restraints at the ends and at intermediate positions along the beam axis, the material properties, the magnitude and distribution of residual stresses, initial imperfections of geometry, changes in the cross section (steps or taper in the cross section, holes), and interaction between local and overall buckling.

When a beam is laterally braced at discrete points along its length and is loaded such that it is bent about its strong axis, the possibility that the beam will buckle laterally and with a torsion before reaching its plastic moment or local buckling moment must be investigated. Figure 2.1 shows moment resistance versus unbraced length of a flexural member.
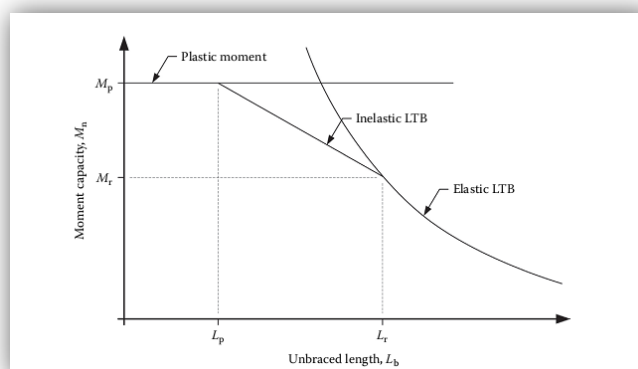


**Figure 2.1 Lateral-torsional buckling solution space**

### 2.7.3 Theory of LTB

Traditionally, the theoretical study of LTB mentioned phenomenon starts for the basic case representing members with rectangular section. A particular interest of slender sections, I-shaped of classes 3 and respectively, in which the ratio of $I_y/I_z$ is large as they are mainly concerned by the LTB. These type of section are very common in the steel structures having large span. The manner in which the point of application of loads in the top flange , the shear centre or at the lower flange, affects considerably the global behaviour of flexural members in their resistance with regard to the lateral-torsional buckling. In order to understand the real behaviour (inelastic) of the so-called real beams, the initial imperfection must be considered.

The following assumptions are considered to understanging the LTB phenomenon in the particular case of I-shaped steel sections:

- The beam is prismatic.
- The beam is initially undistorted.
- The member cross section retains its original shape during buckling.
- The externally applied loads are conservative.
- The global behaviour is elastic (no yielding).
 -The analysis is limited within the elastic limit.
- The transverse load passes through the axis of symmetry in the plane of
bending.
- Residual stresses are not considered.
- Simply supported vertically and laterally bouandring conditions.

In order to determine the lateral torsional buckling capacity of beams, different structural steel design standards (e.g., CAN-CSA S16-14 (2014), AISC-ANSI 360-10 (2010), AS 4100 (1998), and Eurocode 3 (2005)) provide different algebraic equations. However, in a general sense, all of them start with calculating the elastic LTB resistance Mu of a simply supported beam under uniform moments.

The finite element method is a numerical technique used to solve problems that may be otherwise difficult to solve analytically. The basic concept behind the finite element method is to model a continuum with infinite degrees of freedom and as a system of elements having finite degrees of freedom. These elements are assembled to accurately approximate the behavior of the entire system. The next point will be the causes of failures for beams is the lateral-torsional buckling LTB either elastically or inelastically. A beam can fail by reaching $M_{pl}$, and a plastic hinge will be created. The failure can be one of the three types of bucklings: LTB is the first reason for failur and also the flange local buckling (FLB) in elastic or inelastic manners.

### 2.8 Parameters effecting the design background of members subjected to LTB

### 2.8.1  General

The buckling is essentially flexure behaviour. Due to their high strength, steel beams are characterized by small thicknesses of section walls, which leads to various forms of stability loss. Structural stability problems have substantial effects on the design steps of steel structures. Stability is a potent issue in the design of steel structures which may cause serious structural failure. Lateral-torsional buckling is a kind of failure that occurs when the in-plane bending capacity of a member exceeds its resistance to out-of-plane lateral buckling and twisting.  Physically, the phenomenon of LTB in which the overall behaviour of steel member changes from initially in-plane bending to combined a large lateral displacement and twist angle due to an application of load on an unsupported beam.

### 2.8.2 LTB codes provisions

The elastic stability of flexural members has been an important consideration in civil engineering design since the beginning of the 20th century. In fact, International design codes in United States, Australia, Europe and Canada contain relative provisions for designing flexural members considering the limit state. Therefore, LTB is one of the most important stability problems and may often be a controlling parameter in steel beam design. Various design standards and codes recommend methods in order to calculate lateral torsional buckling of steel members. Critical elastic lateral torsional buckling moment capacities for I-shaped steel members are considered in various standards and codes: AISC 360-10, EC3, BS 5950 etc.

With regard of LTB, the effect of moment distribution between supports and the effect of load height with respect to the shear centre, the beam being or not laterally restrained etc. The LTB can cause partial failure or whole failure in the structure. The stress at which buckling occurs depends on a variety of factors ranging from the dimensions of the member to the boundary conditions to the properties of the material of the member.

### 2.8.3 Effect of moment distribution

To designate the effects of moment distribution between supports codes used an expression termed the equivalent uniform moment factor. This factor is an attempt at modifying the basic strength of a loaded member by referring its strength versus the strength of a member loaded with a constant moment distribution. The factors used by these codes are inaccurate for some loading circumstances on both the conservative and unconservative ends of capacity prediction. This issue arises due to the broad range of moment distributions for which the factor is intended to predict capacities. Current efforts to improve the effectiveness of these moment factors involve producing expressions for specific loading types. Although extensive effort has been put into producing solutions for possible

distributions, many loading scenarios remain uncharacterized. Without solutions for a comprehensive range of load distributions, it is unlikely design codes will alter their methods and use moment factors tailored to specific load distribution types.

### 2.8.4 Effect of load position in the cross section

The effects of load locations are characterized in the design codes that consider this effect by modifying the members' effective length. In the case of a sagging bending moment, when a member is loaded below its shear centre, the effective capacity of the member increases because the load acts to correct the torsional displacement tendency (tension zone). When the load is above the shear centre, however, the capacity decreases significantly as the load produces additional destabilizing forces in the torsional direction.

It is worth to recall that neglecting the fact of actual location of the applied load, the design codes at risk of producing weak structural components and therefore entire the entire structures are structurally deficient during critical phases of their life. The most significant of these phases being the construction period, as many of the members will be loaded in a standalone temporary fashion where they do not have suitable lateral bracing to ensure negation of the load height effect.

### 2.9 Lateral-Torsional Buckling according to EC3

### 2.9.1 Cross-section classification

- **Basis:** The role of cross section classification is to identify the extent to which the resistance and rotation capacity of cross sections is limited by its local buckling resistance as shown in (Figure 4.1).

- **Classification:** Four classes of cross-sections are defined, as follows:
    - *Class 1* cross-sections are those which can form a plastic hinge with the rotation capacity required from plastic analysis without reduction of the resistance.
    - *Class 2* cross-sections arc those which can develop their plastic moment resistance, but have limited rotation capacity because of local buckling.
    - *Class 3* cross-sections are those in which the stress in the extreme compression fiber of the steel member assuming an elastic distribution of stresses can reach the yield strength, but local buckling is liable to prevent development of the plastic moment resistance.
    - *Class 4* cross-sections are those in which local buckling will occur before the attainment of yield stress in one or more parts of the cross-section.
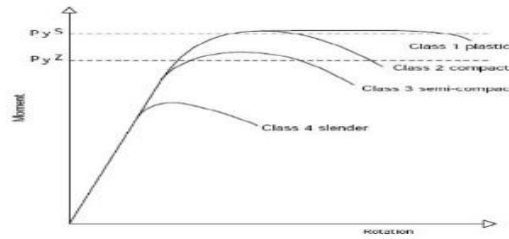
**Figure 2.2 Classification of cross-section [EN 1993-1-1:2005]**

- **Classification criteria**

    - For the particular case of Class 4, the cross sections effective widths may be used to make the necessary allowances for reductions in resistance due to the effects of local buckling, [EN 1993-1-5, 4.4].

    - The classification of a cross-section depends on the width to thickness ratio of the parts subject to compression.

    - Compression parts include every part of a cross-section which is either totally or partially in compression under the load combination considered.

    - The various compression parts in a cross-section (such as a web or flange) can, in general, be in different classes.

    - A cross-section is classified according to the highest (least favourable) class of its compression parts.

- **Particular remarks**

    Alternatively, the classification of a cross-section may be defined by quoting both the flange classification and the web classification. The limiting proportions for Class 1, 2, and 3 compression parts should be obtained from Table 4.1. A part which fails to satisfy the limits for Class 3 should be taken as Class 4. Except as given in (10) Class 4 sections may be treated as Class 3 sections if the width to thickness ratios are less than the limiting proportions for Class 3 obtained from (Table 4.2) when £ is increased by $\sqrt{\dfrac{\frac{f_y}{\gamma_{M_0}}}{\sigma_{com.Ed}}}$ , Where $\sigma_{com.Ed}$ is the maximum design compressive stress in the part taken from first order or where necessary second order analysis.

    However, when verifying the design buckling resistance of a member using section 6.3 [EN 1993-1-1:2005], the limiting proportions for Class 3 should always be obtained from Tables

    Cross-sections with a Class 3 web and Class I or 2 flanges may be classified as class 2 cross sections with an effective web in accordance with 6.2.2.4 [EN 1993-1-1:2005].

Where the web is considered to resist shear forces only and is assumed not to contribute to the bending and normal force resistance of the cross section, the cross section may be designed as Class 2, 3 or 4 sections, depending only on the flange class.

### 2.9.2 Uniform members in bending: buckling resistance

In order to analyses buckling effect on a structure subjected to transverse loading, and according to section EN-1993-1, where no lateral-torsional buckling checking is needed, two main cases are considered:

**1.** Beams with sufficient restraint to compression flange, which are not susceptible to lateral-torsional buckling.

**2.** Beams with particular cross-section shape, such as square or circular hollow sections, fabricated circular tubes or square box sections are not susceptible to lateral-torsional buckling.

According to  EN-1993-1-1, lateral-torsional bukling checking for a member laterally unrestrained subject to major axis bending, should be verified as the follow:

$$\frac{M_{Ed}}{M_{b,Rd}} \leq 1 \qquad\qquad (2.1)$$

Where,          $\mathbf{M_{Ed}}$              is the design value of the moment

$\mathbf{M_{b,\,Rd}}$                 is the design buckling resistance moment

If the  ratio $\frac{M_{Ed}}{M_{b,Rd}} \leq 1.0$ then $M_{b,\,Rd}$ is the highest value that section can reach, so $M_{Ed}$ cannot exceed it.

The design buckling resistance moment is calculated as:

$$M_{b,Rd} = \chi_{LT}.W_y \frac{f_y}{\gamma_{M1}} \qquad\qquad (2.2)$$

Where, $W_y$ is the appropriate section modulus as follows:

In which $W_y$ is $\mathbf{W_{pl,\,y}}$ for Class 1 or 2 cross-sections, and $W_y$ is $\mathbf{W_{el,\,y}}$ for Class 3 cross-sections.

For Class 4 cross-sections $W_y$ is $\mathbf{W_{eff,\,y}}$

And,  $\boldsymbol{\gamma_{M1}}$        Is the partial factor for buckling resistance.

$\boldsymbol{f_y}$       Is the yield strength of the material.

$\boldsymbol{\chi_{LT}}$        Is the  non-dimensional reduction factor for lateral-torsional buckling that ranges from 0 to 1. Further details will be provided later in the chapter.

### 2.9.3 Lateral-torsional buckling parameter and buckling curves

For bending members of constant cross-section, the value of   $\chi_{LT}$ for the appropriate non-dimensional slenderness$\bar{\lambda}_{LT}$ , should be determined from the given formulation:

$$\chi_{LT} = \frac{1}{\Phi_{LT}+\sqrt{\Phi_{LT}^2-\bar{\lambda}_{LT}^2}} \quad , \lambda_{LT} \leq 1. \qquad\qquad (2.3)$$

Where, $\Phi_{LT} = 0.5\big(1 + \alpha_{LT}(\bar{\lambda}_{LT} - 0.2) + \bar{\lambda}_{LT}^2\big)$and  ranges  from  0  to  1.  It  is  a  non-dimensional parameter.

$\alpha_{LT}$ Is an imperfection factor and must be taken from Table 4.3. It is a non-dimensional parameter.

$\bar{\lambda}_{LT}$ Is the non-dimensional slenderness, it is calculated as:

$$\bar{\lambda}_{LT} = \sqrt{\frac{W_y * f_y}{M_{cr}}} \qquad\qquad (\,2.4\,)$$

$M_{cr}$ Is the elastic critical moment for lateral-torsional buckling. It is based on gross cross sectional properties and takes into account the loading conditions.

The Standard provides a table to determine what buckling curve we must chose and other recommended values that belongs to each curve (see Table 4.2 and Table 4.3).

In addition, EN-1993-1-1 says that it is not necessary check the phenomenon for $\bar{\lambda}_{LT} < 0.4.$ Table 4.2 Recommended values for lateral torsional buckling curves for cross-sections using for $\chi_{LT}$ [EN-1993-1-1, Table 6.4]

**Table 2.1 Recommended values for imperfection factors for lateral-torsional buckling curves [EN-1993-1-1, Table 6.3]**

| Cross-section | Limits | Buckling curve |
|---|---|---|
| Rolled I sections | h/b ≤ 2 | a |
| | h/b > 2 | b |
| Welded I sections | h/b ≤ 2 | c |
| | h/b > 2 | d |
| Other cross-sections | - | d |

**Table 2.2 Recommended values for lateral torsional buckling curves for cross-sections using for $\chi_{LT}$ [EN-1993-1-1, Table 6.4]**

| Buckling curve | a | b | c | d |
|---|---|---|---|---|
| Imperfection factor $\alpha_{LT}$ | 0,21 | 0,34 | 0,49 | 0,76 |

**Buckling curves:**

The graphical representation of these curves is the following one:
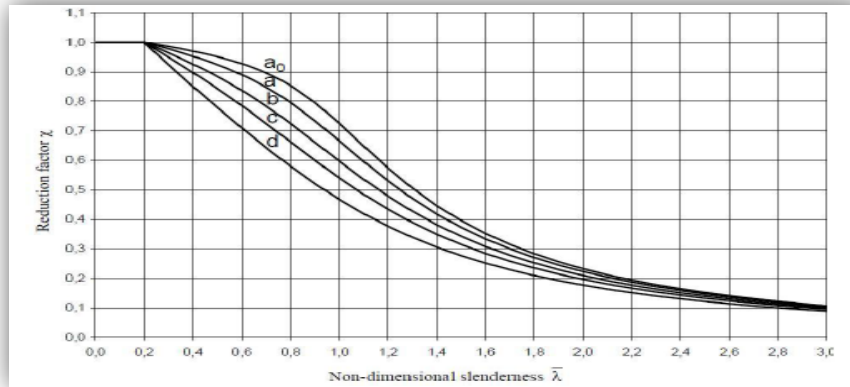
Figure 2.3 Buckling curves. [EN-1993-1-1, 2005]

- Curve a, represents quasi perfect shapes.

- Curve b, represents shapes with medium imperfections.

- Curve c, represents shapes with a lot of imperfections.

- Curve d, represents shapes with maximum imperfections.

## 2.10 Elastic critical moment, Mcr

**The 3-factor formula (EC3)**

When finding the lateral-torsional buckling resistance of a beam, a certain maximum theoretical moment is needed which applies for the beam if it was ideal. That moment is the elastic critical moment, $M_{cr}$. It depends on number of factors, for example the length of the beam, the moment diagram, the support conditions, the stiffness of the beam about the minor axis and the torsional stiffness.

The elastic critical moment is used to find the non-dimensional slenderness of a beam in the process of designing it according to Eurocode3. However, there is nothing stated about how to determine *Mcr* in Eurocode3. In an earlier version of Eurocode3, the pre-standard ENV 1993-1-1:1992, an approximating formula is presented to estimate *Mcr*, which gives conservative results. The formula is valid for beams in a major axis bending with a uniform cross section that is symmetric about the minor axis (ECCS 2006, p. 229). Beams in reality are not ideal. That is why a reduction factor must be used to find the design capacity. The formula mentioned above is often called the 3-factor formula and is expressed as follows:

$$\mathbf{M_{cr}} = \mathbf{C_1} \cdot \frac{\pi^2 EI_{z_i}}{(K_Z \cdot L)^2} \left[ \sqrt{\left(\frac{K_z}{K_w}\right)^2 \frac{I_{w_i}}{I_{z_i}} + \frac{(K_Z \cdot L)^2 GI_{t_i}}{\pi^2 EI_{z_i}} + \left(C_2 Z_g - C_3 Z_j\right)^2} - \left(C_2 Z_g - C_3 Z_j\right) \right] \quad (2.5)$$

Where,

$C_1$ = factor depending on the moment diagram and the end restraints.

$C_2$ = factor depending on the moment diagram and the end restraints, related to the vertical position of loading.

$C_3$ = factor depending on the moment diagram and the end restraints, related to the mono-symmetry of the beam.

**E** = Young is modulus of elasticity.

**G** = shear modulus.

$I_t$ = Torsional constant.

$I_W$ = Warping constant.

$I_Z$ = second moment of area about the minor axis.

**L** = length of the beam between points which have lateral restraints.

$K_W$ = effective length factor which refers to end warping.

$K_Z$ = effective length factor which refers to end rotation in plan.

$Z_g$ = coordinate of the point of load application w.r.t the shear Centre in the z-direction.

**Zj** = mono-symmetry parameter.

Values of the factorsC1, $C_2$, and $C_3$ referred to as the C-factors, for the two load cases studied in the present theses, given by ECCS (2006) are presented in Table 4.4. Different values for the C-factors can be found in other literature, such as in Access Steel (2010) and Access Steel (2006), where only $K_Z=K_W=1$ is considered and in the pre-standard ENV 1993-1-1:1992, where various load cases are considered but some values are overestimated as shown in Mohri et al. (2003).

The shear modulus is calculated as follows:     $$G = \frac{E}{2(1+\vartheta)}$$     (2.6)

Where,    $\vartheta$ = Poisson's ratio

The parameter $Z_g$ describes the vertical position of the PLA ??. In lateral-torsional buckling, the PLA has a significant influence. If the load acts on the compression flange, i.e. above the SC, the parameter $Z_g$ is positive and $M_{cr}$ lower than for $Z_g=0$, so the load has a destabilizing effect. If the load acts below the SC, like on the tension flange, the parameter $Z_g$ is negative and $M_{cr}$ higher than for $Z_g$ =0 so the load has a stabilizing effect.

## 2.11 Lateral-Torsional Buckling according to ANSI/AISC 360-16 (June 2018)

### 2.11.1 Cross-section classification

For members subject to axial compression, sections are classified as non-slender element or slender-element sections. For a non-slender-element section, the width-to- thickness ratios of its compression elements shall not exceed $\lambda r$ from *Table 4.5(sheet 1 of 2).* If the width-to-thickness ratio of any compression element exceeds $\lambda r$, the section is a slender-element section.

For members subject to flexure, sections are classified as compact, noncompact or slender-element sections. For a section to qualify as compact, its flanges must be-continuously connect to the web or webs, and the width-to-thickness ratios of its compression elements shall not exceed the limiting width-to-thickness ratios, λp, from *Table 4.5(sheet 2 of 2).* If the width-to-thickness ratio of one or more compression elements exceeds λp, but does not exceed λr from *Table 4.5(sheet 2 of 2).*, the section is noncompact. If the width-to-thickness ratio of any compression element exceeds $λ_r$, the section is a slender-element section.

### 2.11.2 Doubly symmetric compact I-shaped members and Channels

When Lb ≤ Lp, the limit state of lateral-torsional buckling does not apply.

✓        When $L_p < L_b \leq L_r$        $M_n = C_b \left[ M_p - (M_p - 0.7F_y S_x)(\frac{L_b - L_p}{L_b - L_p}) \right] \leq M_P$        (2.7)

✓        When $L_b > L_r$        $M_n = F_{cr} S_x \leq M_p$        (2.8)

where

- $L_b$ = length between points that are either braced against lateral displacement of the compression flange or braced against twist of the cross section in (mm)

- $F_{cr} = \frac{C_b \pi^2 E}{(\frac{L_b}{r_{ts}})^2} \sqrt{1 + 0.078 \frac{J_c}{S_x h_0} (\frac{L_b}{r_{ts}})^2}$ = critical stress, ksi (MPa)        (2.9)

- E = modulus of elasticity of steel = 29,000 ksi (200 000 MPa)

- J = torsional constant, in.4 (mm4)

- $S_x$ = elastic section modulus taken about the x-axis, in.3 (mm3)

- ho = distance between the flange centroids, in. (mm)

The square root term in Equation (2.10) may be conservatively taken equal to 1.0.

Equations (2.9) and (2.10) provide identical solutions to the following expression for lateral-torsional buckling of doubly symmetric sections that has been presented in past editions of this Specification:

$$M_{cr} = C_b \frac{\pi}{L_b} \sqrt{EI_y GI + (\frac{\pi E}{L_b})^2 I_y C_w}$$        (2.10)

The advantage of Equations (4.8) and (4.9) is that the form is very similar to the expression for lateral-torsional buckling of singly symmetric sections given in Equations (2.9) and (2.10).

- $L_p$, the limiting laterally unbraced length for the limit state of yielding, in. (mm), is:

$$L_p = 1.76r_y \sqrt{\frac{E}{F_y}}$$        (2.11)

- $L_r$, the limiting unbraced length for the limit state of inelastic lateral-torsional buckling, in.

(mm), is:

$$L_r = 1.95 r_{ts} \frac{E}{0.7F_y} \sqrt{\frac{J_c}{S_x h_0} + \sqrt{\left(\frac{J_c}{S_x h_0}\right)^2 + 6.76 \left(\frac{0.7F_y}{E}\right)^2}} \qquad (2.12)$$

Where

- $r_y$ = radius of gyration about y-axis, in. (mm)

- $r_{ts}^2 = \frac{\sqrt{I_y C_w}}{S_x}$ $\qquad\qquad\qquad\qquad\qquad\qquad\qquad\qquad$ (2.13)

and the coefficient c is determined as follows:

- For doubly symmetric I-shapes $\qquad c=1$ $\qquad\qquad\qquad\qquad\qquad\qquad$ (2.14)

- For channels $\qquad c = \frac{h_0}{2}\sqrt{\frac{I_y}{C_w}}$ $\qquad\qquad\qquad\qquad\qquad\qquad$ (2.15)

Where

- $I_y$ = moment of inertia about the y-axis, in.4 (mm4)

  For doubly symmetric I-shapes with rectangular flanges, $C_w = \frac{I_y h_0}{4}$ $\qquad$ (2.16)

  Hence, $r_{ts}^2 = \frac{I_y h_0}{2S_x}$ $\qquad\qquad\qquad\qquad$ (2.17)

$r_{ts}$ may be approximated accurately and conservatively as the radius of gyration

of the compression flange plus one-sixth of the web:

$$r_{ts} = \frac{b_f}{\sqrt{12\left(1 + \frac{1}{6}\frac{h t_w}{b_f t_f}\right)}} \qquad\qquad (2.18)$$

---

**User Note:** All current ASTM A6 W, S, M, C and MC shapes except W21×48, W14×99, W14×90, W12×65, W10×12, W8×31, W8×10, W6×15, W6×9, W6×8.5 and M4×6 have compact flanges for Fy = 50 ksi (345 MPa); all current ASTM A6 W, S, M, HP, C and MC shapes have compact webs at Fy ≤ 70 ksi (485 MPa)

---

# CHAPTER 3:

# EFFECTIVE LENGTH APPROACH AND HAND CALCULATIONS OF GEOMETRIC PROPERTIES

### 3.1 INTRODUCTION

In this chapter full details will be provided on calculations of geometrical properties of the selected slender sections becoming to class 4 as per EC4. Determining the resistance (or strength) of structural steel components requires the designer to consider firstly the cross-sectional behaviour and secondly the overall member behaviour. Clauses 5.5.1 and 6.2 cover the cross-sectional aspects of the design process. Whether in the elastic or inelastic material range, cross-sectional resistance and rotation capacity is limited by the effects of local buckling.

As this research work is devoted to the study of the elastic and inelastic buckling behaviour of slender section of class 4, more interest in the theoretical back ground of such type of sections will be discussed.

### 3.2 DESIGN OF THE CROSS SECTIONS TO EC3

### 3.2.1 Introduction

In Eurocode 3, cross-sections are placed into one of four behavioural classes depending upon the material yield strength, the width-to-thickness ratios of the individual compression parts (e.g. webs and flanges) within the cross-section, and the loading arrangement.

➢ Class 1 cross-sections are those which can form a plastic hinge with the rotation capacity required from plastic analysis without reduction of the resistance.

➢ Class 2 cross-sections are those which can develop their plastic moment resistance, but have limited rotation capacity because of local buckling.

➢ Class 3 cross-sections are those in which the elastically calculated stress in the extreme compression fibre of the steel member assuming an elastic distribution of stresses can reach the yield strength, but local buckling is liable to prevent development of the plastic moment resistance.

➢ Class 4 cross-sections are those in which local buckling will occur before the attainment of yield stress in one or more parts of the cross-section.

N.B The classifications from BS 5950 of plastic, compact, semi-compact and slender are replaced in Eurocode 3 with Class 1, Class 2, Class 3 and Class 4, respectively[De Gardner et al,2010].

### .3.2.2 Behavioural classes

The moment–rotation characteristics of the four classes are shown in Figure 4.1.

Class 1 cross-sections are fully effective under pure compression, and are capable of reaching and maintaining their full plastic moment in bending (and may therefore be used in plastic design).

Class 2 cross-sections have a somewhat lower deformation capacity, but are also fully effective in pure compression, and are capable of reaching their full plastic moment in bending.

Class 3 cross sections are fully effective in pure compression, but local buckling prevents attainment of the full plastic moment in bending; bending moment resistance is therefore limited to the (elastic) yield moment.

For Class 4 cross-sections, local buckling occurs in the elastic range. An effective cross-section is therefore defined based on the width-to-thickness ratios of individual plate elements, and this is used to determine the cross-sectional resistance. In hot-rolled design the majority of standard cross-sections will be Class 1, 2 or 3, where resistances may be based on gross section properties obtained from section tables. Effective width formulations are not contained in Part 1.1 of Eurocode 3, but are instead to be found in Part 1.5; these are discussed later in this section.

It must be notated that both compression parts include every part of a cross-section which is either totally or partially in compression under the load combination considered.

The various compression parts in cross-section such as web or flange can be in different classes as per EC3.
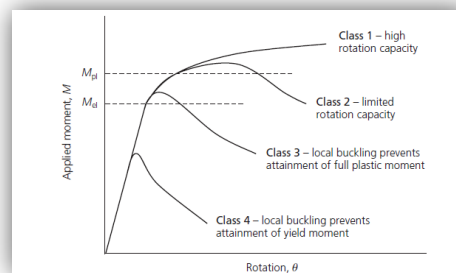


**Figure 3.1 The four behavioural classes of cross-section defined by Eurocode 3[De Gardner et al, 2010]**

### 3.3 Class 4 cross-sections according to EC3

### 3.3.1 General

For class 4 cross-sections it is assumed that parts of the area under compression due to local instability phenomena do not have any resistance (lost area): typically, the compressed portions of the cross-sections, which have to be neglected for the resistance checks, are the parts close to the free end of an outstand flange or the central part of an internal compressed element. It is worth to note that the design principles of Class 4 sections are very specific and usually more difficult than for normal sections. The local buckling of cross sections affects their resistance and rotation capacity and must be considered in design. The evaluation of the influence of local buckling of a cross section on

the resistance or ductility of a steel member is complex. Consequently, a deemed-to-satisfy approach was developed in the form of cross section classes that greatly simplify the problem.

### 3.3.2 Class 4 to EC3

Class 4 cross-sections (see clause 6.2.2.5 of EC3) contain slender elements that are susceptible to local buckling in the elastic material range. It is well-known that allowance for the reduction in resistance of Class 4 cross-sections as a result of local buckling is made by assigning effective widths to the Class 4 compression elements see Chapter 1.

The formulae for calculating effective widths are not contained in Part 1.1 of Eurocode 3; instead, the designer is directed to Part 1.3 for cold-formed sections, to Part 1.5 for hot-rolled and fabricated sections, and to Part 1.6 for circular hollow sections. The calculation of effective properties for Class 4 cross-sections is described in detail in Section 6.2.2 of this guide [De Gardner et al,2010].

### 3.3.3 Load type effect on the classification under combined bending and axial force

Cross-sections subjected to combined bending and compression should be classified based on the actual stress distribution of the combined loadings. For simplicity, an initial check may be carried under the most severe loading condition of pure axial compression; if the resulting section classification is either Class 1 or Class 2, nothing is to be gained by conducting additional calculations with the actual pattern of stresses. However, if the resulting section classification is Class 3 or 4, it is advisable for economy to conduct a more precise classification under the combined loading.

Once again, for checking against the Class 1 and 2 cross-section slenderness limits, a plastic distribution of stress may be assumed, whereas an elastic distribution may be assumed for the Class 3 limits. To apply the classification limits from Table 5.2 (EC3) for a cross-section under combined bending and compression first requires the calculation of  (for Class 1 and 2 limits) and (for Class 3 limits), where  is the ratio of the compressed width to the total width of an element and is the ratio of end stresses (Figure 3.2).

$$\alpha = \frac{1}{c_w}\left(\frac{h}{2} + \frac{1}{2}\frac{N_{Ed}}{t_w f_y} - (t_f + r)\right) \leq 1$$

where $c_w$ is the compressed width of the web (see Figure 3.2) and $N_{Ed}$ is the axial compression force; use of the plastic stress distribution also requires that the compression flange is at least Class 2.

The ratio of end stresses (required for checking against the Class 3 limits) may be determined by superimposing the elastic bending stress distribution with the uniform compression stress distribution

Design rules for verifying the resistance of structural components under combined bending and axial compression are given in clause 6.2.9 for cross-sections and clause 6.4.3 for members. An example demonstrating cross-section classification for a section under combined bending and compression is given below [De Gardner et al, 2010].
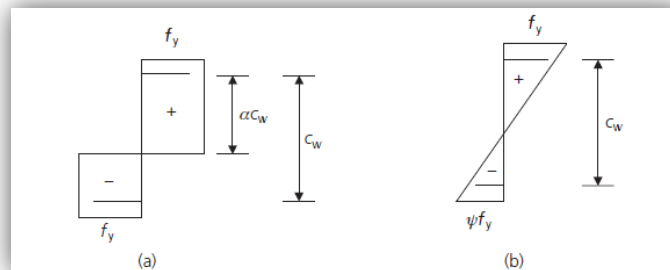


**Figure 3.2. Definitions of  and for classification of cross-sections under combined bending and compression. (a) Class 1 and 2 cross-sections. (b) Class 3 cross-sections EC3 [De Gardner et al, 2010]**

### 3.4 Principles of effective width calculation

To determine the resistance of Class 4 cross sections subject to direct stresses by using the effective width method, the $effective^p$ widths of each plate element in compression are calculated independently. Based on these $effective^p$ widths effective effective geotrical properties of cross section are calculated : $A_{eff}$, $I_{eff}$ and $W_{eff}$ are calculated (see Fig.3.3 , Fig.3.4 , Fig3.5).

**Compression :** For compression elements the effective widths are determined by taking into account the combined effect of shear lag and plate buckling.

**Tension :** For tension elements, $effective^s$ widths come only from shear lag effects. Tension elements without shear lag effects are taken as fully effective. *The effective cross section is then treated as an equivalent Class 3 cross section,* with the assumption of a linear elastic strain and stress distribution over the reduced cross section. The ultimate resistance is reached with the onset of yielding in the centre of the compressed plate located furthest from the centroid of the cross section.

The maximum stress may be calculated in the mid-plane of the critical plate – for I girders, for instance in the mid-plane of flanges (see Fig.4.3).

**Combined loadings:** If axial force and bending moment act simultaneously, the calculation of effective widths may be based on the resulting stress distribution. EN 1993-1-5 allows a simplified approach where $A_{eff}$ is calculated only for stresses due to pure compression and $W_{eff}$ only for stresses due to pure bending.

In non-symmetrical cross sections subject to an axial force $N_{ed}$, a shift $e_N$ occurs (of the centroid $G'$ of the effective area $A_{eff}$ relative to the centre of gravity of the gross cross section $G$, see Fig.4.4). This shift results in an additional bending moment $\Delta M = e_N N_{ed}$ that should be taken into account in the cross-section verification (see section 2.4.6). According to clause 4.3(3) of EN 1993-1-5 the shift $e_M$ (see Fig3.5) of the centre of gravity due to pure bending can be disregarded in the calculation of $\Delta M$, even if the cross section is subject to the combination of axial force and bending moment.

**N. B.** The following material including figures is mainly taken from Beg et al 2012, see bibliography [De Beg, Darko et al, 2012]
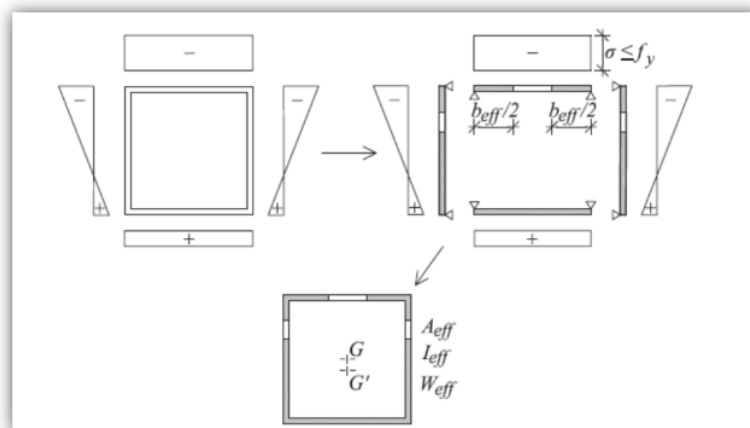


**Figure 3.3: Effective cross section [De Beg, Darko et al, 2012]**
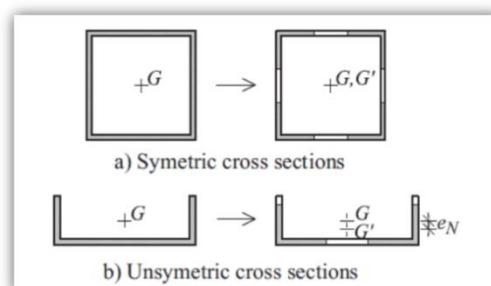


**Figure 3.4: Class 4 cross sections in pure compression [De Beg, Darko et al, 2012]**
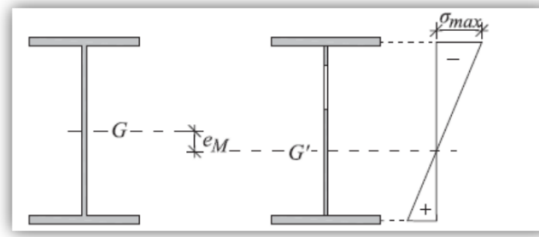
**Figure 3.5: Class 4 cross section in pure bending [De Beg, Darko et al, 2012]**

## 3.5 Iterative procedure

### 3.5.1 General

Generally, the calculation of $effective^p$ widths requires an iterative procedure shown in Fig. 4.6 that ends when the differences between two steps are sufficiently small.
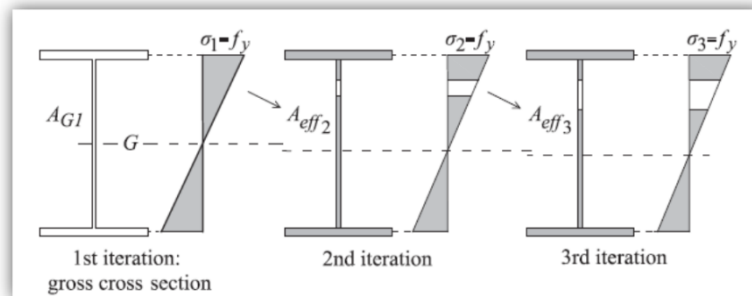


**Figure 3.6 Determination of effective area by iterative procedure [De Beg, Darko et al ,2012]**

The first iteration starts with the stress distribution on the gross cross section AG1. The effective area for the second iteration $A_{eff2}$ is calculated from this stress distribution and the effective area for the third iteration Aeff3 from the stresses on $A_{eff2}$.

### 3.5.2 Step

For I-section and box cross section in bending EN 1993-1-5 allows a simplified approach that ends in two steps.

**In the first step**: effective widths in flanges (if they are in Class 4) are determined from the stress distribution on the gross cross section.

**In the second step**: the stresses are determined on the cross section composed of the $effective^p$ area of the compressed flanges and the gross areas of the web and the tension flanges. The $effective^p$ width in the web is calculated based on these stresses and this is taken as the final result.

### 3.5.3 Cases of stages of construction

When different stages of construction have to be considered, which is a normal case in the design of composite bridges, the following simplified approach proposed in a Note to clause 4.4 (2) of EN 1993-1-5 may be used:

- In all relevant construction stages (e.g. concreting of the slab, normal use of a bridge) the stresses should be calculated on the gross cross section of the web and effective cross section of the flanges (plate buckling and/or shear lag), when relevant.

- The stresses from different construction stages are summed up and used to determine a single effective cross section of the web that is used for all construction stages.

  - Finally, the stresses for individual construction stages are calculated on corresponding effective cross sections and summed up to get the final cumulative stresses [De Beg, Darko et al ,2012].

### 3.6 Effective width implanted in EC3 method for section properties calculation

### 3.6.1. An overview

It is well known that a side supported thin steel plate with aspect ratio $\alpha = a/b \geq 1$ (Fig 3.7) subject to direct loading along in-plane direction tends to buckle at a stress level $\sigma_{cr}$ less than the yield stress $f_y$. However, after $\sigma_{cr}$ is reached, resistance of the plate is not completely exhausted and it shall have sufficient post-buckling strength due to stress redistribution. According to the ultimate resistance of the plate will be reached after yielding occurred at the two supported sides and this will result in final a non-uniform stress distribution $\sigma_{act} < f_y$ (Fig. 3.8). This phenomenon is commonly known as "plate like buckling" and is most obvious for geometrical prefect elastic plate but less remarkable for a realistic imperfect inelastic plate. It is also well known that as the value of $\alpha$ reduces, the post-buckling resistance of the plate will diminish gradually and the 2D plate like buckling behaviour of the plate will change back to the 1D buckling behaviour like a column. Obviously, the non-uniform distribution of $\sigma_{act}$ is not ideal for design of thin plate subjected to direct stress. Hence, in EC3 Part 1-5, two different design methods, namely the effective width method (Fig. 3.8b) and the effective stress (Fig. 3.8c) method are suggested.

In summary, both methods aim to employ uniform stress block for design. While the effective width method reduces the gross width to an appropriate effective width $b_{eff} = \rho. b < b$ that subjected to the constant yield strength f for design (Fig. 4.8b), the effective stress method maintains a uniform stress $\sigma_{equ} = \chi f < f$ along the whole width. The reduction factors ρ and χ are calculated based on the principle of equivalent in-plane force such that

For the effective width method :
$$\int_0^b \sigma_{act}\,dx = b_{eff}f_y = \rho b f_y \qquad (3.1)$$

For the effective stress method :
$$\int_0^b \sigma_{act}\,dx = b \cdot \sigma_{equ} = b\chi f_y = \chi b f_y \qquad (3.2)$$

It is obvious that for a cross section consisting of a single plate, the two methods are equivalent to each another such that (Fig. 3.8b and Fig. 3.8c) $\chi_b f_y = \rho b_{fy}$ and $\chi = \rho$. However, for cross sections that consist of more than one plate element (e.g. an I section), the two methods are not equivalent to each another and the effective stress method are generally more conservative.

It should be noted that EC Part 1-5 can be considered as largely "biased" towards the effective width method as Sections 4 to 7 (16 pages in length) of EC3 Part 1-5 were written based on this method while only Section 10 (2 pages in length) was devoted to describe the design approach if the effective stress method is employed. Hence, in the design of thin-walled structural components like plate girder and box section using EC3, the calculation of effective width of a Class 4 section is one of the most important steps during the section properties calculation [De Lee, Chi-Kinget, 2019].
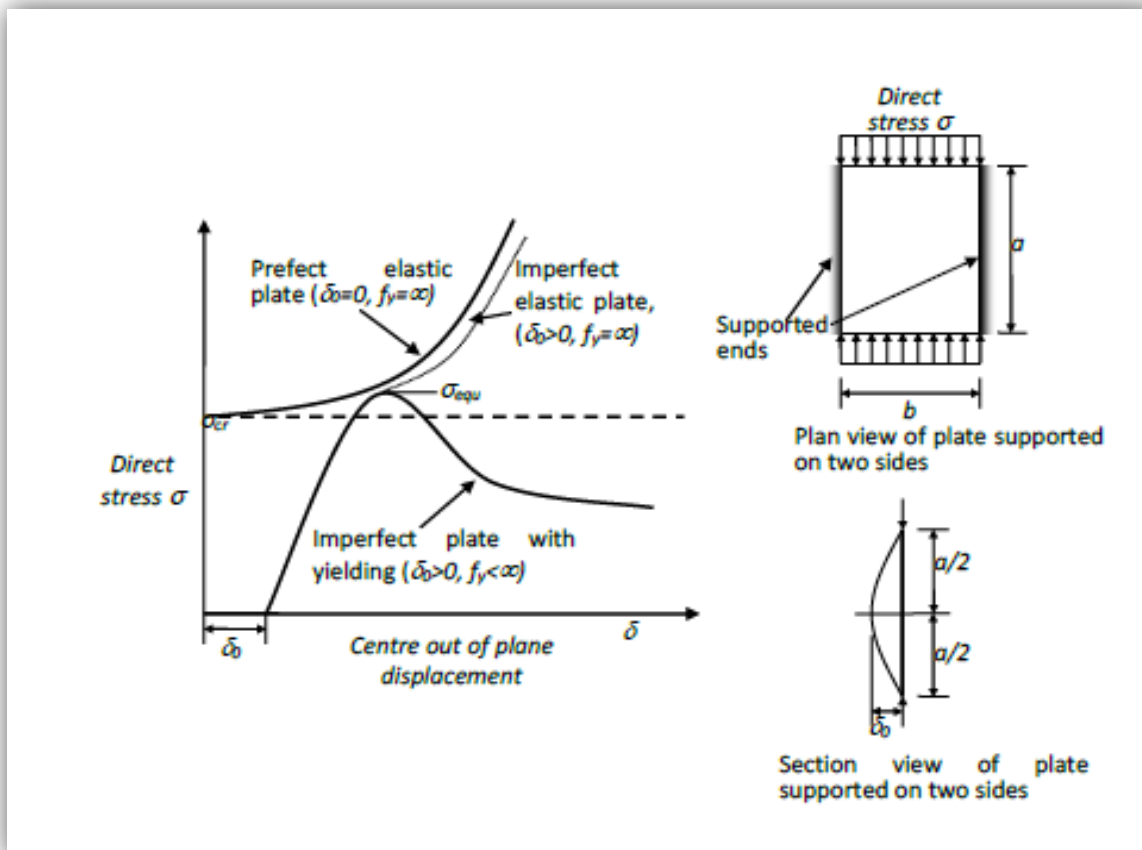


**Figure 3.7Failure of plate with α=a/b >1 subject to in-plane direct loading [De Lee, Chi-Kinget, 2019]**
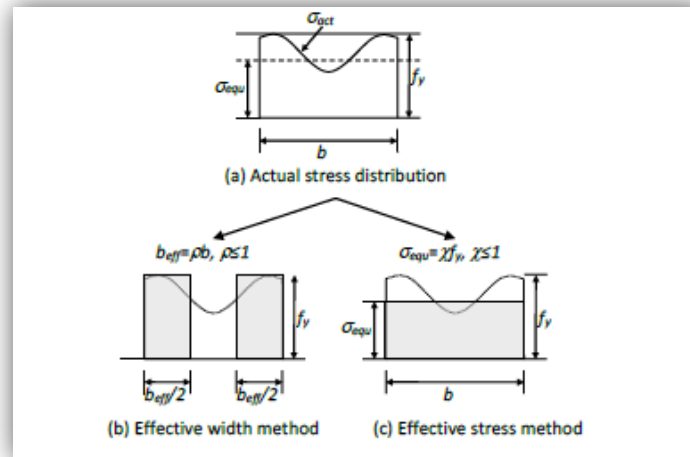
**Figure 3.8 Actual stress distribution at failure, effective width and stress methods [De Lee, Chi-Kinget, 2019]**

### 3.6.2. Effective width calculation procedure

In EC3 Part 1-5, for a given plate element (either supported on a single or on both sides) the effective width reduction factor ρ is solely based on two parameters: (i) $\bar{b}$ /t, the appropriate width ($\bar{b}$) to the plate thickness (t) ratio of the element and (ii) the stress ratio at the two ends $\psi = \sigma_2/\sigma_1$ where $\sigma_2 < \sigma_1$ In general, $\bar{b}$ is the appropriate clear width between the supports of the plate element. $\bar{b}$ is always slightly less than b, the overall width of the plate element, and should be calculated according to the section classification table (Table 5.2) of EC3 [1] and Section 4.4 of [2]. Figs. 3 and 4 respectively show the possible stress distributions for an internal compression element (i.e. the plate is supported at both ends) and an outstanding compression element (i.e. only one end of the plate is supported). Note that in Fig. 3 and Fig. 4, it is assumed that the stress distribution is linear and compressive stress is taken as positive. Furthermore, for $\psi < 0$, the whole plate element is divided into two parts that are under tension and compression respectively with widths equal to $b_t$ and $b_c$, so that $\bar{b} = b_t + b_c$ and $b_c = \bar{b} / (1 - \psi)$ (Fig. 3c, Fig. 4b and Fig. 4d). In general, the effective parts of the plate element consist of those parts that are either under tensile stress (i.e. the stress is negative) or those compressive parts that locate near the supported ends where local buckling is prevented to occur. Once the values of $\bar{b}$ /t and $\psi = \sigma_2/\sigma_1$ are known, the effective width of the plate element could be computed by using the following steps [De Lee, Chi-Kinget, 2019].

### Table 3.1 Calculation of $k_\sigma$ [De Lee, Chi-Kinget, 2019]

| Internal compression part (Fig. 3) | |
|---|---|
| Range of $\psi$ | $k_\sigma$ |
| $-3 \leq \psi < -1$ (Fig. 3c) | $5.98(1-\psi)^2$ |
| $-1 \leq \psi < 0$ (Fig. 3c) | $7.81 - 6.29\psi + 9.78\psi^2$ |
| $0 \leq \psi \leq 1$ (Figs. 3a and 3b) | $8.2/(1.05+\psi)$ |
| Outstand compression part with high stress at supported ends (Figs. 4a and 4b) | |
| Range of $\psi$ | $k_\sigma$ |
| $-1 \leq \psi < 0$ (Fig. 4b) | $1.7 - 5\psi + 17.1\psi^2$ |
| $1 \leq \psi \leq 0$ (Fig. 4a) | $0.578/(\psi+0.34)$ |
| Outstand compression part with lower stress at supported ends (Figs. 4c and 4d) | |
| Range of $\psi$ | $k_\sigma$ |
| $1 \leq \psi < -3$ (Figs. 4c and 4d) | $0.57 - 0.21\psi + 0.07\psi^2$ |

- Use the equations listed in Table 1 to calculate the buckling factor $k_\sigma$ according to the stress ratio $\psi$ for different stress distributions shown in Fig 3.9 and Fig 3.10.

- Compute the plate slenderness $\bar{\lambda}_p$ ratio such that

$$\bar{\lambda}_p = \frac{h_w/t_w}{28.4\,\varepsilon\,\sqrt{K_\sigma}} \rightarrow \varepsilon = \sqrt{\frac{235}{f_y}} \qquad (3.3)$$

- Calculate the reduction factor ρ for the compressive part of the element such that (EC3 Part 1-5, Equations. 3.2 and 3.3) For an internal plate element (Fig.3.10):

$$\rho = \frac{\bar{\lambda}_p - 0.055(3+\psi)}{\bar{\lambda}_p^2} \leq 1.0 \text{ and } \bar{\lambda}_p > 0.5 + \sqrt{0.085 - 0.055\psi}$$

$$(3.4)$$

- For an outstanding plate element (Fig. 4):

$$\rho = \frac{\bar{\lambda}_p - 0.188}{\bar{\lambda}_p^2} \leq 1.0 \text{ and } \bar{\lambda}_p > 0.784$$

$$(3.5)$$

- Calculate $b_{eff}$ , the effective width for the compressive part of the plate element, (Fig. 3.9 and Fig. 3.10)

$$\text{For } \psi \geq 0: \quad b_{eff} = \rho b$$

$$\text{For } \psi < 0: \quad b_{eff} = \frac{\rho \bar{b}}{(1-\psi)} = \rho b_c$$

(3.6)

Note that for the case of an internal compression element with ψ≥0 (i.e. the whole plate element is under compression), the effective width of the element be $b_{eff}$ is further divided into two parts (Figs. 3(a) and 3(b)) with width $b_{e1}$ and $b_{e2}$ such that $b_{e1} + b_{e2} = b_{eff}$ . The relative sizes of be1 and be2 are defined in Fig 3.10.

• Finally, the total effective width of the whole plate elements is computed as $b_{eff}$ (Fig 3.9a, Fig 3.10a and Fig 3.9c) for ψ≥0 when the whole plate element is under compression or $b_{eff} + b_t$ forψ.
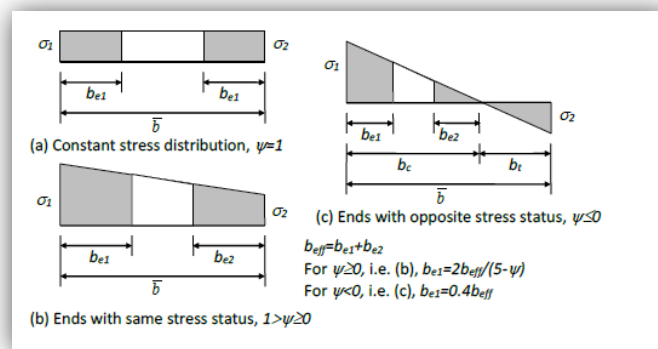


**Figure 3.9 Stress distribution and effective width for internal compression elements (i.e. both ends supported), effective part of the plate is shaded Note: Compressive stress is positive with$\sigma_2 < \sigma_1$. [De Lee, Chi-Kinget, 2019]**
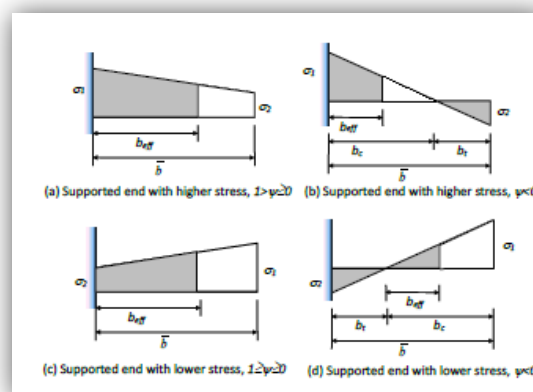


**Figure 3.10 Stress distribution and effective width for outstand compression elements (i.e. only end supported), effective part of the plate is shaded. [De Lee, Chi-Kinget, 2019]**

### 3.7 Full iteration calculation procedure for class 4 section properties calculation

➢ By assuming the whole section is effective, calculate the gross section properties ($G_{gross}$, $A_{gross}$ and $I_{gross}$).

➢ Set $G_{eff} = G_{gross}$, $A_{eff} = A_{gross}$, $I_{eff} = I_{gross}$ and $\Delta y = \Delta z = 0$.

➢ Base on the stress ratio$\psi$, determine the effective area of all plate elements by using Table 3.1 and Fig.3.9 and Fig.3.10.

➢ Compute the new centroid of the effective area $\grave{G}_{eff}$ and the corresponding effective area $\grave{A}_{eff}$ and effective second moment of area $\grave{I}_{eff}$ .

➢ Determine the shift of the centroid $G_{eff}$ - $\grave{G}_{eff}$ =($\Delta y$, $\Delta z$) and the relative change of effective area and effective second moment of area such that

$$S_G(\%) = \frac{\sqrt{\Delta y^2 + \Delta y^2}}{min(b,h)} \times 100\%$$

(3.7)

$$C_A(\%) = \frac{|A_{eff} - A_{eff}'|}{A_{eff}} \times 100\% \quad and \quad C_I(\%) = \frac{|I_{eff} - I_{eff}'|}{I_{eff}} \times 100\%$$

(3.8)

where b and h in Equation 10a is the overall width and depth of the section.

➢ Update the section properties so that $G_{eff} \leftarrow \grave{G}_{eff}$, $A_{eff} \leftarrow \grave{A}_{eff}$ and $I_{eff} \leftarrow \grave{I}_{eff}$.

➢ Check for convergence of the section properties: The section

properties are assumed to be converged if the following criteria are satisfied.

$S_G \leq S_{tol}$ $\qquad\qquad\qquad$ $C_A \leq C_{Atol}$ $\qquad\qquad\qquad$ $C_I \leq C_{Itol}$ .

where $S_{tol}$ , $C_{Atol}$ and $C_{Itol}$ are tolerances for the convergences of $G_{eff}$, $A_{eff}$ and $I_{eff}$, respectively.

➢ If the section properties are converged, output the value of $G_{eff}$, $A_{eff}$ and $I_{eff}$ and stop. Otherwise, go to step. [De Lee, Chi-Kinget, 2019]

### 3.8 Section properties calculation examples

### 3.8.1 General

In the present study, sections, three sections: S1, S2 and S3 will be designed with different flange thicknesses. All sections are being bi-symmetric. The design procedure concern beams which

are predominantly loaded in bending, that is, where axial loads, if any, are small and transverse shear forces are not excessive. In all models, the elastic analysis of simply supported beams undergoing uniformed transverse load is carried out.

All members subject to bending should be checked for the following at critical sections:

      (a)     A combination of bending and shear force

      (b)     Deflection

      (c)     Lateral restraint

      (d)     Local buckling

      (e)     Web bearing and buckling.

The application of a theoretical treatment of the problem would be too complex for routine design so a combination of theory and test results is required to produce a reliable (safe) design approach.

Before considering the analysis of the problem, it is useful to attempt to gain an insight into the physical behaviour by considering a simplified model. Since bending of an I-section beam is resisted principally by the tensile and compressive forces developed in two flanges, as shown in Figure 3.11, the compression flange may be regarded as a strut.

Generally, compression members buckle in the weaker direction i.e. the flange buckles downwards. However, this is prevented by the presence of the web. Therefore the flange is forced to buckle sideways, which will induce some degree of twisting in the section as the web too is required to deform. Whilst this approach neglects the real influence of torsion and the role of the tension flange, it does approximate the behaviour of very deep girders with very thin webs or of trusses or open web joists. Indeed, early attempts at analysing lateral-torsional buckling started with this approach [Abutair. Baker Wael].
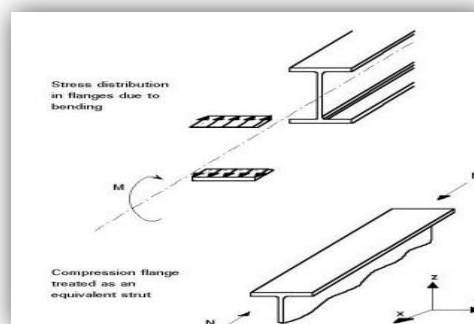


**Figure 3.11 the analogy and approximation of beam buckling problem as a strut problem [Abutair. Baker Wael, 2017]**

### 3.8.2 Case 1 studied

Once again, we will present only one type of cross section will be studied with different thickness of flanges for a single spanned beam, supported at both ends.

### 3.8.3 Sections bi-symmetric

The beam with the bi-symmetric I-section chosen to be modelled will be made of elastic material, with E = 210 Gpa and $v = 0.4$. The beam length is L = 20 m.

The beam will be subjected to a uniform distributed load along of the beam, with different position of load.
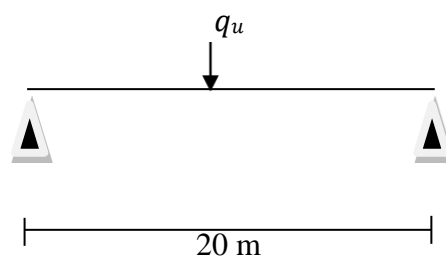


**Figure 3.12 Beam with supports under uniform distributed load**

M(x) > 0

$$M(x) = q_{ell} \cdot \frac{X}{2}$$

$$x = \frac{L}{2} \rightarrow M(x = \frac{L}{2}) = q_{ell} \cdot \frac{X}{2} = M_{max}(x) = q_{ell} \cdot \frac{L}{4}$$

L20 m; S355 → $f_y$ =355 Mpa → $f_u$ = 470 Mpa or 510 Mpa
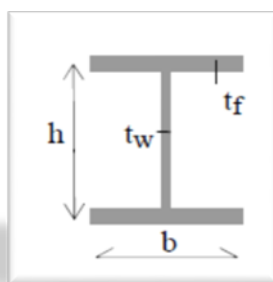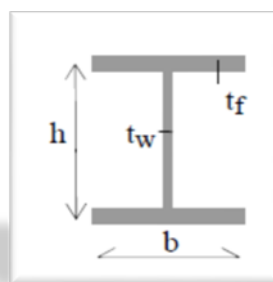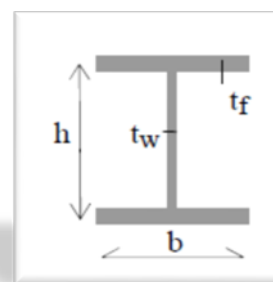


|  a) Section 1 | b) Section 2 | c) Section 3 |
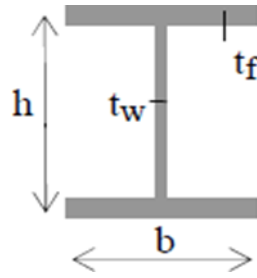
**Figure 3.13 bi-symmetric cross-section of the beam (elastic)**

### 3.8.4 Pre-defining

$h_w = \frac{1}{15}. L = \frac{1}{15} . 20000 = 1300$ mm

$t_w = \frac{1}{130} . h_w = \frac{1}{130} . 1300 = 10$ mm

$b = \frac{hw}{5.2} = \frac{1300}{5.2} = 250$ mm

$t_{f1} = \frac{1}{12.5} . b = \frac{1}{12.5} . 250 = 20$ mm

$t_{f2} = \frac{1}{20} . b = \frac{1}{20} . 250 = 12$ mm

$t_{f3} = \frac{1}{25} . b = \frac{1}{25} . 250 = 10$ mm

### 3.8.5 Geometrical proprieties (section 1)

➢ **Cross-sectional area**

$A_1 = h. t_w + 2b. t_{f1} = (1300. 10) + (2.250.20) = 23000 \ mm^2 = 230 \ cm^2$

➢ **Moment of inertia**

$I_{y1} = \frac{bH^3 - ( b - t_w ). h^3}{12} = \frac{250.1340^3 - (250 - 10).1300^3}{12} = 6187166667 \ mm^4 = 618716.66 \ 67 cm^4$

$I_{z1} = \frac{2 \ b^3. t_{f1} + h. tw^3}{12} = \frac{2.250^3. \ 20 \ + \ 1300.10^3}{12} = 52191666.67 \ mm^4 = 5219.1667 \ cm^4$

➢ **Elastic resistance modulus**

$Wel_{y1} = 2. \frac{I_{y1}}{H} = 2. \frac{618716.6667}{134} = 9234.5771 \ cm^3$

➢ **Elastic moment**

$Mel_{y1} = Wel_{y1} . f_y = 9234.5771. 3550 = 32782748.7100$ dan. cm = 3278.2749 KN. m

➢ **Inertia of torsion**

$I_{t1} = \frac{1}{3}$ (h. $tw^3$ + 2b. $t_{f1}^3$) = $\frac{1}{3}$ (1300. $10^3$ + 2.250. $20^3$) = 1766666.6670 $mm^4$ = 176.6667 $cm^4$

➢ **Factor of warping**

$I_{w1} = I_{z1} * (\frac{H - t_{f1}}{2})^2 = 52191666.67 * (\frac{1340 - 20}{2})^2 = 2.273469. 10^{13} \ mm^6 = 22734690 \ cm^6$

➢ **Shear modulus**

$$G = \frac{E}{2\,(1+\vartheta\,)} = \frac{210000}{2\,(1+0.3\,)} = 80769.2308 \text{ Mpa}$$

**Table 3.2 Section 1 e p (with thickness of flange =20 mm)**

| CHARACTERISTIC GEOMETRIC | $A_1$ [$cm^2$] | $I_{y1}$ [$cm^4$] | $I_{z1}$ [$cm^4$] | $Wel_{y1}$ [$cm^3$] | $Mel_{y1}$ [KN.m] | $I_{t1}$ [$cm^4$] | $I_{w1}$ [$cm^6$] | G [Mpa] | E [Mpa] |
|---|---|---|---|---|---|---|---|---|---|
| Section 1 | 230 | 618716.667 | 5219.167 | 9234.577 | 3278.275 | 176.667 | 22734690 | 80769.231 | 210000 |

**Table 3.3 Section 2 (with thickness of flange =12 mm)**

| CHARACTERISTIC GEOMETRIC | $A_2$ [$cm^2$] | $I_{y2}$ [$cm^4$] | $I_{z2}$ [$cm^4$] | $Wel_{y2}$ [$cm^3$] | $Mel_{y2}$ [KN.m] | $I_{t2}$ [$cm^4$] | $I_{w2}$ [$cm^6$] | G [Mpa] | E [Mpa] |
|---|---|---|---|---|---|---|---|---|---|
| Section 3 | 190 | 441292.133 | 3135.833 | 6666.044 | 2366.446 | 72.1333 | 13494619.59 | 80769.231 | 210000 |

**Table 3.4 Section 3 (with thickness of flange =10 mm)**

| CHARACTERISTIC GEOMETRIC | $A_3$ [$cm^2$] | $I_{y3}$ [$cm^4$] | $I_{z3}$ [$cm^4$] | $Wel_{y3}$ [$cm^3$] | $Mel_{y3}$ [KN.m] | $I_{t3}$ [$cm^4$] | $I_{w3}$ [$cm^6$] | G [Mpa] | E [Mpa] |
|---|---|---|---|---|---|---|---|---|---|
| Section 3 | 180 | 397600 | 2615 | 6024.242 | 2138.606 | 60.000 | 11219003 | 80769.231 | 210000 |

### 3.8.6 Classifications of the used sections

➢ **Web**

✓ **Section 1**

$$\frac{d}{t_w} \le 124\,\varepsilon \rightarrow \varepsilon = 0.81$$

$$\frac{1300}{10} = 130 \ge 100.44 \rightarrow classe04$$

✓ **Section 2**

$$\frac{d}{t_w} \le 124\,\varepsilon \rightarrow \varepsilon = 0.81$$

$$\frac{1300}{10} = 130 > 100.44 \rightarrow classe04$$

✓ **Section 3**

$$\frac{d}{t_w} \le 124\,\varepsilon \rightarrow \varepsilon = 0.81$$

$$\frac{1300}{10} = 130 \ge 100.44 \rightarrow classe04$$

➢ **Flange**

$C = \frac{250}{2} - \frac{10}{2} = 120$ mm

✓ **Section 1**

$\frac{c}{t_{f1}} \le 9\,\varepsilon \to \varepsilon = 0.81$

$\frac{120}{20} = 6 \le 9\,\varepsilon = 7.44 \to$ *classe 01*

✓ **Section 2**

$\frac{c}{t_{f2}} \le 14\,\varepsilon \to \varepsilon = 0.81$

$\frac{120}{12} = 10 \le 14\,\varepsilon = 11.34 \to$ *classe 3*

✓ **Section 3**

$\frac{c}{t_{f3}} \le 14\,\varepsilon \to \varepsilon = 0.81$

$\frac{120}{10} = 12 > 14\,\varepsilon = 11.34 \to$ *classe 4*

### 3.8.7 Determining the elastic loading acing on the beam

$Mel_{y1} = M_{max} = \frac{q_1\,L}{4}$         for the section 1.

$3278.275 = \frac{q_1.20}{4} \to q_1 = 655.656$ KN /m

| Section 1 | $q_1 = 655.656$ KN /m |
|-----------|------------------------|
| Section 2 | $q_2 = 473.289$ KN /m |
| Section 3 | $q_3 = 427.721$ KN /m |

### 3.8.8 Case 2 studied

Once again, we will present one type of cross section will be studied with different thickness of flanges for a single spanned beam, supported at both ends.

### 3.8.9   Sections bi-symmetric

The beam with the bi-symmetric I-section chosen to be modelled will be made of effective material, with E = 210 Gpa and 9 = 0.4. The beam length is L = 20 m.

The beam will be subjected to a uniform distributed load along of the beam, with different position of load.
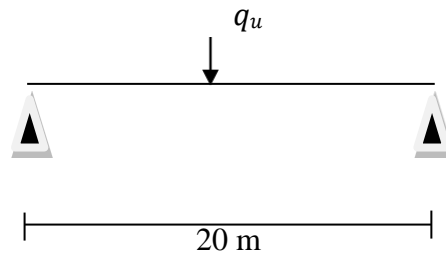
**Figure 3.14 Beam with supports under uniform distributed load**
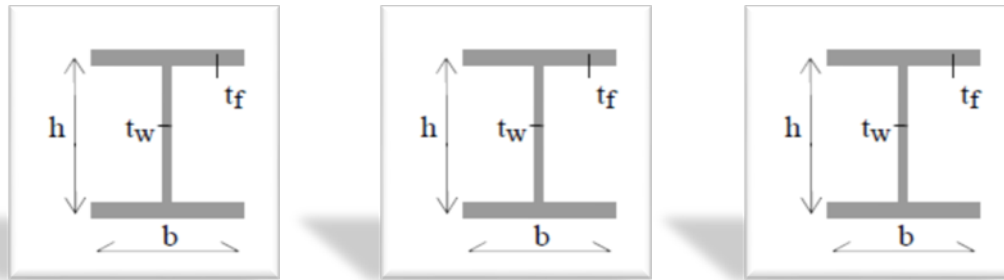


a) **Section 1**                              b) **Section 2**                              c) **Section 3**
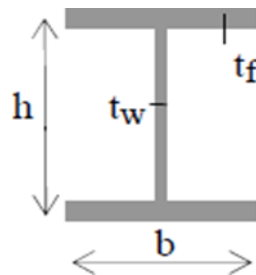


**Figure 3.15 bi-symmetric cross-section of the beam (elastic)**

$M(x) > 0$

$M(x) = q_{eff} \cdot \dfrac{X}{2}$

$x = \dfrac{L}{2} \rightarrow M(x = \dfrac{L}{2}) = q_{eff} \cdot \dfrac{X}{2} = M_{max}(x) = q_{eff} \cdot \dfrac{L}{4}$

L20 m; S235 $\rightarrow f_y = 235$ Mpa $\rightarrow f_u = 360$ Mpa or 510 Mpa

### 3.8.10 Geometrical proprieties effective (section 3)

The gross section properties of the section are given by: $h_w$=1300mm, $t_w$=10mm, $A_{gross}$=18000 $mm^2$ , $I_{gross}$=397600.000 $mm^4$ and $W_{el}$=6024.242 $mm^3$

➢     **Flange**

✓     Determine the stress ratio, ψ:

From Table 4 of EN 1993-1-5, the buckling factor ψ = +1, $K_\sigma$ =0.43

✓     The normalized slenderness ratio $\bar{\lambda}_p$ is given by

$$\bar{\lambda}_p = \frac{c/t}{28.4\ \varepsilon\ \sqrt{K_\sigma}} = \frac{120/10}{28.4.\ 0.81.\ \sqrt{0.43}} = 0.795$$

$$\bar{\lambda}_p > 0.673$$

✓     The reduction factor ρ for an internal compression member is given by

$$\rho = \frac{\overline{(\lambda_p} - 0.22\ )}{\bar{\lambda}_p{}^2} = 0.910$$

✓     The effective depth $b_{eff}$ is given by

$$b_{eff3} = \rho.\ c = 0.910.\ 120 = 109.2$$

➤     **WEB SECTION**

✓     **First iteration**

        ❖   Calculation of effective area, $A_{eff3}$

✓     Determine the stress ratio, ψ:

   From Table 4.1 of EN 1993-1-5, the buckling factor $K_\sigma = 23,9$ for ψ = −1,0.

✓     The normalized slenderness ratio $\bar{\lambda}_p$ is given by

$$\bar{\lambda}_p = \frac{h_w/t_w}{28.4\ \varepsilon\ \sqrt{K_\sigma}} = \frac{1300/10}{28.4.\ 0.81.\ \sqrt{24.9}} = 1.156\ \ > \ \ 1.08$$

✓     The reduction factor ρ for an internal compression member is given by

$$\rho = \frac{\bar{\lambda}_p - 0.055(3+\psi\ )}{\bar{\lambda}_p{}^2} = \frac{1.156 - 0.055(3-1\ )}{1.156^2} = \ 0.783$$

✓     The effective depth $b_{eff}$ is given by

$$b_{eff}\ = \frac{\rho h_w}{1 - \psi} = \frac{0.784.1300}{1 - (-1)} = 508.95 \text{ mm}$$

✓     The depth of web left at the top $b_{e1}$:

$$b_{e1} = 0.4\ b_{eff} = 0.4 \times 508.95 = 204.58 \text{ mm}$$

✓     The depth of web left at the bottom (above the centroidal axis), be2:

$$b_{e2} = 0.6\ b_{eff} = 0.6 \times 508.95 = 305.37 \text{ mm}$$

✓     The ineffective portion of web has a length

$$l_w = \text{x} = \frac{h_w}{2}\ - \ b_{e1} - \ b_{e2} = 650 - 204.58 - 305.37 = 141.05 \text{ mm}$$

✓     The net loss of area of the web, $A_w$ is given by

✓     $A_w = \ l_w.t_w = 141.05.\ 10 = 1410.50\ mm^2$

- ✓ Effective area of section, $A_{eff}$:

$A_{eff3} = A - A_w = 18000\text{-}1410.50 = 16589.50 \ mm^2 = 165.895 \ cm^2$

$C_A(\%) = \frac{|A_{eff} - A_{eff'}|}{A_{eff}} \times 100\% \rightarrow C_A(\%) = 7.84\% > 0.1\%$
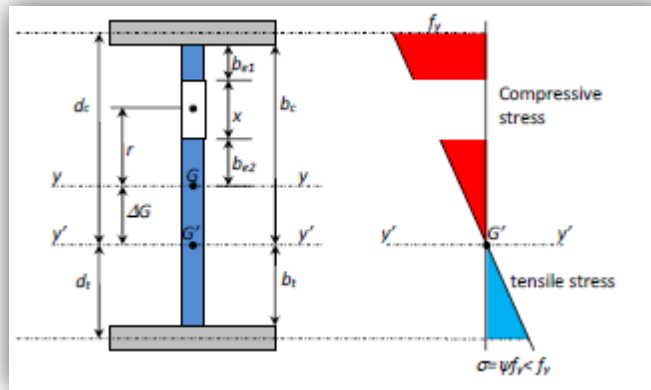


❖ **Figure 3.16 Calculation of effective cross section.** [Lee, Chi-King & Chiew, Sing-Ping, 2019]

- ✓ Calculation of $A_{eff3}$ Position of effective centroid, $z_{eff}$:

r $= \frac{hw}{2} - b_{e1} - \frac{x}{2} = \frac{1300}{2} - 204.58 - \frac{141.05}{2} = 375.89$mm

r. $A_w + A_{eff}. \Delta G = 0$ or $\Delta G = \frac{-375.89. \ 1410.50}{16589.50} = \text{-}31.96$mm

Note, $z_{eff,prev}$ is the neutral axis position at the previous iteration.

For the first iteration, $z_{eff,prev} = h/2$

- ✓ Effective second moment of area, $I_{eff3}$

$I_{eff3} = I_{gross} + A \ (\Delta G)^2 - (\frac{x^3.tw}{12} + A_w \ (r + \Delta G)^2 )$

$= 397600.10^4 + 18000(31.96)^2 - (\frac{141.05^3.10}{12} + 1410.50 \ (375.89 \ 31.96)^2 )$

$= 3757422587 \ mm^4 = 375742.259 \ cm^4$

$C_I \ (\%) = \frac{|I_{eff} - I_{eff'}|}{I_{eff}} \times 100\% = \frac{|397600 - 375742.259 \ |}{397600} \times 100\% \rightarrow C_I = 5.49\% > 0.1\%$

$d_c = \frac{hw}{2} + \frac{tw}{2} - \Delta G = 650 + 5 + 31.96 = 686.96$ mm

$d_t = \frac{hw}{2} + \frac{tw}{2} + \Delta G = 650 + 5\text{-}31.96 = 624.04$ mm

- ✓ The lesser elastic section modulus $W_{eff}$ is given as

$W_{eff3} = \frac{I_{eff3}}{d_c} = \frac{375742.259}{68.696} = 5469.638 \ cm^3$

Since both $C_A$ and $C_I$ >0.1%, further iteration is carried out.

✓ Effective moment

$Meff_3 = Weff_3 . f_y = 19417214.9$ dan .cm

=1941721490 N. cm = 1941.721 KN. cm

✓ <u>Second iteration</u>

❖ Calculation of effective area, $A_{eff}$

✓ Determine the stress ratio, ψ:

$$\Psi = - \frac{(\frac{h_w}{2} - \Delta G)}{(\frac{h_w}{2} + \Delta G)} = - \frac{(\frac{1300}{2} - 31.96)}{(\frac{1300}{2} + 31.96)} = -0.906$$

$K_\sigma = 7.81 - 6.29\psi + 9.78\ \psi^2 = 21.536$

✓ The normalized slenderness ratio $\bar{\lambda}_p$ is given by

$$\bar{\lambda}_p = \frac{h_w/t_w}{28.4\ \varepsilon\ \sqrt{K_\sigma}} = \frac{1300/10}{28.4.\ 0.81.\ \sqrt{21.536}} = 1.218\ >\ 1.08$$

✓ The reduction factor ρ for an internal compression member is given by

$$\rho = \frac{\bar{\lambda}_p - 0.055(3 + \psi)}{\bar{\lambda}_p{}^2} = \frac{1.218 - 0.055(3 - 0.906)}{1.218^2} = 0.743$$

✓ The effective depth $b_{eff}$ is given by

$b_c = hw\ /2 + \Delta G = 1300/2 + 31.96 = 681.96$ mm

$b_{eff} = \rho.\ b_c = 0.744.\ 681.96 = 506.70$ mm

✓ The depth of web left at the top $b_{e1}$:

$b_{e1} = 0.4\ b_{eff} = 0.4 \times 506.70 = 202.68$ mm

✓ The depth of web left at the bottom (above the centroidal axis), be2:

$b_{e2} = 0.6\ b_{eff} = 0.6 \times 506.70 = 304.02$ mm

✓ The ineffective portion of web has a length

$l_w = x = b_c - b_{e1} - b_{e2} = 681.96 - 202.68 - 304.02 = 175.26$ mm

✓ The net loss of area of the web, $A_w$ is given by

$A_w = l_w.t_w = 175.26.10 = 1752.60$ mm$^2$

✓ Effective area of section, $A_{eff}$:

$A_{eff3}$ = A $- A_w$ = 18000-1752.60 = 16247.40$mm^2$

$C_A(\%) = \frac{|A_{eff3}-A_{eff3}{}'|}{A_{eff3}} \times 100\% \rightarrow C_A(\%) = \frac{|16589.50-16247.40|}{16589.50} \times 100\%$ $C_A(\%)$

$\qquad$ = 2.06 % > 0.1%

$\qquad$ ❖ Calculation of $A_{eff3}$

✓ $\qquad$ Position of effective centroid, $z_{eff}$:

$\qquad$ r = $\frac{hw}{2}$ - $b_{e1} - \frac{x}{2} = \frac{1300}{2}$ - 202.68 $- \frac{175.26}{2}$ = 359.69mm

$\qquad$ r. $\varDelta A + A_{eff}.\Delta G$=0 or $\Delta G$ =- $\frac{359.69. \ 1752.60}{16247.40}$ = -38.80mm

This means that shift of G' to G''=(-31.96–(-38.80))= 6.84mm (downward)

$\qquad$ Note, $z_{eff,prev}$ is the neutral axis position at the previous iteration. For

the first iteration, $z_{eff,prev}$ = h/2

✓ $\qquad$ Effective second moment of area, $\quad I_{eff3}$

$\qquad$ $I_{eff3} = \quad I_{gross} + A \ (\Delta G)^{\ 2} - ( \ \frac{x^3.tw}{12} \quad + A_w \ (r \ + \ \Delta G)^{\ 2} \ )$

$\qquad$ = 397600.$10^4$+18000(38.80)$^{\ 2}$ $-(\frac{175.26^3.10}{12}$+1752.60 (359.69 + 38.80)$^{\ 2}$ )

$\qquad$ = 372030898.1 $mm^4$ = 372030.898 $cm^4$

$\qquad$ $C_I(\%) = \frac{\left|I_{eff}-I'_{eff}\right|}{I_{eff}} \times 100\% = \frac{|375742.259 - 372030.898|}{375742.259} \ 100\% \rightarrow C_I$

$\qquad$ = 0.99% > 0.1%

$\qquad$ $d_c = \frac{hw}{2} \ + \frac{tw}{2} - \Delta G = $ 650+5+38.80= 694.8 mm

$\qquad$ $d_t = \frac{hw}{2} \ + \frac{tw}{2} + \Delta G = $650+5-38.80 = 616.20 mm

✓ $\qquad$ The lesser elastic section modulus $\quad W_{eff3}$ is given as

$\qquad$ $W_{eff3} = \frac{I_{eff3}}{d_c} = \frac{372030.898}{69.38}$ = 5362.221 $cm^3$

✓ $\qquad$ Effective moment

$\qquad$ $M_{eff3} = \ W_{eff3} \cdot f_y$ = 5362.221. 3550 = 19035884.55dan .cm

$\qquad$ =1903588455 $\quad$ N. cm = 1904.588 KN. cm

✓ $\qquad$ third iteration

$\qquad\qquad$ ❖ Calculation of effective area, $A_{eff3}$

✓    Determine the stress ratio, ψ:

$$\Psi = -\frac{(\frac{h_w}{2} - \Delta G)}{(\frac{h_w}{2} + \Delta G)} = -\frac{(\frac{1300}{2} - 38.80)}{(\frac{1300}{2} + 38.80)} = -0.887$$

$$K_\sigma = 7.81 - 6.29\psi + 9.78\ \psi^2 = 21.020$$

✓    The normalized slenderness ratio $\bar{\lambda}_p$ is given by

$$\bar{\lambda}_p = \frac{h_w/t_w}{28.4\ \varepsilon\ \sqrt{K_\sigma}} = \frac{1300/10}{28.4.\ 0.81.\ \sqrt{21.02}} = 1.233\ >\ 1.08$$

✓    The reduction factor ρ for an internal compression member is given by

$$\rho = \frac{\bar{\lambda}_p - 0.055(3+\psi)}{\bar{\lambda}_p{}^2} = \frac{1.233 - 0.055(3 - 0.887)}{1.233^2} = 0.734$$

✓    The effective depth $b_{eff}$ is given by

$b_c = hw\ /2 + \Delta G = 1300/2 + 38.8 = 688.80$ mm

$b_{eff}\ = \rho.\ b_c = 0.734.\ 688.80 = 505.58$ mm

✓    The depth of web left at the top  $b_{e1}$:

$b_{e1} = 0.4\ b_{eff} = 0.4 \times 505.58 = 202.23$ mm

✓    The depth of web left at the bottom (above the centroidal axis), be2:

$b_{e2} = 0.6\ b_{eff} = 0.6 \times 505.58 = 304.35$ mm

✓    The ineffective portion of web has a length

$l_w = $ x $ =\ b_c - b_{e1} -\ b_{e2} = 688.80 - 202.23 - 304.35 = 184.22$ mm

✓    The net loss of area of the web,  $A_w$ is given by

$A_w =\ l_w. t_w = 184.22.\ 10 = 1832.2\ mm^2$

✓    Effective area of section, $A_{eff3}$:

$A_{eff3} = $ A $- A_w\ = 18000 - 1832.20 = 16167.80 mm^2 = 161.678\ cm^2$

$C_A(\%) = \frac{|A_{eff} - A_{eff}'|}{A_{eff}} \times 100\% \rightarrow C_A(\%) = \frac{|16247.40 - 16167.80|}{16247.40} \times 100\%$

$\rightarrow C_A(\%) = 0.49\% > 0.1\%$

❖    Calculation of $A_{eff}$

✓    Position of effective centroid, $z_{eff}$:

$r = \dfrac{hw}{2} - b_{e1} - \dfrac{x}{2} = \dfrac{1300}{2} - 202.23 - \dfrac{184.22}{2} = 356.16\text{mm}$

$r \cdot \Delta A + A_{eff} \cdot \Delta G = 0$ or $\Delta G = -\dfrac{356.16 \cdot 1832.20}{16167.40} = -40.36\text{mm}$

This means that shift of G' to G''= (-38.80–(-40.36)) =1.56mm (downward)

Note, $z_{eff,prev}$ is the neutral axis position at the previous iteration. For the first iteration, $z_{eff,prev} = h/2$

✓   Effective second moment of area,   $I_{eff3}$

$$I_{eff3} = I_{gross} + A\,(\Delta G)^2 - \left(\dfrac{x^3 \cdot t_w}{12} + A_w\,(r + \Delta G)^2\right)$$

$$= 397600.10^4 + 18000(40.36)^2 - \left(\dfrac{184.22^3 \cdot 10}{12} + 1832.20\,(356.16 + 40.36)^2\right)$$

$$= 3712121875\ mm^4 = 371212.187\ cm^4$$

$$C_I(\%) = \dfrac{\left|I_{eff} - I'_{eff}\right|}{I_{eff}} \times 100\% = \dfrac{|\,372030.898 - 371212.187\,|}{372030.898}\ 100\%$$

$$\rightarrow C_I = 0.22\% > 0.1\%$$

$$d_c = \dfrac{hw}{2} + \dfrac{tw}{2} - \Delta G = 650 + 5 + 40.36 = 695.36\text{mm}$$

$$d_t = \dfrac{hw}{2} + \dfrac{tw}{2} + \Delta G = 650 + 5 - 40.36 = 614.64\text{mm}$$

✓   The lesser elastic section modulus   $W_{eff}$ is given as

$$W_{eff3} = \dfrac{I_{eff3}}{d_c} = \dfrac{371212.187}{69.536} = 5338.417$$

✓   Effective moment

$$M_{eff3} = W_{eff3} \cdot f_y = 5338.417 \cdot 3550$$

$$= 18951380.35\ dan\,.cm = 1895138035\text{N. mm} = 1895.138\ KN.\,m$$

✓   For iteration

❖   Calculation of effective area, $A_{eff}$

✓   Determine the stress ratio, ψ:

$$\Psi = -\dfrac{\left(\dfrac{h_w}{2} - \Delta G\right)}{\left(\dfrac{h_w}{2} + \Delta G\right)} = -\dfrac{\left(\dfrac{1300}{2} - 40.36\right)}{\left(\dfrac{1300}{2} + 40.36\right)} = -0.883$$

$$K_\sigma = 7.81 - 6.29\psi + 9.78\,\psi^2 = 20.989$$

✓   The normalized slenderness ratio $\bar{\lambda}_p$ is given by

$$\bar{\lambda}_p = \dfrac{h_w/t_w}{28.4\,\varepsilon\,\sqrt{K_\sigma}} = \dfrac{1300/10}{28.4 \cdot 0.81 \cdot \sqrt{20.989}} = 1.233 > 1.08$$

✓　　The reduction factor ρ for an internal compression member is given by

$$\rho = \frac{\overline{\lambda}_p - 0.055(3 + \psi)}{\overline{\lambda}_p{}^2} = \frac{1.233 - 0.055(3 - 0.883)}{1.233^2} = 0.734$$

✓　　The effective depth $b_{eff}$ is given by

$b_c$=hw /2+ΔG=1300/2+40.36= 690.36 mm

$b_{eff}$　= ρ. $b_c$ = 0.734. 690.36= 506.72mm

✓　　The depth of web left at the top $b_{e1}$:

$b_{e1}$= 0.4 $b_{eff}$ = 0.4× 506.72= 202.69 mm

✓　　The depth of web left at the bottom (above the centroidal axis), be2:

$b_{e2}$= 0.6 $b_{eff}$ = 0.6 × 506.72 = 304.03 mm

✓　　The ineffective portion of web has a length

$l_w$ = x = $b_c$ - $b_{e1}$ − $b_{e2}$ = 690.36− 202.69– 304.03= 184.64 mm

✓　　The net loss of area of the web, $A_w$ is given by

$A_w$ = $l_w . t_w$ = 184.64  10 = 1836.40 $mm^2$

✓　　Effective area of section, $A_{eff}$:

$A_{eff}$ = A − $A_w$ = 18000-1836.40 = 16164.60$mm^2$= 161.636 $cm^2$

$$C_A(\%) = \frac{|A_{eff} - A_{eff}'|}{A_{eff}} \times 100\% \rightarrow C_A(\%) = \frac{|16167.80 - 16164.60|}{16167.80} \times 100\%$$

$$\rightarrow C_A(\%) = 0.025\% < 0.1\%$$

❖　Calculation of $A_{eff}$

✓　　Position of effective centroid, $z_{eff}$:

r = $\frac{hw}{2}$ - $b_{e1}$ − $\frac{x}{2}$ = $\frac{1300}{2}$ - 202.69 − $\frac{184.64}{2}$ = 355.49mm

r. $\Delta A$ + $A_{eff} . \Delta G$=0 or ΔG =- $\frac{355.49.\ 1836.40}{16164.60}$ = -40.39mm

This means that shift of G' to G''= (-40.36–(-40.39))=0.03mm (downward)

Note, $z_{eff,prev}$ is the neutral axis position at the previous iteration. For the first iteration, $z_{eff,prev}$ = h/2

✓     Effective second moment of area,    $I_{eff3}$

$$I_{eff3} = I_{gross} + A\,(\Delta G)^{\,2} - (\ \frac{x^{3}\cdot t_{w}}{12}\ + A_{w}\,(r\ +\ \Delta G)^{\,2}\ )$$

$$= 397600.10^{4} + 18000(40.39)^{\,2} - (\frac{184.64^{3}.10}{12} + 1836.40\ (355.49 +\ 40.39)^{\,2}\ )$$

$$= 3712401098\ mm^{4} = 371240.110\ cm^{4}$$

$$C_{I}(\%) = \frac{\left| I_{eff} - I'_{eff} \right|}{I_{eff}} \times 100\% = \frac{\left| 371241.240 - 371240.110 \right|}{371240.110}\ 100\%$$

$$\rightarrow\ C_{I} = 0.003\% < 0.1\%$$

$$d_{c} = \frac{hw}{2} + \frac{tw}{2} - \Delta G = 650 + 5 + 40.39 = 695.39\text{mm}$$

$$d_{t} = \frac{hw}{2} + \frac{tw}{2} + \Delta G = 650 + 5 - 40.39 = 614.61\text{mm}$$

✓     The lesser elastic section modulus   $W_{eff}$ is given as

$$W_{eff3} = \frac{I_{eff3}}{d_{c}} = \frac{371240.110}{69.54} = 5338.512\ cm^{3}$$

✓     Effective moment

$$M_{eff3} = W_{eff3}\,.\,f_{y} = 5338.512.\ 3550 = 18951717.60\ \text{dan .cm}$$

$$= 1895171760\ \text{N. mm} = 1895.172\ \text{KN. m}$$

**Table 6.5 Section 1 (with thickness of flange =20 mm)**

| Iteration | $A_{eff1}$ [cm$^2$] | $I_{eff1}$ [cm$^4$] | $W_{eff1}$ [cm$^3$] | $M_{eff1}$ [KN. m] | $\Delta G$ [mm] | $\psi$ |
|---|---|---|---|---|---|---|
| 0 (Gross) | 230 | 618716.667 | 9234.577 | 3278.275 | | -1 |
| 1 | 215.895 | 597251.355 | 8724.602 | 3097.234 | 24.56 | -0.927 |
| 2 | 214.271 | 594496.113 | 8634.531 | 3065.258 | 28.51 | -0.916 |
| 3 | 212.901 | 594161.381 | 8624.157 | 3061.221 | 29.03 | -0.914 |
| 4 ( Full ) | 212.820 | 594069.425 | 8620.196 | 3060.169 | 29.16 | -0.913 |
| Simplified | 215.895 | 597251.355 | 8724.602 | 3097.234 | 24.56 | -0.927 |
| Full/Simplified | 0.99 | 0.99 | 0.99 | 0.99 | | |

### Table 3.6 Section 1 (with thickness of flange =12 mm)

| Iteration | $A_{eff2}$ [$cm^2$] | $I_{eff2}$ [$cm^4$] | $W_{eff2}$ [$cm^3$] | $M_{eff2}$ [KN. m] | $\Delta G$ [mm] | ψ |
|---|---|---|---|---|---|---|
| 0 (Gross) | 190.000 | 441292.133 | 6666.044 | 2366.446 | | -1 |
| 1 | 175.895 | 419530.153 | 6114.352 | 2170.595 | 30.14 | -0.911 |
| 2 | 172.793 | 416247.068 | 6015.305 | 2135.433 | 35.98 | -0.895 |
| 3 | 172.096 | 415522.590 | 5994.180 | 2127.934 | 37.21 | -0.892 |
| 4 ( Full ) | 171.995 | 415440.014 | 5991.520 | 2126.990 | 37.38 | -0.891 |
| Simplified | 175.895 | 419530.153 | 6114.352 | 2170.595 | 30.14 | -0.911 |
| Full/Simplified | 0.98 | 0.99 | 0.98 | 0.98 | | |

### Table 3.7 Section 1 (with thickness of flange =10 mm)

| Iteration | $A_{eff3}$ [$cm^2$] | $I_{eff3}$ [$cm^4$] | $W_{eff3}$ [$cm^3$] | $M_{eff3}$ [KN. m] | $\Delta G$ [mm] | ψ |
|---|---|---|---|---|---|---|
| 0 (Gross) | 180.000 | 397600.000 | 6024.242 | 2138.606 | | -1 |
| 1 | 165.895 | 375742.259 | 5469.638 | 1941.721 | 31.96 | -0.906 |
| 2 | 162.474 | 372030.898 | 5362.221 | 1904.588 | 38.80 | -0.887 |
| 3 | 161.674 | 371241.240 | 5338.569 | 1895.192 | 40.36 | -0.883 |
| 4 (Full) | 161.636 | 371240.110 | 5338.512 | 1895.172 | 40.39 | -0.882 |
| Simplified | 165.895 | 375742.259 | 5469.638 | 1941.721 | 31.96 | -0.906 |
| Full/Simplified | 0.98 | 0.99 | 0.98 | 0.98 | | |

## 3.8.11 Determining the effective loading acing on the beam

$$M_{eff3} = M_{max} = \frac{q_3\,L}{4} \qquad \text{for the section 4.}$$

$$1941.721 = \frac{q_3.20}{4} \rightarrow q_{eff3} = 388.344 \text{ KN /m}$$

| Section 1 | $q_{eff1} = 619.447$ KN /m |
|---|---|
| Section 2 | $q_{eff2} = 434.119$ KN /m |
| Section 3 | $q_{eff3} = 388.344$ KN /m |

$C$HAPTER 4:

# FINITE ELEMENT MODELLING FOR

# SLENDER BEAM SECTIONS

## 4.1 General introduction to stability of members in bending

This chapter deals the technics of modelling structures with finite element. This modelling concerns the elastic and inelastic buckling behaviour of slender sections. The author suggests a brief introduction to the stability theory and the types of analysis of buckling. A general introduction to software used in modelling the considered sections. The used software, the first is a free (LTBEAM) and the second is the more general purpose: well-known (ABAQUS).

The main material described in this chapter is extracted from Master thesis previously submitted under the supervision of A. Labed in The University of Tebessa.

A study of the stability of structures is aimed at calculating the elastic critical load and deducing appropriate design loads for elements under compression to ensure that buckling does not occur. This is generally a complex procedure although the techniques can be built up from the matrix analysis methods are available. Fortunately, the stability analysis of a structure can be considered subsequent to the linear elastic analysis. Further, in many cases Codes of Practice offer sufficient guidance for a stability analysis not to be necessary. Nevertheless, important structures are subjected to stability analysis and the computational effort required is continually being reduced by developments in computer applications.

LTB can be considered as a critical condition for laterally unsupported beams. Like members in compression, the resistance of members in bending to lateral torsional buckling depends on the non-dimensional slenderness and an allowance for initial imperfections. However, no simple expression is given for non-dimensional slenderness for lateral torsional buckling. Its value is to be derived from the elastic critical buckling moment for the member. There are two methods for determining LTB slenderness manually, without the need to determine elastic critical moment. Both are based on empirical simplifications that give conservative values of slenderness [Abutair. Baker Wael,2017].

## 4.2 Solution by Finite Element Analysis for stability problems

### 4.2.1 Introduction

The recourse can be made to finite element analysis software (LTBEAM, ABAQUS ANSYS) when it is not possible to isolate uniform structural components, the loading on the components is complex or the interaction between components makes it difficult to determine boundary conditions for the critical components in order to determine elastic critical buckling loads using matrix analysis.

The eigenvalue of interest to the designer is therefore not the lowest value but the one relevant to the first global LTB mode. The eigenvalue of interest to the designer is therefore not the lowest value but the one relevant to the first global LTB mode. The Eigen value of interest to the designer is therefore not the lowest value but the one relevant to the first global LTB mode.

Two types of analysis i.e. elastic buckling analysis and non-linear analysis are performed to estimate the ultimate load carrying capacity of beams. Firstly, an eigenvalue analysis is performed for elastic buckling analysis in which eigenvalues of corresponding Eigen modes are determined using the linear perturbation buckling analysis. In this study, four eigenvalues for each run are extracted. Finally,RIKS method (ABAQUS 2014) is selected for non-linear post buckling analysis since it is suitable for predicting the instability as well as for understanding the non-liner behaviour of geometric collapse (ABAQUS 2014). RIKS method is based on Arc-length method and a form of Newton-Raphson iteration method, in which an additional unknown, named load proportionality factor is introduced to provide solutions concurrently for load and displacement [Abutair. Baker Wael, 2017].

### 4.2.2 First order analysis

First order analysis software will determine buckling loads by considering a particular loading situation and evaluating the eigenvalues for the stiffness matrix. Each eigenvalue has a corresponding eigenvector that defines the particular buckling mode associated with that value. The eigenvalues thus represent the critical buckling loads for each possible mode of buckling. Each eigenvalue gives the multiple of the applied loading at which the structure buckles in that particular mode and thus it is only the lowest values that are of relevance.

First order buckling analysis will be adequate for determining elastic critical buckling loads for most situations, which means that material non-linearity and geometric deformation are not taken into account. Note, however, that since the software for determining elastic critical loads generally uses stress stiffness matrices, which are based on initial linear stress and displacements, the destabilizing effect of any loads applied above the member centroid is automatically taken into account.

The effects of initial imperfections are not considered in first order analysis.

The primary result of an FE buckling analysis is a series of eigenvalues representing the load factors (multipliers on the magnitude of the given loading) at which the various buckling modes are critical (such as the higher harmonic modes referred to for flexural buckling). The results are normally presented in ascending order and only the lowest modes are of interest. However, the effective design resistance is not necessarily given by the lowest eigenvalue. To determine the design resistance, the designer must consider not just the eigenvalues but also the associated eigenvectors (which reveal the mode shape): when there are slender plate elements, local buckling can occur at a lower load than member buckling but the local buckling does not represent failure and does not determine the slenderness that is needed in the evaluation of design resistance of the member.

The top flange in a mid-span region may well be proportioned such that it is close to the out stand limit for Class 3 or 4, this occurs when its slenderness is about 0.75. If the slenderness for LTB were the

same as this value (and thus the eigenvalues for the two buckling modes would be the same), then the reduction factor for LTB (assuming a welded section and buckling curve d) would be about 0.6. In practice, economic design would probably require a 'better' (higher) reduction factor and thus a lower slenderness and a greater elastic critical buckling load. In such a situation, the eigenvalue for LTB (the ratio of elastic critical load to load applied to the model) would be higher than that for flange buckling. The eigenvalue of interest to the designer is therefore not the lowest value but the one relevant to the first global LTB mode.

To analyse members in bending, shell elements should be used for the webs and the flanges. Generally, the FE mesh size should be sufficiently fine that the model is able to represent torsional effects in the elements and the overall buckling modes. The mesh will also be able to model the local buckling of the compression flange and the webs in bending, although not with accuracy unless the mesh is fine. Shear buckling of the web will not normally be modelled as it would require a much finer mesh than is appropriate for determining member buckling [Abutair. Baker Wael, 2017]

### 4.2.3 Second order analysis

A full second order analysis takes account of material non-linearity and geometric deformation. To carry out such an analysis to determine failure load in accordance with Eurocodes requires complex software. It can determine failure loads directly, without reference to buckling curves, but the model does need to incorporate initial imperfections that are equivalent to those assumed in the Euro code design rules; it should be noted that the design imperfections exceed the geometrical limits given in EN 1090-2 because the former also include the effects of residual stresses through additional equivalent geometric imperfection. Evaluation of appropriate imperfections for the analysis requires a thorough understanding of the design basis in Eurocode3.

Second order analysis is essential when the buckling behaviour is influenced by the modified geometry of the structure under load. First order buckling analysis would only give eigenvectors for buckling modes related to the original geometry. However, the axial strain in the arch members will cause the arch to flatten, which increases the axial forces and strains. (In a sufficiently flat arch, the arch will snap through.) The true buckling load is thus only given by a second order analysis.

Nonlinear FE model is developed using the commercial finite element software package ABAQUS (ABAQUS 2014). Both geometric and material nonlinearities are considered in modelling. Since shell element is the most suitable element for complex buckling behaviour and has the capability of providing accurate solutions in case of a structure whose thickness is much smaller than the other dimensions (Smalberger 2014), a 8-node doubly curved shell element with reduced integration S8R (ABAQUS 2014) has been chosen from ABAQUS element library to model the web and flanges of I

sections (i.e. W and WWF) [Abutair. Baker Wael].

## 4.3 Overview of Software used in this thesis

In this chapter the following tow commercial structural engineering software tools will be introduced:

- LTBEAM v1.0.11
- ABAQUS v6.14-1

The software will hereinafter be referred to as LTBEAM and ABAQUS respectively. Information about their background will be given. Their methods for finding the elastic critical moment $M_{cr}$ described and their possibilities and limitations in that area discussed.

Two types of analysis i.e. elastic buckling analysis and inelastic analysis are conducted to estimate the ultimate load carrying capacity of simply supported beam subjected to uniform loading. Firstly, as it was the case with LTBEAM, an eigenvalue analysis is performed for elastic buckling analysis in which eigenvalues of corresponding Eigen modes are extracted using the linear perturbation buckling analysis. In this study, four eigenvalues for each run were extracted. From the eigenvalue analysis a suitable pattern of imperfection is obtained and incorporated into nonlinear analysis.

Nonlinear buckling analysis is usually the more accurate approach and is therefore recommended for design or evaluation of actual structures. This technique employs a nonlinear static analysis with gradually increasing loads to seek the load level at which your structure becomes unstable. Using the nonlinear technique, the model can include features such as initial imperfections, plastic behaviour, gaps, and large-deflection response [Abutair. Baker Wael, 2017].

## 4.4 Modelling beams of class 4 using LTBEAM (CTICM LTBeam)

### 4.4.1 General

The Centre Technique Industrial de la Construction Métallique (CTICM) in France have developed a computer program which enables the designer to quickly calculate the elastic critical lateral torsional buckling moment in a matter of seconds. The elastic critical lateral torsional buckling moment is determined using an iterative calculation process in which a linear eigenvalue analysis is performed. The behaviour of the beam is treated using the finite element method and the discretization of the beam can be varied from 100 elements up to 200 elements.

LTBEAM is software used in the field of the computational structural steel. It was developed by CTICM within a European research project, partly funded by the European Coal and Steel Community (ECSC), and completed in 2002 (CTICM, n.d.). LTBEAM is software that deals with elastic lateral-torsional buckling of beams subjected to bending about their major axis (CTICM, n.d.).It uses FEM

to obtain it´s results. This software applies to straight beams with one or more spans under simple bending about their major axis. The cross section must be symmetric about the minor axis, but can vary along the x-axis. Each node has four degrees of freedom (DOFs). At the beam ends, the user can choose which one of them to restrain. The four DOFs are:

- Lateral displacement
- Torsion rotation
- Lateral flexural rotation
- Warping

Along the beam the following restraints can be applied:

- Lateral displacement, local and continuous

Torsional rotation, local and continuous Supports conditions in the bending plane and externally applied loads are taken into account by the bending moment distribution [A. Galea].

### 4.4.2 User interface

The program provides a database of different steel profiles, saving the designer time to input the material and geometrical properties of the beam. Of course a manual input is possible .The next step is to choose the support conditions at the end of the beam. The program also allows the designer to apply one, two, or a continuous lateral restraint at different heights to the beam. After that, the load conditions must be chosen. Many types of load combinations can be chosen. The point of application is located in the shear Centre by default; however, the distance from the shear Centre can be varied as well. The program also calculates the maximum bending moment for the chosen loads. The final step is to calculate the elastic critical lateral torsional buckling moment with just a mouse click. As a result, the value of the elastic critical lateral torsional buckling moment is given as well as a graphical example of the deformed shape [A. Galea].

Two input methods are available; the simple input mode and the file input mode, shown in Figure 4.1. As the name indicates the simple input mode is simpler and therefore faster. It is unnecessary to use the file input mode unless the beam to be checked has a variable cross section or if complex loading conditions are present.

### 4.4.3 Simple input mode

The software gives the possibility to choose members from its built-in catalogue, or to manually enter the geometry. Additionally, it can be entered as in the following sectional properties: The second moment of area about the minor axis, the torsional constant, the warping constant and the Wagner's coefficient. The last option must be used if beams with a channel section are to be modelled. No channel sections or mono-symmetric I-sections are available from the built-in catalogue.

BI-symmetric I-sections can be defined by choosing the **By Dimensions** option, as shown in Figure 5.1. Then the corresponding sectional properties will be calculated by the software. The user can choose between 100, 120, 150 and 200 elements. When lateral restraints are chosen, fixed, and free or spring restraints are the alternatives but for the end supports in the plane of bending, fixed and free are the only options. No spring supports are available in simple input mode. It is also a possibility to apply local lateral restraints or a continuous lateral restraint along the whole beam. Different types of loading can be applied; a point load, a distributed load and a point moment about the major axis. The location of the forces can be chosen along the beam and the point load and the distributed load can be placed at different heights as well. The cross section must be constant along the x-axis in the simple input mode. In order to model a multi-span beam, the interior supports in the plane of bending must be replaced by its reactions and applied as point loads[Abutair. Baker Wael, 2017].
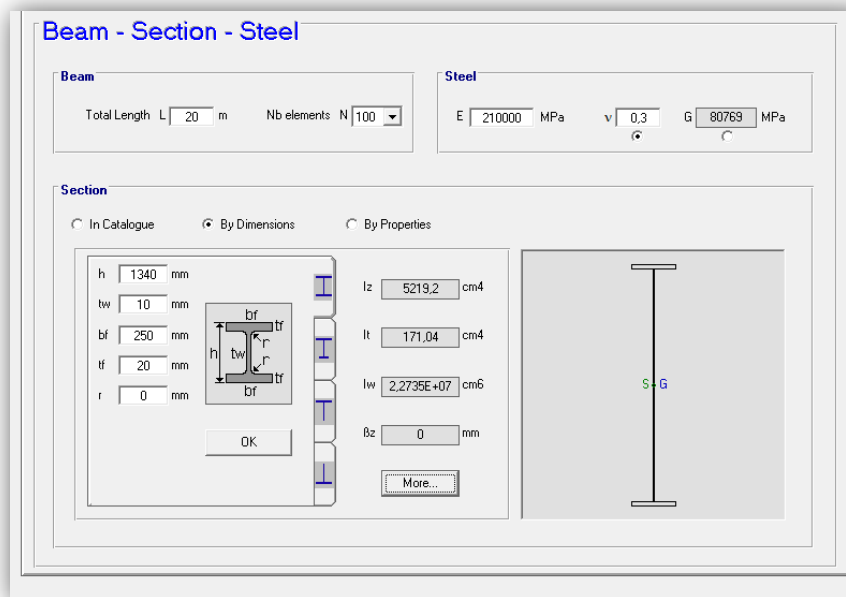


**Figure 4.1 User interface of the simple input mode in LTBEAM**

### 4.4.4 File input mode

To use the file input mode for more complex cases, a preparation and even pre calculations are sometimes needed. Here the cross section can vary, but the user must then define the sectional properties in each element. Between 50 and 300 elements can be chosen. The bending moment distribution for the whole beam has to be established and specified, it is defined by the values of bending moment in the endpoints of each element. Any loading, such as external moments and loads, and support reactions in the plane of bending are taken into account by the bending moment distribution. In addition to that, loads that are not applied at the shear Centre of the beams cross section, and result in destabilising or stabilising effects, need to be specifically stated [A. Galea].

### 4.5 Modelling beams of class 4 using ABAQUS (Manuel of ABAQUs)

### 4.5.1 Prologue

Undoubtedly, the finite element method represents one of the most significant achievements in the field of computational methods in the last century. Historically, it has its roots in the analysis of weight-critical framed aerospace structures. These framed structures were treated as an assemblage of one-dimensional members, for which the exact solutions to the differential equations for each member were well known. These solutions were cast in the form of a matrix relationship between the forces and displacements at the ends of the member. Hence, the method was initially termed matrix analysis of structures. Later, it was extended to include the analysis of continuum structures. Since continuum structures have complex geometries, they had to be subdivided into simple components or "elements" interconnected at nodes. It was at this stage in the development of the method that the term "finite element" appeared. However, unlike framed structures, closed form solutions to the differential equations governing the behavior of continuum elements were not available. Energy prin-ciples such as the theorem of virtual work or the principle of minimum potential energy, which were well known, combined with a piece-wise polynomial interpolation of the unknown displacement, were used to establish the matrix relationship between the forces and the interpolated displacements at the nodes numerically. In the late 1960s, when the method was recognized as being equivalent to a minimization process, it was reformulated in the form of weighted residuals and variational calculus, and expanded to the simulation of nonstructural problems in fluids, thermo-mechanics, and electromagnetics. More recently, the method is extended to cover multiphysics applications where, for example, it is possible to study the effects of temperature on electromagnetic properties that might affect the performance of electric motors [Khennane. A. 2013].

### 4.5.2 General

FEA is widely useful tool for studying the behaviour of various structural and mechanical designs. It can also be used to predict the ability of a design to withstand extreme loading conditions that cannot be duplicated in an experiment. Hopefully these extreme loading conditions will be considered early in the design process. An example of such a finite element analysis is the simulation of the ability of an offshore platform to withstand the forces produced by a storm.

With the advances in modern computing techniques, finite element analysis has become a practical and powerful tool for engineering analysis and design. In Structural Engineering, development of structural design code equations, their redeveloping is a continuous process and requires a wide range of experimental studies. However, performing many numbers of experiments is

costly, time consuming and hence uneconomical. On the other hand, conducting experiments is a compulsion for the research to progress.

ABAQUS is a suite of powerful engineering simulation programs based on the Finite Element Method, sold by Dassault Systems as part of their SIMULIA Product Life-cycle Management (PLM) software tools. Abaqus is a software package that is widely used in various industries and in the field of construction to solve a wide variety of problems in structural mechanics. It allows the implementation of very complex and customized material behaviours, up to the definition of failure criteria. The problem gets enormously simplified with the use of ABAQUS 6.9 (2009). ABAQUS is a highly sophisticated, general purpose finite element program, designed initially to model the behaviour of solids and structures under various externally applied loadings .

### 4.5.3 Brief introduction to ABAQUS

The ABAQUS 6.14.1 software was used for the finite element analysis (FEA). Which is a general-purpose finite element analysis program, capable of handling non-linear static analysis and elasto-plastic materials? In addition, Abaqus allows to take into account very complex contact behaviours that consider large rotations and friction.

Designed as a general-purpose simulation tool, ABAQUS can be used to study more than just structural (stress/displacement) problems. It can simulate problems in such diverse areas as heat transfer, mass diffusion, thermal management of electrical components (coupled thermal-electrical analyses), acoustics, soil mechanics (coupled pore fluid-stress analyses), and piezoelectric analysis. ABAQUS contains an extensive library of elements that can model virtually any geometry. It has an equally extensive list of material models that can simulate the behaviour of most typical engineering materials including metals, rubber, polymers, composites, reinforced concrete, crushable and resilient foams, and geotechnical materials such as soils and rock.

ABAQUS includes the following features:

- Capabilities for analysing both static and dynamic problems;
- The ability to model very large changes in shape of solids, in both two and three dimensions;
- A very extensive element library, including a full set of continuum elements, beam elements, shell and plate elements.
- A sophisticated capability to model contact between solids
- An advanced material library, including the usual elastic and elastic– plastic solids; models for foams, concrete, soils, piezoelectric materials and many others

- Capabilities to model a number of phenomena of interest, including vibrations, coupled fluid/structure interactions, acoustics, buckling problems and so on.

ABAQUS is simple to use and offers the user a wide range of capabilities, even the most complicated analyses can be modelled easily [Marwa Boudjadja, 2019].

### 4.5.4 Modelling sequence

Every complete finite-element analysis consists of 3 separate stages:

Pre-processing or modelling: this stage involves creating an input file, which contains an engineer's design for a finite-element analyser (also called "solver").

Processing or finite element analysis: This stage produces an output visual file.

Post-processing or generating report, image, animation, etc. from the output file: This stage is a visual interpretation stage.

In fact, ABAQUS/CAE is capable of pre-processing, post-processing, and monitoring the processing stage of the solver; however, the first stage can also be done by other compatible CAD software, or even a text editor.

ABAQUS/Standard, ABAQUS/Explicit or ABAQUS/CFD is capable of accomplishing the processing stage. Assault Systems also produces ABAQUS for CATIA for adding advanced processing and post processing stages to a pre-processor like CATIA.

As shown in the picture below, 11 modules are implanted in ABAQUS CAE which have to be used one after the other in order to modelling, loading, defining boundary conditions and finally analysis and then showing the results, diagrams and etc. These11 modules are named: Part-Property-Assembely-Step-Intreaction-Load-Mesh-Optimization-Job-vizualation-Sketch.

In the following, some details will be provided for each module:

- PART MODULE: This module allows the creation of the geometry required for the problem. Prior to create a 3-D geometry, the creation of 2-D must be performed and then manipulate it to obtain the solid geometry.

- PROPERTY MODULE: For defining material properties for the analysis and assigning them to available parts.

- ASSEMBLY MODULE: For assembling created parts together. Even with a single part, assembly is needed.

- INTERACTION MODULE: Permits to rely different parts by Tie, Rigid body, etc.

- STEP MODULE: To select the kind of analysis to be performed and define the parameters associated with it. variables to include can be also selected.in the output files in this module.

Load is applied over a step; the sequence of loads creates several steps and define the loads for each of them. Most complex analysis are likely to have a sequence of steps. An analysis step during which the response is nonlinear is called general analysis step. An analysis step during which the response is linear is called a linear perturbation step. A linear perturbation analysis step provides the linear response of the system about the base state i.e. the state at the end of the last nonlinear analysis step prior to the linear perturbation step.

- <u>LOAD MODULE</u>: Allows defining the loads and boundary conditions of the model for a particular step (indicated in the toolbar below).

- <u>MESH MODULE</u>: The mesh module controls how to mesh your model: the type of element, their size etc.

- <u>JOB MODULE</u>: To submit the model for analysis.

- <u>VISUALIZATION MODULE</u>: To look at the deformed model. A plot of values of stress, displacement, reaction forces, etc. with the possibility of using contours, surface, vectors or tensors.

- <u>MODEL TREE</u>**:** Provides a graphical overview of the model and the objects that it contains, such as parts, materials, steps, loads, and output requests. In addition, the Model Tree provides a convenient, centralized tool for moving between modules and for managing objects. If the model database contains more than one model, Model Tree can be used to move between models.

- <u>RESULTS TREE</u>**:** provides a graphical overview of your output databases and other session-specific data such as *X–Y* plots. When more than one output database is open in the session, the Results Tree can used to move between output databases.

**N.B.** There is no inherent set of units used in ABAQUS. It is up to the user to decide on a consistent set of units and use that unit [ABAQUS].
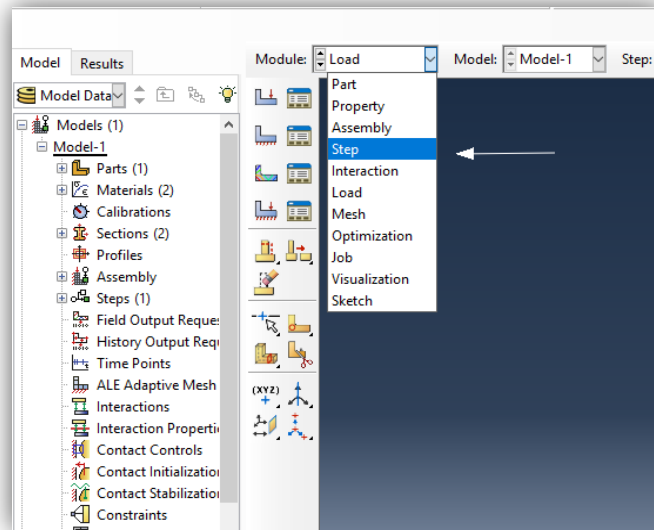
**Modelling demonstration**

**Figure 4.2**: ABAQUS Modules [ABAQUS]

## 4.6 Elements in ABAQUS

### 4.6.1 Element types

Wide range of elements in the ABAQUS/Explicit element library are available and provides flexibility in modelling different geometries and structures.

Each element can be characterized by:

- Family: Continuum, shell, membrane, rigid, beam, truss elements, etc. Figure 4.3
- Number of nodes: Element shape and Geometric order. Figure 4.4
- Linear or quadratic interpolation
- Degrees of freedom: Displacements, rotations, temperature: translation towards1; translation towards 2; translation direction 3; rotations around the axis 1; rotations around the axis 2; rotations around the axis 3.

Directions 1, 2 and 3 correspond to the global directions 1, 2 and 3, respectively; unless a local coordinate system has been defined at the nodes. Figure 4.5

- Formulation: Small and finite strain shells, etc.
- Integration: Reduced and full integration

Each element in ABAQUS has an assigned name: S4R, B31, M3D4R, C3D8R and C3D4 and the element name identifies primary element characteristics.

Each element can be differed by family, number of nodes, and Degrees of freedom.

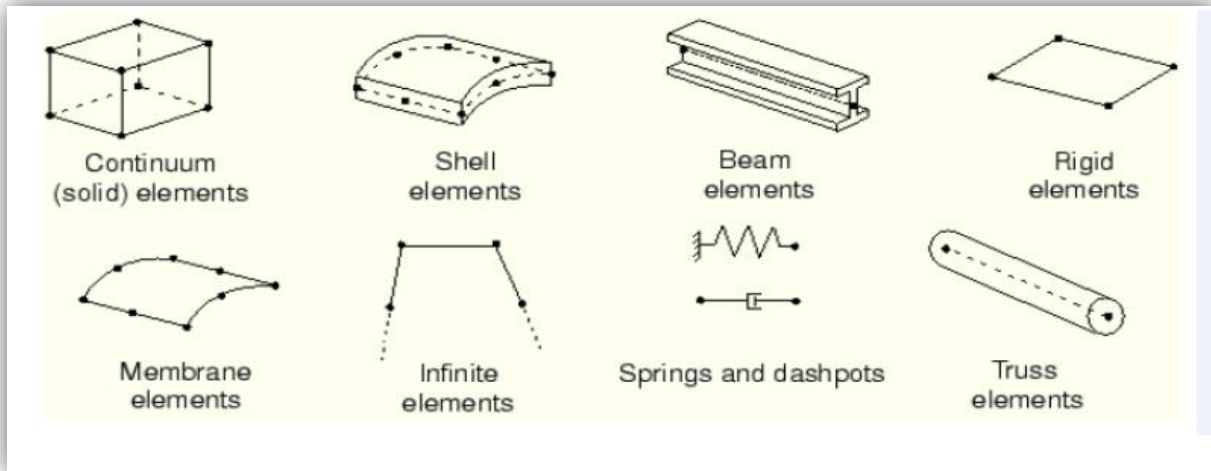- Family: solid (Continuum), shell, membrane, rigid, beam, truss elements, etc.

**Figure 4.3** Family of element in ABAQUS [Marwa Boudjadja, 2019]
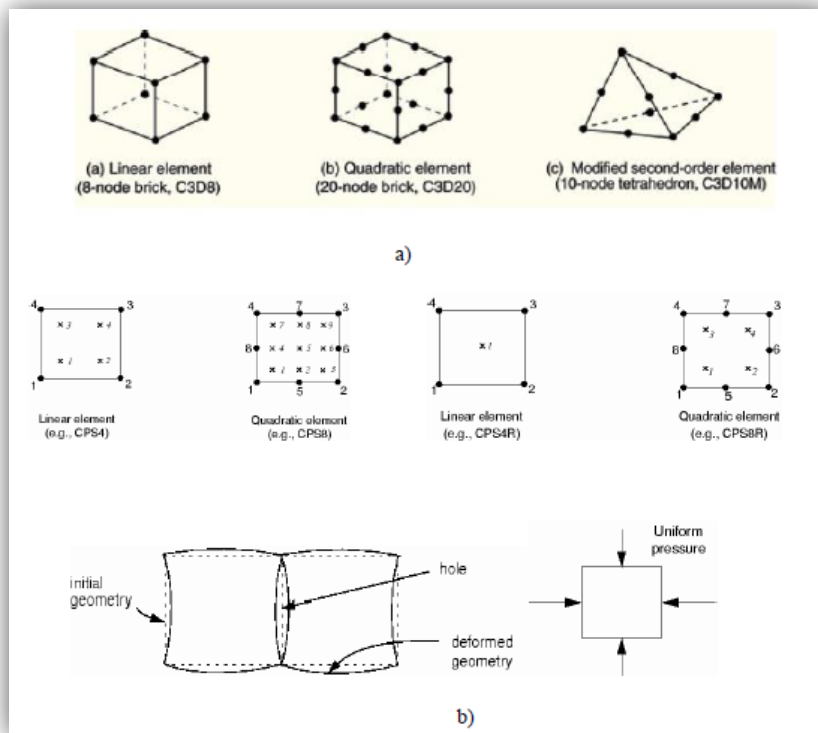
- Number of nodes



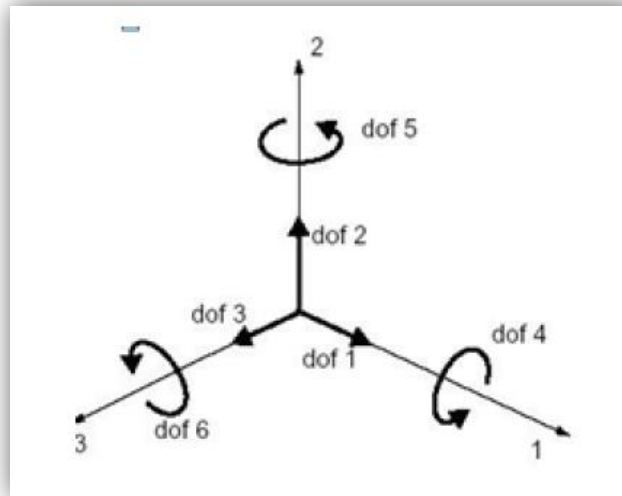**Figure 4.4:** Number of nodes of element in ABAQUS [Marwa Boudjadja, 2019]

**Figure 4.5** Displacement and Rotational degrees of freedom [Marwa Boudjadja, 2019]



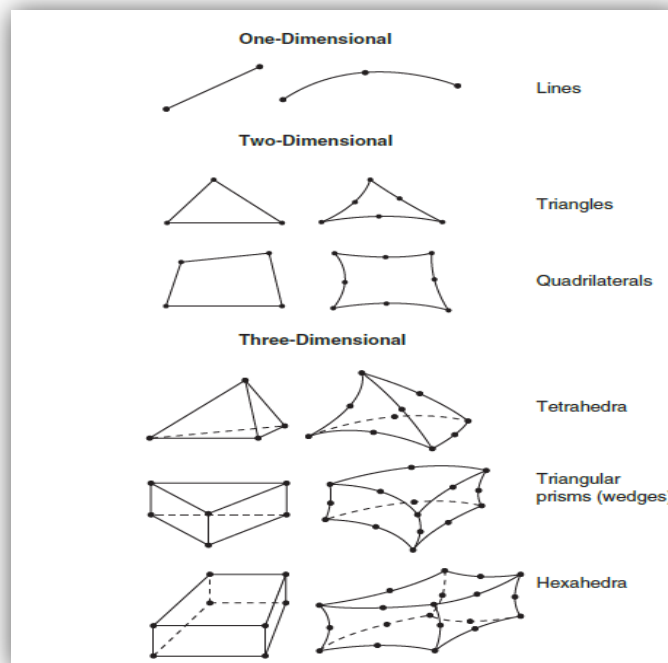**Figure 4.6 Elements Shapes in ABAQUS [Marwa Boudjadja, 2019]**

**4.6.2 Shell element overview**

Shell elements are needed for out-of-plane loading. Shell elements can also be used where the loading is planar but the material is made of composites. Since shell elements by definition allow for through thickness variation of material properties these are the appropriate elements to be used in these cases.

The ABAQUS shell element library provides elements that allow the modelling of curved, intersecting shells that can exhibit nonlinear material response and undergo large overall motions (translations and rotations). ABAQUS shell elements can also model the bending behaviour of composites.

The library is divided into three categories consisting of general-purpose, thin, and thick shell elements. Thin shell elements provide solutions to shell problems that are adequately described by classical (Kirchhoff) shell theory, thick shell elements yield solutions for structures that are best modelled by shear flexible (Mindlin) shell theory, and general-purpose shell elements can provide solutions to both thin and thick shell problems. All shell elements use bending strain measures that approximate those of Koiter-Sanders shell theory. While ABAQUS/Standard provides shell elements in all three categories, ABAQUS/Explicit provides only general-purpose shell elements. For most applications the general-purpose shell elements should be the user's first choice from the element library. However, for specific applications it may be possible to obtain enhanced performance by choosing one of the thin or thick shell elements. It should also be noted that not all ABAQUS shell elements are formulated for large-strain analysis.

The general-purpose shell elements are axisymmetric elements SAX1, SAX2, and SAX2T and three-dimensional elements S3, S4, S3R, S4R, S4RS, S3RS, and S4RSW, where S4RS, S3RS, and S4RSW are small-strain elements that are available only in ABAQUS/Explicit. The general-purpose elements provide robust and accurate solutions in all loading conditions for thin and thick shell problems. Thickness change as a function of in-plane deformation is allowed in their formulation. They do not suffer from transverse shear locking, nor do they have any unconstrained hourglass modes. Furthermore, in geometrically nonlinear analyses in ABAQUS/Standard the cross-section thickness of finite-strain shell elements changes as a function of the membrane strain based on a user-defined "effective section Poisson's ratio," $\nu$. In ABAQUS/Explicit, the thickness change is based on the "effective section Poisson's ratio" for all shell elements in large-deformation analyses, unless the user has specified that the thickness change should be based on the element material definition. The thickness change based on the "effective section Poisson's ratio".

SHELL181 is a 4-node 3-D shell element with 6 degrees of freedom at each node. The element has full nonlinear capabilities including large strain and allows 255 layers. The layer information is input using the section commands rather than real constants. Failure criteria is available using the FC commands [Marwa Boudjadja, 2019].

### 4.6.3 Element Shapes

There are various kinds of element shapes in ABAQUS:

- Quad: Use exclusively quadrilateral elements.

- Quad-dominated: Use primarily quadrilateral elements, but allow triangles in transition regions.

- This setting is the default.

- Tri: Use exclusively triangular elements.

- Hex: Use exclusively hexahedral elements. This setting is the default.

- Hex-dominated: Use primarily hexahedral elements, but allow some triangular prisms (wedges) in transition regions.

- Tet: Use exclusively tetrahedral elements.

- Wedge: Use exclusively wedges elements[Marwa Boudjadja, 2019].

# CHAPTER 5:

# RESULTS AND DISCUSSION OF LINEAR BUCKLING ANALYSIS

## 5.1 Introduction

In this chapter, the results and the discussion of the linear elastic buckling for laterally unrestrained beams S1, S2 and S3 made from S355 are provided. Two type of models have been used: Analytical method and Finite Element modelling. The evaluation of the elastic and effective critical lateral torsional buckling moment by means of analytic equation as per EC3 and throughout an eigen analysis by means of two Finite Element software: LTBeam and ABAQUS w sections of cross-sections will be presented. The parameters being investigated are: the class of the flange, the position of applied load and the effect of the effective geometrical properties on the whole behaviour of the considered sections. Also, a comparison of outcomes and some concluding remarks concerning the effect of the studied parameters will be drawn at the end of the chapter.

## 5.2 Elastic critical moment, $M_{cr}$

When looking for the lateral-torsional buckling resistance of a beam, a certain maximum theoretical moment is needed to be applied to the ideal beam. That is the elastic critical moment, noted *$M_{cr}$* as per *EC3*. It depends on number of factors: the lateral length of the beam, the bending moment diagram, the support conditions in both flexure and torsion, the stiffness of the beam about the minor axis and the torsional stiffness.

In this study, two distinct cases are investigated: section with class 4 with different flange classes ranging from 1, 3 and 4.

The elastic critical moment is used to find the non-dimensional slenderness λ $_{LT}$ of a beam to Eurocode3. Eurocode3 proposed an approximating formula to estimate *$M_{cr}$*, which gives conservative results. The formula is valid for when the beam is bent in its major axis bending with a uniform cross section that is symmetric about the minor axis (ECCS 2006, p. 229). Beams are, in reality, are not ideal. That is why a reduction factor must be used to find the design capacity. The formula mentioned above is often called the 3-factor formula and is expressed as follows:

$$M_{cr} = C_1 \cdot \frac{\pi^2 E I_{z_i}}{(K_Z.L)^2} \left[ \sqrt{\left(\frac{K_z}{K_w}\right)^2 \frac{I_{w_i}}{I_{z_i}} + \frac{(K_Z.L)^2 G I_{t_i}}{\pi^2 E I_{z_i}} + \left(C_2 Z_g - C_3 Z_j\right)^2} - \left(C_2 Z_g - C_3 Z_j\right) \right] \qquad (5.1)$$

Details of the above equation are presented in Chapter 3.

### 5.3 Results presentation

In the following, the weakest section, i.e. S3 with flange and web class 4 will be given in details. An evaluation of $M_{cr}$ with the elastic and effective properties will be respectively presented.  It

must be recalled that this investigation considers three types of cross sections belonging to class 4, slender sections to AISC and three loading conditions. For the remaining sections: S1 and S2, summarising tables display their results for both elastic and effective properties. Each table provides $M_{cri}$ in terms section $S_i$ namely the class of flange ($t_{fi}$) and the load position. A comparative table provides the differences is provided to express the percentage in the prediction of $M_{cr}$. Finally, a plot representing the variation of $M_{cr}$.in terms of flange's thicknesses for the whole analysed section. Similarly, the results will be displayed in the same manner for the sections with effective properties.

### 5.3.1 Linear analyse using elastic properties (EC3)

- ## Worked example of the analytical evaluation of $M_{cr}$ for S3

Cross-section of the beam with the thickness of flange = 10 mm (load applied at the top of flange).
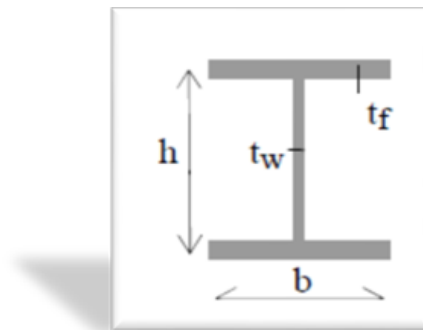


**Figure 5.1 bi-symmetric cross-section of the beam**

$$M_{cr} = C_1 . \frac{\pi^2 EI_{z_i}}{(K_Z . L)^2} \left[ \sqrt{\left(\frac{K_z}{K_w}\right)^2 \frac{I_{w_i}}{I_{z_i}} + \frac{(K_Z . L)^2 GI_{t_i}}{\pi^2 EI_{z_i}} + \left(C_2 Z_g - C_3 Z_j\right)^2} - \left(C_2 Z_g - C_3 Z_j\right) \right]$$

C1 = 1.35      ; C2 = 0.59     ; C3 = 0.411

$K_w = K_z = 1$

$E = 210. 10^6$ KN/m$^2$

$I_z = 2.615. 10^{-5}$ m$^4$; L = 20 m; $I_w = 1.122. 10^{-5}$ m$^6$; G = 80769230 KN/m$^2$

$I_t = 6.00 * 10^{-7}$ m$^4$

$Z_g = 0.66$ m

$M_{cr} = 182.92 * [\sqrt{0.429 + 0.357 + 0.151} - 0.389]$

$M_{cr} = 106.09\ KN.m$

## Table 5.1 Results of Section S1 ($t_f$ =20 mm)

| SECTION 1 | | $c_i$ | | | $K$ | | S355 | | $I_z$ $[m^4]$ | $I_w$ $[m^6]$ | $I_t$ $[m^4]$ | $Z_g$ $[m]$ | $M_{cr}$ $[KN.m]$ |
|---|---|---|---|---|---|---|---|---|---|---|---|---|---|
| POSITION OF LOAD | | $c1$ | $c2$ | $c3$ | $Kw$ | $Kz$ | $G$ $[mpa]$ | $E$ $[KN/m^2]$ | | | | | |
| | TOP | | | | | | | | | | | 0.67 | 241.98 |
| | SHEAR CENTRE | 1.35 | 0.59 | 0.411 | 1 | 1 | 80769230 | 210. $10^6$ | 5.219. $10^{-5}$ | 2.273. $10^{-5}$ | 1.767. $10^{-6}$ | 0 | 358.25 |
| | BOTTOM | | | | | | | | | | | -0.67 | 530.38 |

## Table 5.2 Results of Section S2 ($t_f$ =12 mm)

| SECTION 2 | | $c_i$ | | | $K$ | | S355 | | $I_z$ $[m^4]$ | $I_w$ $[m^6]$ | $I_t$ $[m^4]$ | $Z_g$ $[m]$ | $M_{cr}$ $[KN.m]$ |
|---|---|---|---|---|---|---|---|---|---|---|---|---|---|
| POSITION OF LOAD | | $c1$ | $c2$ | $c3$ | $Kw$ | $Kz$ | $G$ $[mpa]$ | $E$ $[KN/m^2]$ | | | | | |
| | TOP | | | | | | | | | | | 0.662 | 127.20 |
| | SHEAR CENTRE | 1.35 | 0.59 | 0.411 | 1 | 1 | 80769230 | 210. $10^6$ | 3.135. $10^{-5}$ | 1.349. $10^{-5}$ | 7.213. $10^{-7}$ | 0 | 194.79 |
| | BOTTOM | | | | | | | | | | | -0.662 | 298.25 |

## Table 5.3 Results of Section S3 ($t_f$ =10 mm)

| SECTION 3 | | $c_i$ | | | $K$ | | S355 | | $I_z$ $[m^4]$ | $I_w$ $[m^6]$ | $I_t$ $[m^4]$ | $Z_g$ $[m]$ | $M_{cr}$ $[KN.m]$ |
|---|---|---|---|---|---|---|---|---|---|---|---|---|---|
| POSITION OF LOAD | | $c1$ | $c2$ | $c3$ | $Kw$ | $Kz$ | $G$ $[mpa]$ | $E$ $[KN/m^2]$ | | | | | |
| | TOP | | | | | | | | | | | 0.66 | 106.09 |
| | SHEAR CENTRE | 1.35 | 0.59 | 0.411 | 1 | 1 | 80769230 | 210. $10^6$ | 2.615. $10^{-5}$ | 1.122. $10^{-5}$ | 6.00. $10^{-7}$ | 0 | 162.27 |
| | BOTTOM | | | | | | | | | | | -0.66 | 248.41 |

**Table 5.4 Comparison of the whole considering the elastic properties**

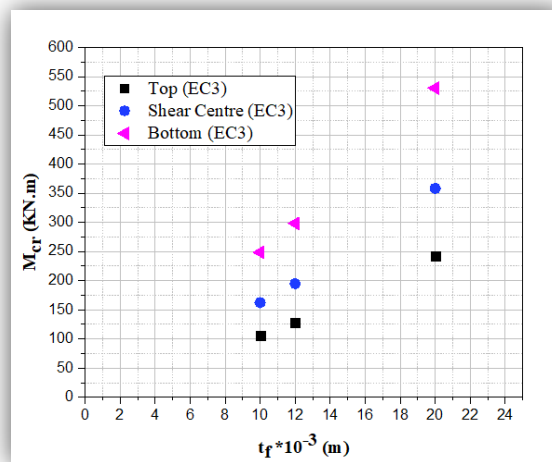| EC3 POSITION OF LOAD | S1 | $M_{cr}$ | DIFFERENCE | S2 | $M_{cr}$ | DIFFERENCE | S3 | $M_{cr}$ | DIFFERENCE |
|---|---|---|---|---|---|---|---|---|---|
| TOP | | 241.98 | 0.675<1 | | 127.20 | 0.653<1 | | 106.09 | 0.653<1 |
| SHEAR CENTRE | | 358.25 | 1 | | 194.79 | 1 | | 162.27 | 1 |
| BOTTOM | | 530.38 | 1.480>1 | | 298.25 | 1.531>1 | | 248.41 | 1.530>1 |



**Figure 5.2 Results as per EC3 of the variation of $M_{cr}$ in terms of flange's thickness**

- **Discussion of the results**

The overall results for the elastic linear analysis are shown in tables (5.1 to 5.4), and figure 5.2 depicts the variation of the of $M_{cr}$ in terms of flange's thickness. Broadly speaking, one can notice from the above shown results that the values of the elastic critic moment depend mainly on the slenderness of flange, that the position of the applied load. For each section as expected, $M_{cr}$ values depends on the load position with larger values in the bottom flange (tension zone). These values decrease when P is applied at the shear centre and less values are found when the applied load is located at the top flange (compressive zone). However, the differences of the amount of $M_{cr}$ varies from S1 to S3. In fact, the differences are being quasi- constant ranging from around 0.7 in the compressive flanges to 1.5 for tension flanges.

### 5.3.2 Linear analyse using effective properties (EC3)

- **Worked example of the analytical evaluation of $M_{cr}$ for S1 and S2**

It must be reminded that S1 and S2 are of class 4 with flanges belonging to class 1 and 3 respectively. Carrying the hand calculations of effective properties, the only difference from the case previously presented is the fact that the down translation of G.

Cross-section of the beam with the thickness of flange = 20 mm (load applied at the top of flange).
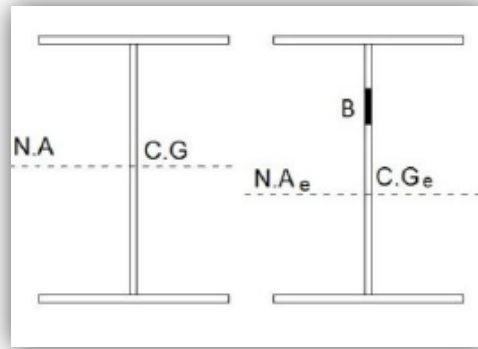


**Figure 5.3 Bi-symmetric cross-section of the beam (effective)**

$$M_{cr} = C_1 \cdot \frac{\pi^2 EI_{z_i}}{(K_z.L)^2} \left[ \sqrt{\left(\frac{K_z}{K_w}\right)^2 \frac{I_{w_i}}{I_{z_i}} + \frac{(K_z.L)^2 GI_{t_i}}{\pi^2 EI_{z_i}} + \left(C_2 Z_g - C_3 Z_j\right)^2} - \left(C_2 Z_g - C_3 Z_j\right) \right]$$

C1 = 1.35      ; C2 = 0.59     ; C3 = 0.411

$K_w = K_z = 1$

$E = 210. \ 10^6 \ KN/m^2$

$I_z = 5.219 * 10^{-5} \ m^4$; L = 20 m; $I_w = 2.273 * 10^{-5} \ m^6$; G = 80769230 $KN/m^2$

$I_t = 1.767 * 10^{-6} \ m^4$

$Z_g = 0.64544 \ m$

$M_{cr} = 365.073 * [\sqrt{0.435 \ + \ 0.528 \ + \ 0.145} - 0.381]$

$M_{cr} = 245.189 \ KN.m$

**Table 5.5 Results of Section S1 with effective properties ($t_f$ =20 mm)**

| SECTION 1 | | ci | | | K | | S355 | | $I_z$ [$m^4$] | $I_w$ [$m^6$] | $I_t$ [$m^4$] | $Z_g$ [m] | $M_{cr}$ [KN. m] |
|---|---|---|---|---|---|---|---|---|---|---|---|---|---|
| POSITION OF LOAD | | c1 | c2 | c3 | Kw | Kz | G [mpa] | E [KN/$m^2$] | | | | | |
| | TOP | | | | | | | | | | | 0.64544 | 245.18 |
| | SHEAR CENTRE | 1.35 | 0.59 | 0.411 | 1 | 1 | 80769230 | 210. $10^6$ | 5.219. $10^{-5}$ | 2.273. $10^{-5}$ | 1.767. $10^{-6}$ | - 0.02456 | 363.40 |
| | BOTTOM | | | | | | | | | | | - 0.64544 | 523.37 |

### Table 5.6 Results of Section S2 with effective properties ($t_f$ =12 mm)

| SECTION 2 | ci | | | K | | S355 | | $I_z$ $[m^4]$ | $I_w$ $[m^6]$ | $I_t$ $[m^4]$ | $Z_g$ $[m]$ | $M_{cr}$ $[KN. m]$ |
|---|---|---|---|---|---|---|---|---|---|---|---|---|
| POSITION OF LOAD | c1 | c2 | c3 | Kw | Kz | G [mpa] | E [KN/$m^2$] | | | | | |
| TOP | | | | | | | | | | | 0.63186 | 129.45 |
| SHEAR CENTRE | 1.35 | 0.59 | 0.411 | 1 | 1 | 80769230 | 210. $10^6$ | 3.135. $10^{-5}$ | 1.349. $10^{-5}$ | 7.213. $10^{-7}$ | - 0.03014 | 198.77 |
| BOTTOM | | | | | | | | | | | - 0.63186 | 293.05 |

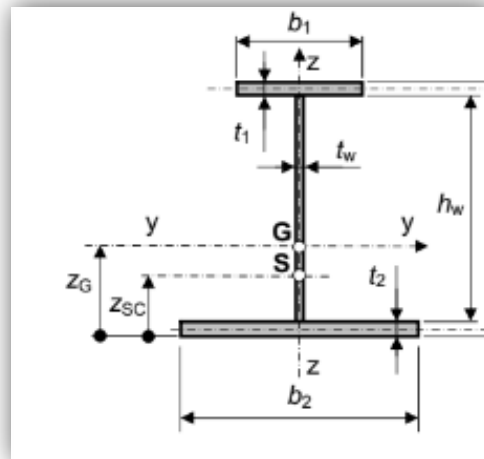Cross-section of the beam with the thickness of flange = 10 mm (load applied at the top of flange).



### Figure 5.4 Sections mono-symmetric (effective)

$$M_{cr} = C_1 . \frac{\pi^2 EI_{z_i}}{(K_Z . L)^2} \left[ \sqrt{\left(\frac{K_z}{K_w}\right)^2 \frac{I_{w_i}}{I_{z_i}} + \frac{(K_Z . L)^2 GI_{t_i}}{\pi^2 EI_{z_i}} + \left(C_2 Z_g - C_3 Z_j\right)^2} - \left(C_2 Z_g - C_3 Z_j\right) \right]$$

C1 = 1.35                        ; C2 = 0.59        ; C3 = 0.411

$K_w = K_z = 1$

E = 210. $10^6$ KN/$m^2$

$I_z$ = 2.306 * $10^{-5}$ $m^4$; L = 20 m; $I_w$ = 9.727 * $10^{-6}$ $m^6$; G = 80769230 KN/$m^2$

$I_t$ = 5.931 * $10^{-7}$ $m^4$

$Z_g$ = 0.636 m

$M_{cr}$ = 161.306 * [$\sqrt{0.422 + 0.401 + 0.141}$− 0.375]

$M_{cr} = 97.886\ KN.m$

**Table 5.7 Results of Section S3 with effective properties ($t_f$ =10 mm)**

| SECTION 3 | | ci | | | K | | S355 | | $I_z$ | $I_w$ | $I_t$ | $Z_g$ | $M_{cr}$ |
|---|---|---|---|---|---|---|---|---|---|---|---|---|---|
| | | | | | | | | | $[m^4]$ | $[m^6]$ | $[m^4]$ | $[m]$ | $[KN.m]$ |
| POSITION OF LOAD | | c1 | c2 | c3 | Kw | Kz | G [mpa] | E [KN/$m^2$] | | | | | |
| | TOP | | | | | | | | | | | 0.6360 | 97.88 |
| | SHEAR CENTRE | | | | | | | | | | | -0.03196 | 149.42 |
| | BOTTOM | 1.35 | 0.59 | 0.411 | 1 | 1 | 80769230 | 210.$10^6$ | 2.306.$10^{-5}$ | 9.727.$10^{-6}$ | 5.931.$10^{-7}$ | -0.6360 | 216.092 |

**Table 5.8 Comparison of the whole considering the effective properties**

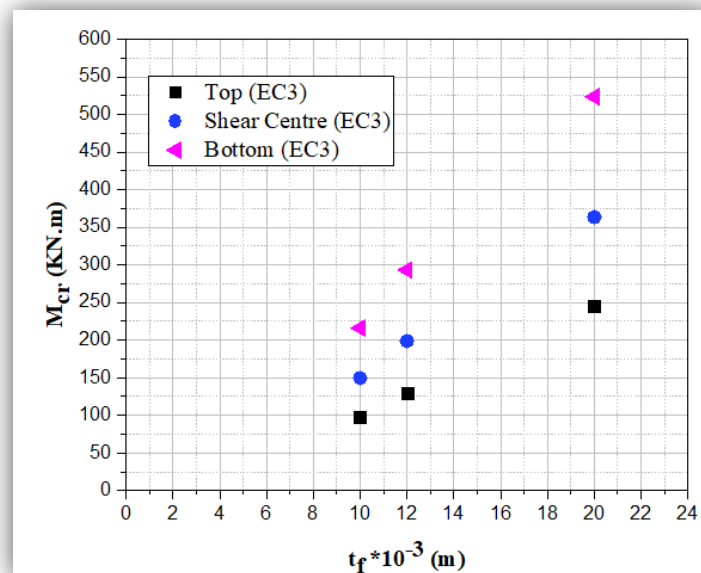| EC3 POSITION OF LOAD | S1 | $M_{cr}$ | DIFFERENCE | S2 | $M_{cr}$ | DIFFERENCE | S3 | $M_{cr}$ | DIFFERENCE |
|---|---|---|---|---|---|---|---|---|---|
| TOP | | 245.18 | 0.674<1 | | 129.45 | 0.651<1 | | 97.88 | 0.655<1 |
| SHEAR CENTRE | | 363.40 | 1 | | 198.77 | 1 | | 149.42 | 1 |
| BOTTOM | | 523.37 | 1.440>1 | | 293.05 | 1.474>1 | | 216.09 | 1.446>1 |



**Figure 5.5 Results as per EC3 of the Variation of $M_{cr}$ in terms of flange's thickness**

• **Discussion of the results**

The overall results for the elastic linear analysis are shown in tables (5.5 to 5.8), and figure 5.5 depicts the variation of the of $M_{cr}$ in terms of flange's thickness. Similarly, with changing the geometrical properties from elastic to effective, the tendency of $M_{cr}$ is quite similar and the same remarks can be made as it was discussed in previous section. Once again, the impact of the investigated parameters shown their importance. In fact, one can notice from the above shown results that the values of the effective moment depend mainly on the slenderness of flange, that the position of the applied load. For each section as expected, $M_{cr}$ values depends on the load position with larger values in the bottom flange (tension zone). These values decrease when P is applied at the shear centre and less values are found when the applied load is located at the top flange (compressive zone). However, the differences of the amount of $M_{cr}$ varies from S1 to S3. In fact, the differences are being quasi- constant ranging from around 0.7 in the compressive flanges to 1.45 for tension flanges.

**N.B.** From the above results of the elastic analysis to EC3, it can be concluded that changing the geometrical properties from elastic to effective has no important effect as the $M_{cr}$ are of the same range.

### 5.4 Linear Buckling Analysis by LTBEAM

### 5.4.1 Elastic characteristics

• **Presentation of a sample of results**

As previously mentioned in chapter 4, LTBEAM is free Finite Element software dealing with the linear buckling analysis throughout an eigen analysis mode. Firstly, the geometrical properties of the used section are displayed before running the linear buckling analysis. It gives also several modes with the $\mu_{cr}$ for each mode. In the following, only the first mode (fundamental mode) of buckling is considered. The extracted value of $\mu_{cr}$ permits the evaluation of the $M_{cr}$ which is given by the software. The following demonstration is devoted to section S3 that is web and flanges of class 4.

In this section, the elastic critical lateral torsional buckling moment is calculated for unrestrained beam with different position of loads that is applied at the top flange, at the shear centre and at the bottom flange for all bi-symmetric sections. The demonstration considers the following:
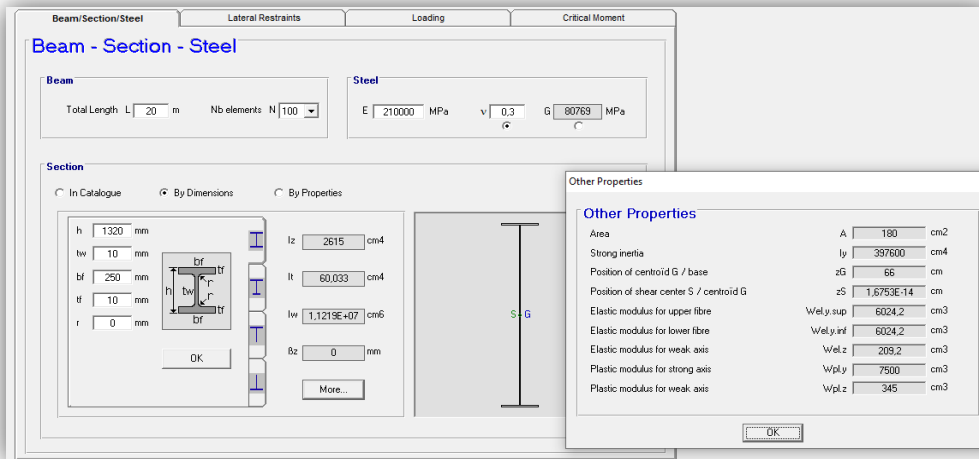
Figure 5.6 shows how to introduce the input file of the elastic properties of the studied section.
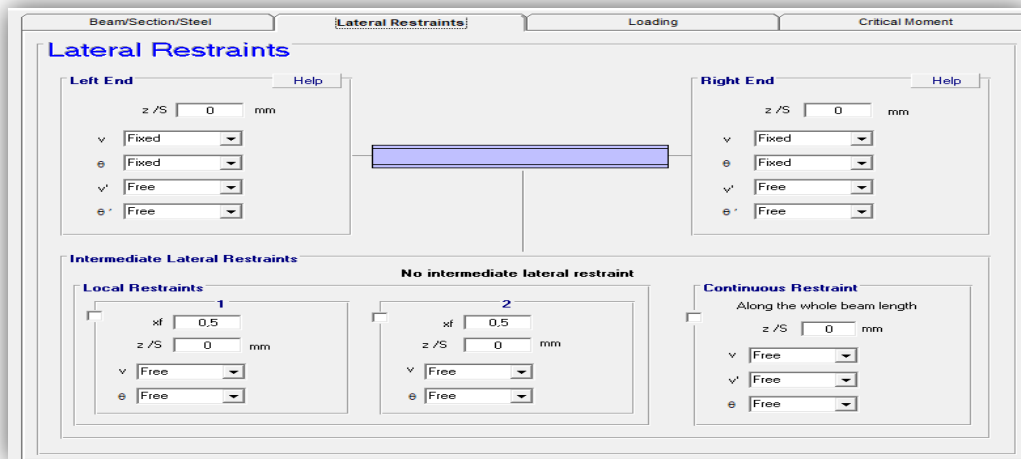
Figure 5.7 shows how to introduce the boundary conditions including torsion limitation.

Figure 5.8 shows how to introduce the applied load and location in the cross section.

Figure 5.9 shows how to get the results: $\mu_{cr}$ and $M_{cr}$

**Figure 5.6 Shows how to introduce the input file of the elastic properties of the studied section**



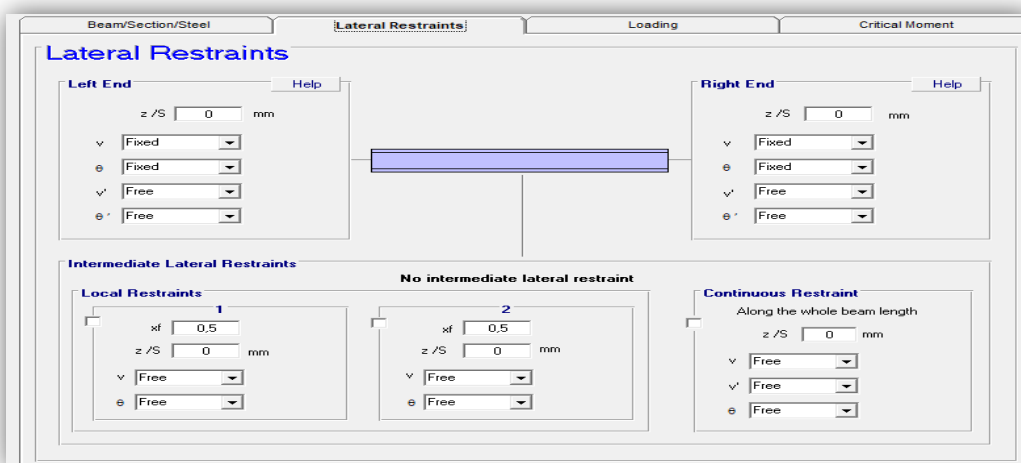**Figure 5.7 Shows how to introduce the boundary conditions including torsion limitation**



**Figure 5.8 Shows how to introduce the applied load and location in the cross section**
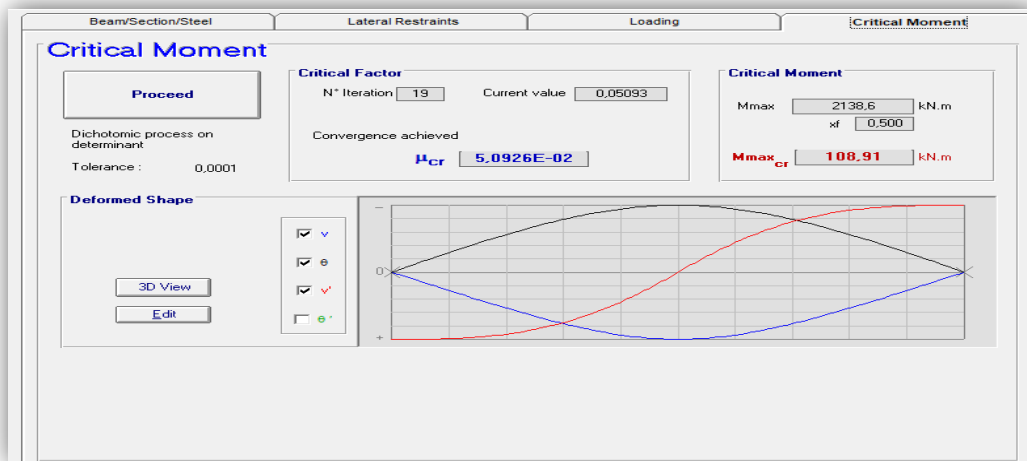
Figure 5.9 Shows how to get the results: $\mu_{cr}$ and $M_{cr}$

Table 5.9 Results of Section S1 ($t_f$ =20 mm)

| Section | Position of load | $q_{el}$[KN] | $\mu_{cr}$ | $M_{cr}(KN.m)$ |
|---------|------------------|--------------|------------|----------------|
| 1 | Top | 655.656 | $7.476*10^{-2}$ | 245.09 |
| 1 | Shear Centre | 655.656 | 0.10933 | 358.41 |
| 1 | Bottom | 355.656 | 0.15892 | 520.98 |

Table 5.10 Results of Section S2 ($t_f$ =10 mm)

| Section | Position of load | $q_{el}$[KN] | $\mu_{cr}$ | $M_{cr}(KN.m)$ |
|---------|------------------|--------------|------------|----------------|
| 2 | Top | 473.289 | $5.5153*10^{-2}$ | 130.52 |
| 2 | Shear Centre | 473.289 | $8.3038*10^{-2}$ | 196.51 |
| 2 | Bottom | 473.289 | 0.12424 | 294.02 |

Table 5.11 Results of Section S3 ($t_f$ =10 mm)

| Section | Position of load | $q_{el}$[KN] | $\mu_{cr}$ | $M_{cr}(KN.m)$ |
|---------|------------------|--------------|------------|----------------|
| 3 | Top | 427.721 | $5.0926*10^{-2}$ | 108.91 |
| 3 | Shear Centre | 427.721 | $7.6591*10^{-2}$ | 163.80 |
| 3 | Bottom | 427.721 | 0.11449 | 244.86 |

Table 5.12 Comparison of the whole considering the elastic properties

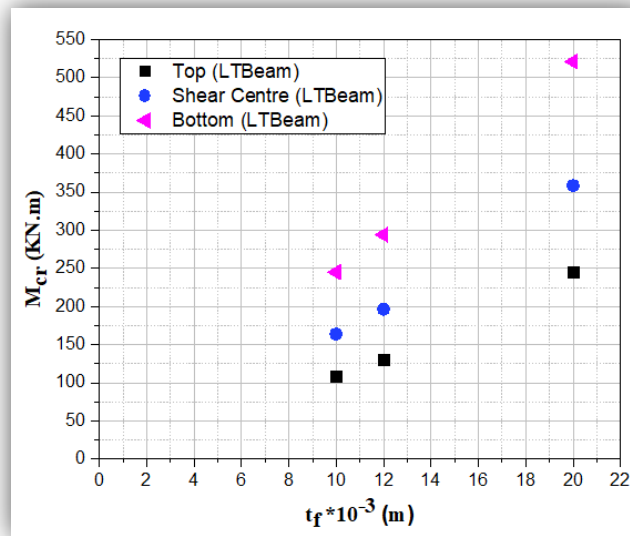| LTBEAM POSITION OF LOAD | S1 $M_{cr}$ | DIFFERENCE | S2 $M_{cr}$ | DIFFERENCE | S3 $M_{cr}$ | DIFFERENCE |
|-------------------------|-------------|------------|-------------|------------|-------------|------------|
| TOP | 245.09 | 0.683<1 | 130.52 | 0.664<1 | 108.91 | 0.664<1 |
| SHEAR CENTRE | 358.41 | 1 | 196.51 | 1 | 163.80 | 1 |
| BOTTOM | 520.98 | 1.453>1 | 294.02 | 1.496>1 | 244.86 | 1.494>1 |

**Figure 5.10 Results as per LTBEAM of the Variation of $M_{cr}$ in terms of flange's thickness**

- **Discussion of the results**

The overall outcomes from LTBEAM for the elastic linear analysis are shown in tables (5.9 to 5.12), and figure 5.10 depicts the variation of the of $M_{cr}$ in terms of flange's thickness. It can be noticed, once again as discussed in 5.2.1, that the values of the elastic critic moment depend mainly on the slenderness of flange, the position of the applied load with the same proportions: the amount of $M_{cr}$ varies from S1 to S3. In fact, the differences are being quasi- constant ranging from around 0.7 in the compressive flanges to 1.5 for tension flanges.

### 5.4.2 Effective characteristics (LTBEAM)

- **Bi-symmetric sections**

In this section, in the contrary of the previous section, the effective characteristics are rather used to evaluate the effective critical lateral torsional buckling moment. The demonstration concerns the case of bi-symmetric section of unrestrained beam with different position of loads that is applied at the top flange, at the shear centre and at the bottom flange.

**Table 5.13 Results of Section S1 ($t_f$ =20 mm)**

| Section | Position of load | $q_{el}$[KN] | $\mu_{cr}$ | $M_{cr}(KN.m)$ |
|---------|------------------|--------------|------------|----------------|
| 1 | Top | 619.447 | $8.02000*10^{-2}$ | 248.40 |
| 1 | Shear Centre | 619.447 | 0.11738 | 363.55 |
| 1 | Bottom | 619.447 | 0.16605 | 514.18 |

<div align="center">**Table 5.14 Results of Section 2 (t$_f$ =12 mm)**</div>

| Section | Position of load | $q_{el}$[KN] | $\mu_{cr}$ | $M_{cr}(KN.m)$ |
|---------|-----------------|-----------|-----------|--------------|
| 2 | Top | 434.119 | $6.1207*10^{-2}$ | 132.85 |
| 2 | Shear Centre | 434.119 | $9.22702*10^{-2}$ | 200.28 |
| 2 | Bottom | 434.119 | 0.13315 | 289.01 |

- **Mono-symmetric sections**

In this section, the effective geometrical properties of section of a mono-symmetric section in terms of the same parameters as above.

<div align="center">**Table 5.15 Results of Section S3 (t$_f$ =10 mm)**</div>

| Section | Position of load | $q_{el}$[KN] | $\mu_{cr}$ | $M_{cr}(KN.m)$ |
|---------|-----------------|-----------|-----------|--------------|
| 3 | Top | 388.344 | $5.3642*10^{-2}$ | 104.16 |
| 3 | Shear Centre | 388.344 | $8.0627*10^{-2}$ | 156.56 |
| 3 | Bottom | 388.344 | 0.11512 | 223.53 |

<div align="center">**Table 5.16 Comparison of the whole considering the effective properties**</div>

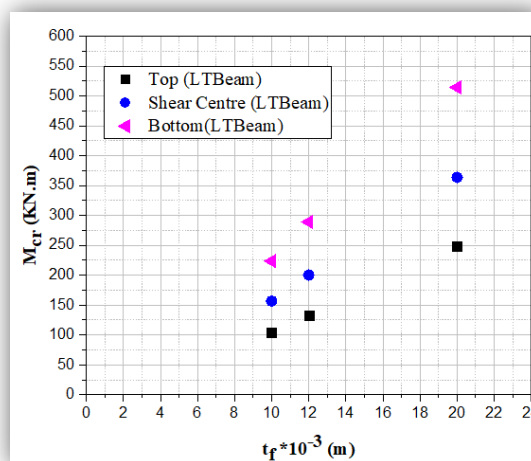| LTBEAM POSITION OF LOAD | S1 | $M_{cr}$ | DIFFERENCE | S2 | $M_{cr}$ | DIFFERENCE | S3 | $M_{cr}$ | DIFFERENCE |
|---|---|---|---|---|---|---|---|---|---|
| TOP | | 248.40 | 0.683<1 | | 132.85 | 0.663<1 | | 254.49 | 0.708<1 |
| SHEAR CENTRE | | 363.55 | 1 | | 200.28 | 1 | | 359.06 | 1 |
| BOTTOM | | 514.18 | 1.414>1 | | 289.01 | 1.444>1 | | 537.80 | 1.497>1 |



<div align="center">**Figure 5.11 Results as per LTBEAM of the Variation of M$_{cr}$ in terms of flange's thickness**</div>

- **Discussion of the results**

The overall results for the elastic linear analysis with effective characteristics are presented in tables (**5.13 to 5.16**), and figure 5.11 depicts the variation of the of $M_{cr}$ in terms of flange's thickness. Similarly, with changing the geometrical properties from elastic to effective does not greatly affect the results. The tendency of $M_{cr}$ is quite similar and the same remarks can be made as it was discussed in previous section. Once again, the impact of the investigated parameters shown their importance. In fact, one can notice from the above shown results that the values of the effective moment depend mainly on the slenderness of flange, that the position of the applied load. For each section as expected, $M_{cr}$ values depends on the load position with larger values in the bottom flange (tension zone). These values decrease when P is applied at the shear centre and less values are found when the applied load is located at the top flange (compressive zone). However, the differences of the amount of $M_{cr}$ varies from S1 to S3. In fact, the differences are being quasi- constant ranging from around 0.7 in the compressive flanges to 1.50 for tension flanges.

**N.B.** From the above results of the elastic analysis to LTBEAM, it can be concluded that changing the geometrical properties from elastic to effective has no important effect as far as the extracted values of $M_{cr}$ are concerned.

### 5.5 Linear Buckling Analysis (ABAQUS)

### 5.5.1 General

To determine the elastic critical lateral torsional buckling load of the beam, a linear buckling analysis (LBA) is performed. During this analysis, the bifurcation point is determined by solving an eigenvalue problem. This eigenvalue problem is solved when the stiffness matrix of the model becomes singular and provides nontrivial solutions.

The software gives the option to choose from two different methods to solve the eigenvalue problem, namely the Lanczos and the subspace iteration method. Both methods provide the option to determine multiple eigenvalues. However, for this research project only the first positive buckling mode is required, therefore only the first positive eigenvalue needs to be determined.

To eventually determine the elastic critical lateral torsional buckling load of the beam, the applied load needs to be multiplied by the eigenvalue resulting from the linear buckling analysis and subsequently, the elastic critical lateral torsional buckling moment can be determined.

### 5.5.2 Results with elastic characteristics

In the same manner, results from LBA of ABAQUS will be presented in tables (5.17 to 5.20) and single figure 5.12.

### Table 5.17 Results of Section S1 (t_f =20 mm)

| Section | Position of load | $q_{el}$[KN] | $\mu_{cr}$ | $M_{cr}(KN.m)$ |
|---------|-----------------|--------------|-----------|----------------|
| 1 | Top | 655.656 | $7.76281*10^{-2}$ | 254.48 |
| 1 | Shear Centre | 655.656 | 0.10799 | 354.02 |
| 1 | Bottom | 655.656 | 0.16404 | 537.78 |

### Table 5.18 Results of Section S2 (t_f =12 mm)

| Section | Position of load | $q_{el}$[KN] | $\mu_{cr}$ | $M_{cr}(KN.m)$ |
|---------|-----------------|--------------|-----------|----------------|
| 2 | Top | 473.289 | $5.84691*10^{-2}$ | 138.36 |
| 2 | Shear Centre | 473.289 | $8.45167*10^{-2}$ | 200.02 |
| 2 | Bottom | 473.289 | 0.13061 | 309.08 |

### Table 5.19 Results of Section S3 (t_f =10 mm)

| Section | Position of load | $q_{el}$[KN] | $\mu_{cr}$ | $M_{cr}(KN.m)$ |
|---------|-----------------|--------------|-----------|----------------|
| 3 | Top | 427.721 | $5.42098*10^{-2}$ | 115.85 |
| 3 | Shear Centre | 427.721 | $7.87790*10^{-2}$ | 168.45 |
| 3 | Bottom | 427.721 | 0.12103 | 258.85 |

### Table 5.20 Comparison of the whole considering the effective properties

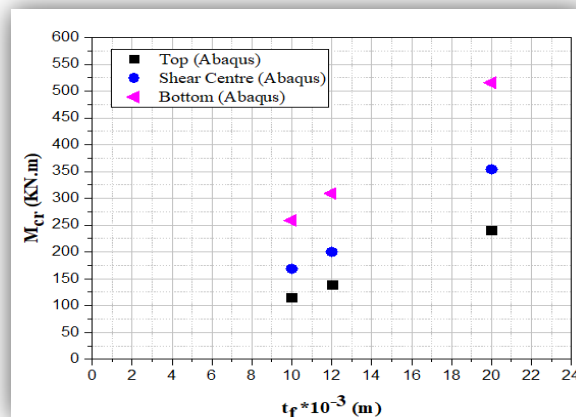| ABAQUS POSITION OF LOAD | S1 | $M_{cr}$ | DIFFERENCE | S2 | $M_{cr}$ | DIFFERENCE | S3 | $M_{cr}$ | DIFFERENCE |
|----------------|------|----------|------------|------|----------|------------|------|----------|------------|
| TOP | | 254.48 | 0.718<1 | | 138.36 | 0.691<1 | | 115.85 | 0.684<1 |
| SHEAR CENTRE | | 354.02 | 1 | | 200.02 | 1 | | 168.45 | 1 |
| BOTTOM | | 537.78 | 1.519>1 | | 309.08 | 1.545>1 | | 258.85 | 1.536>1 |



**Figure 5.12 Results as per ABAQUS of the Variation of M_cr in terms of flange's thickness**

- **Discussion**

The same remarks made in the two-above analysis can be applied to the present analysis by ABAQUS. However, some slight differences can be noticed.

### 5.6 Linear Buckling Analysis with effective characteristics

In the following, a demonstration of the use of ABAQUS for Linear Buckling Analysis (LBA) is presented. A summary of the procedure of defining the model and the steps performed are given.

**1. Part** – defines the geometry of a structural element or model to be used in the analysis.

**2. Property** – defines materials and cross sections.

**3. Assembly** – assembles a number of parts to form the global geometry of a model.

**4. Step** – defines the different analyses to be carried out.

**5. Interaction** – defines connections and interface conditions between different parts.

**6. Load** – defines the boundary conditions of the model.

**7. Mesh** – provides the discretization of the model into finite elements.

**8. Job** – defines the jobs to be carried out by the analysis program.

**9. Visualization** – is utilized for viewing and post processing the results.

**10. Sketch** – can be used as a simple CAD programme for making additional drawings.
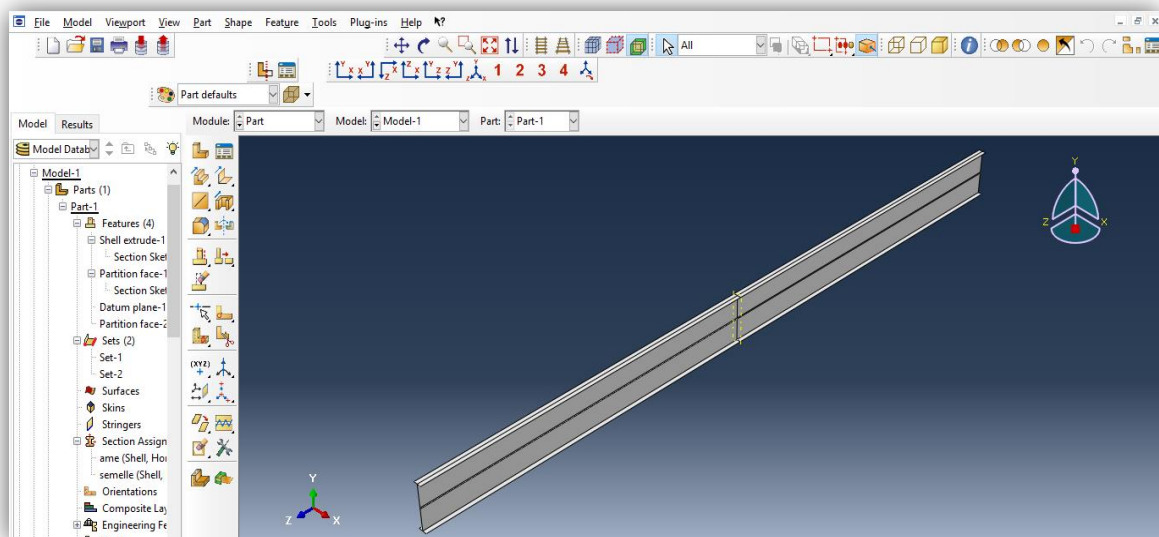

**Defining the geometry**



**Figure 5.13 Typical model**

**Defining the material and cross-sectional properties**
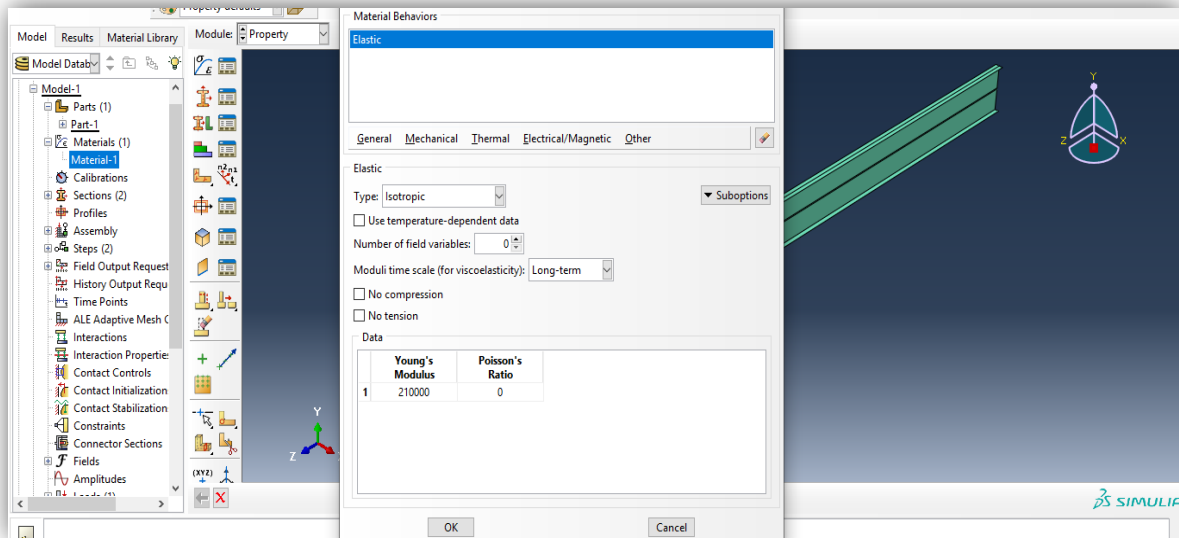
Assigning the values of E= 210000; v =0.3.

**Figure 5.14 Defining material properties**
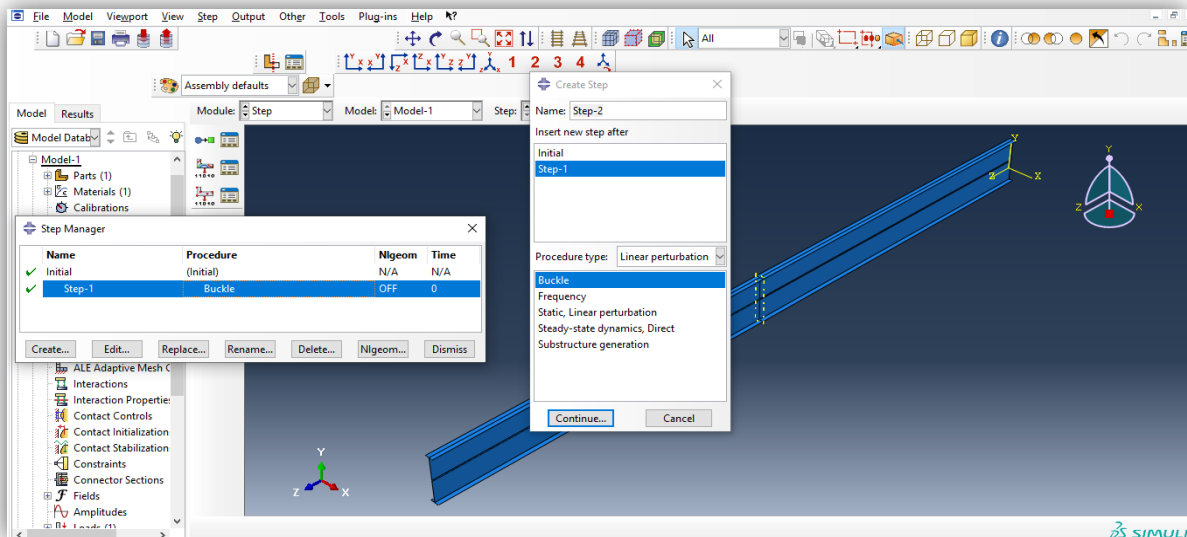
## Setting up the analysis



**Figure 5.15 Setting-up the analysis**

### Defining the boundary conditions Boundary conditions

These conditions are defined in the Load module.

The various boundary conditions are generated in a given Step and may be transferred to subsequent steps, see Figure 5.4.
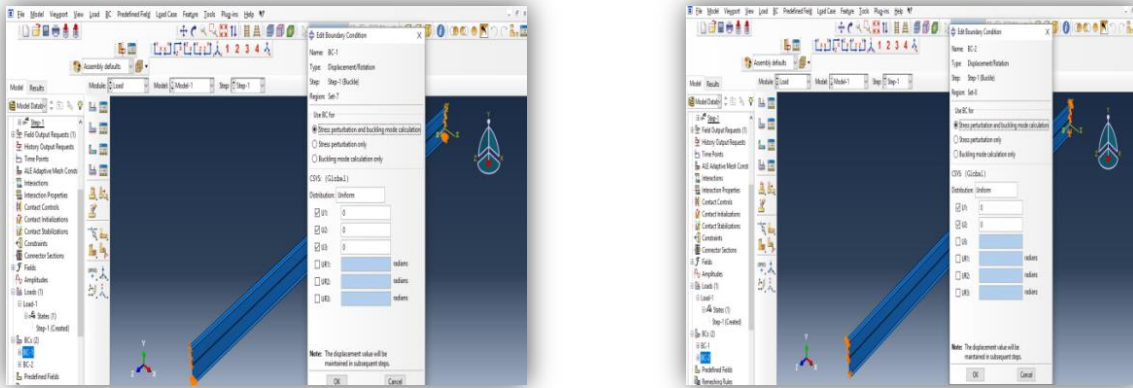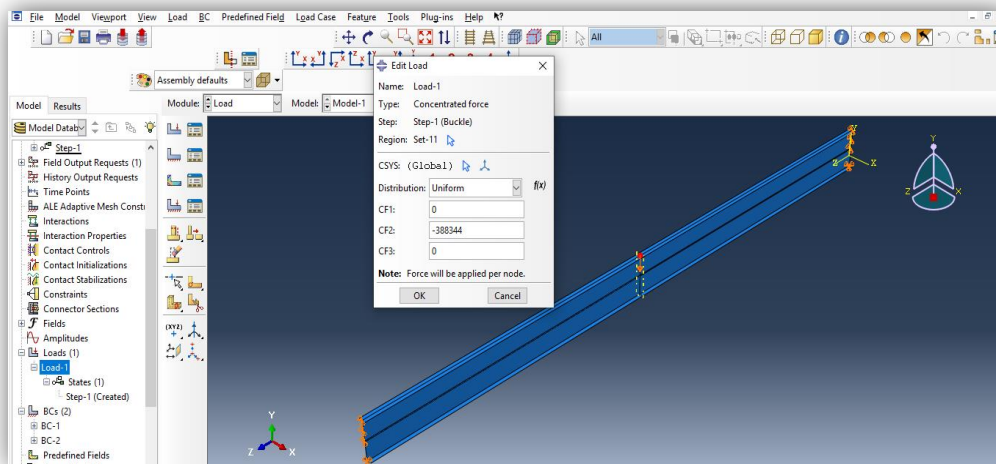
**Figure 5.16 Defining the boundary conditions Boundary conditions**
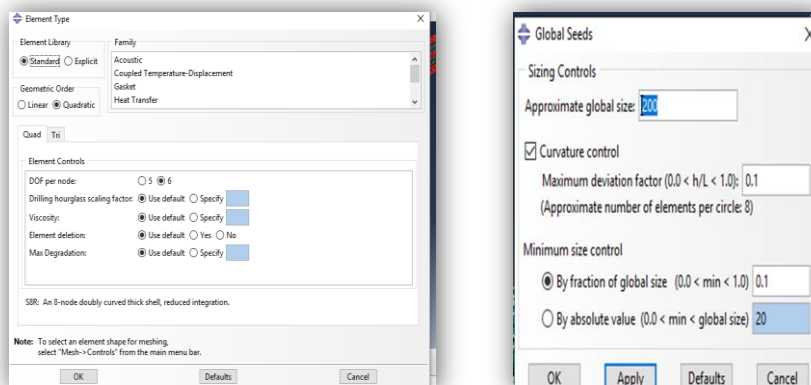
## Defining loads



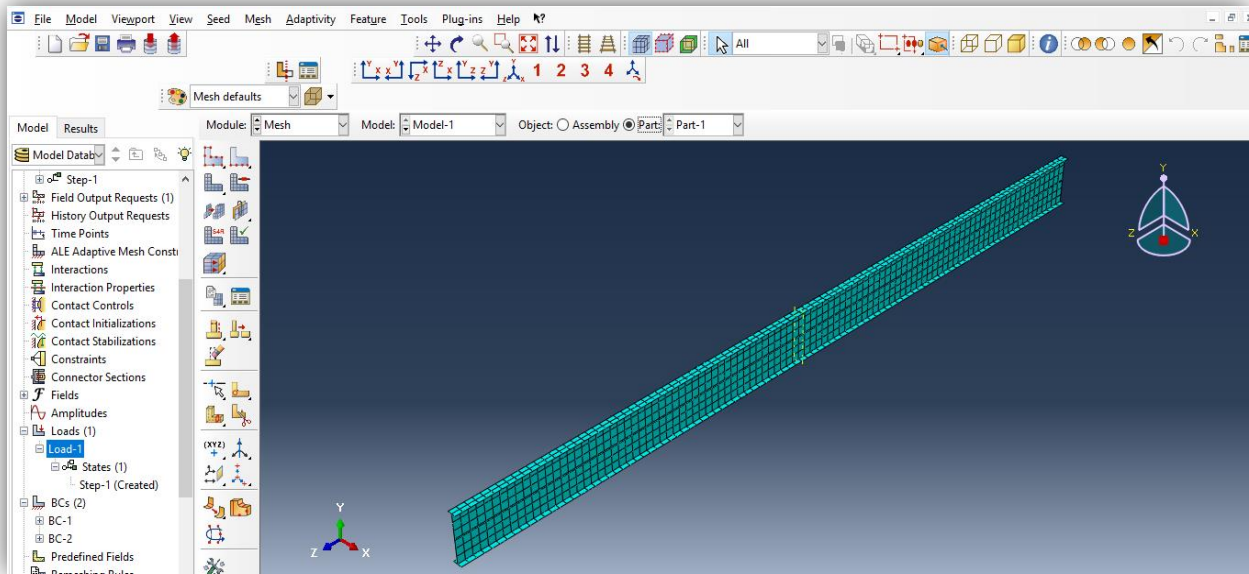**Figure 5.17 Defining the loads**

## Discretization

**Figure 5.18 Discretization**

### Choosing the type of analysis

In the first stage, only the elastic buckling analysis will be selected. This analysis will provide the Eigen values of different buckling modes.

### Running the analysis

In order to submit the analyses to ABAQUS/Standard use the running module. This is the solver, which provides an output database that may later be accessed from ABAQUS/CAE.
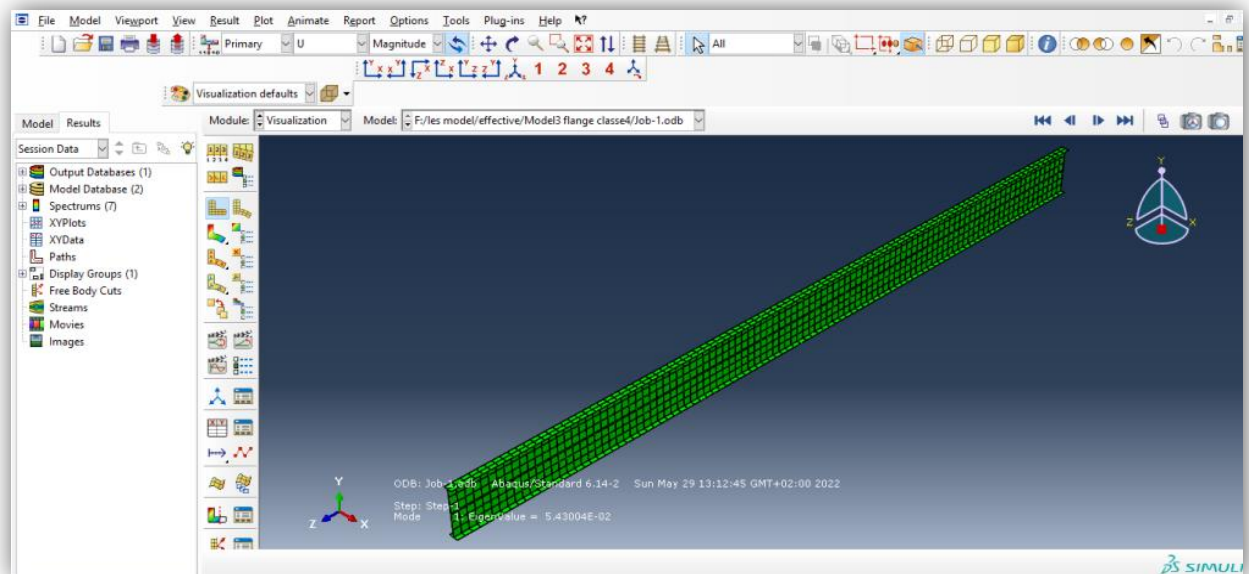
## Visualisation and post- processing of the results



**Figure 5.19 Visualisation and post- processing of the results**
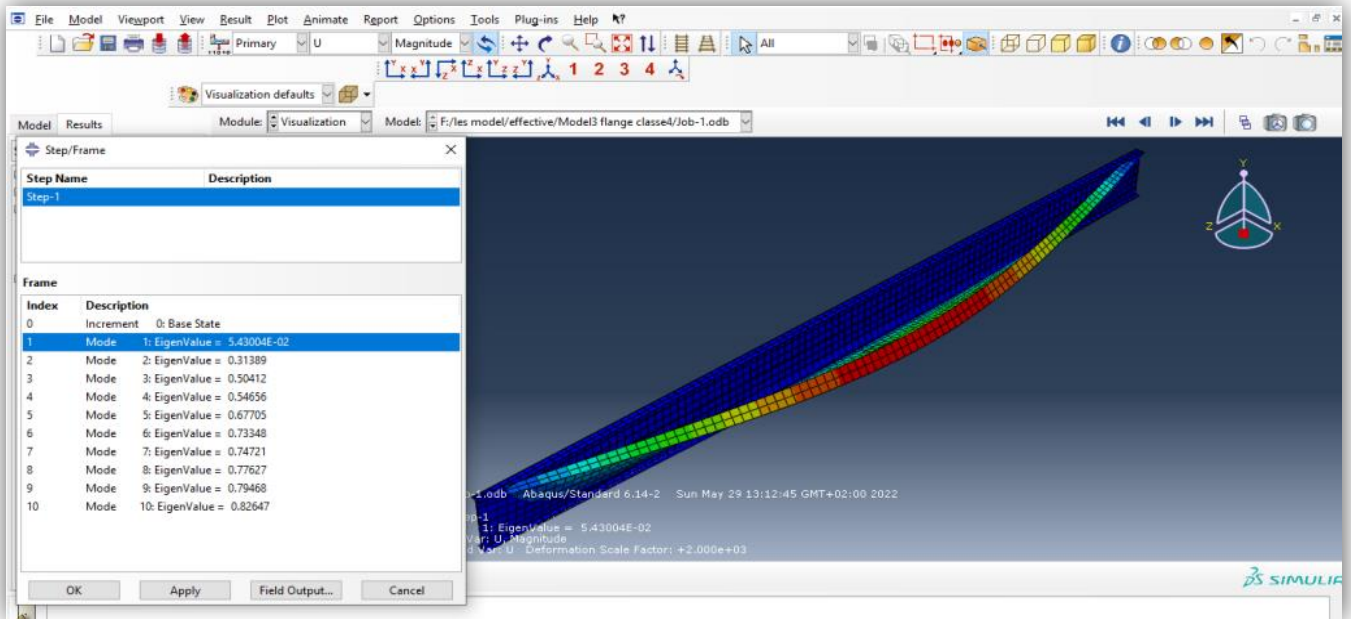
**Result samples of Eigen analysis ; Mode 1**



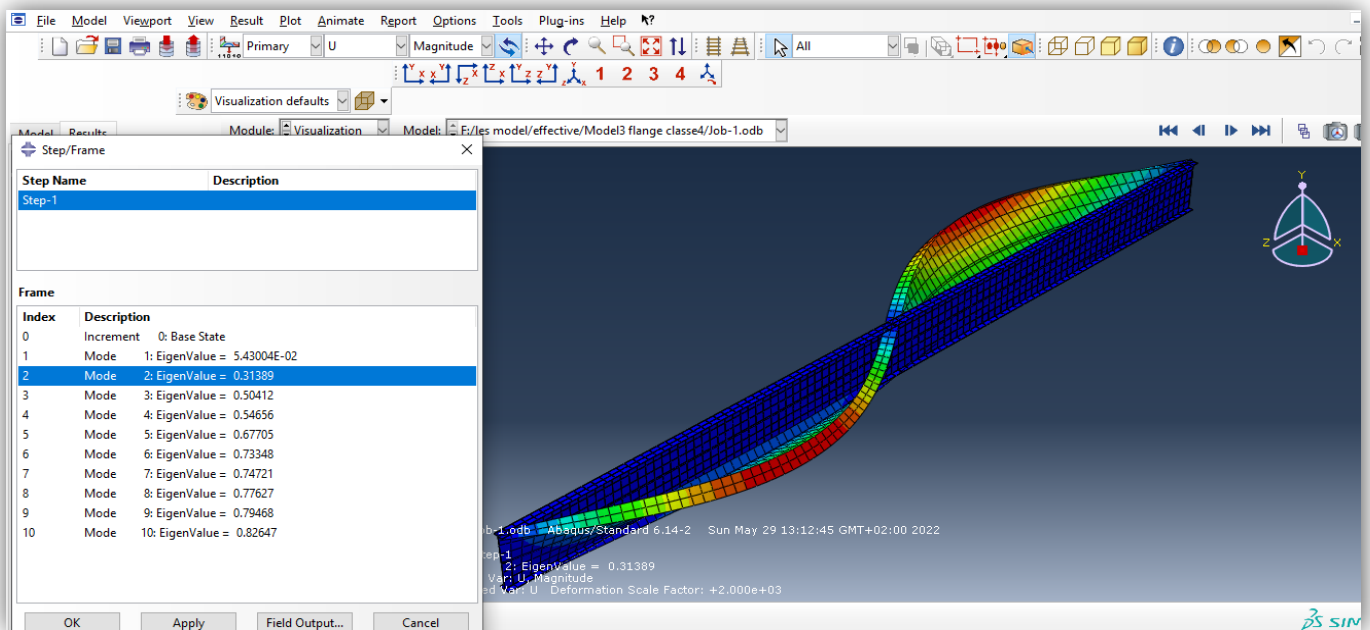Figure 5.20 Linear buckling analysis deformed shape mode 1

**Mode 2**



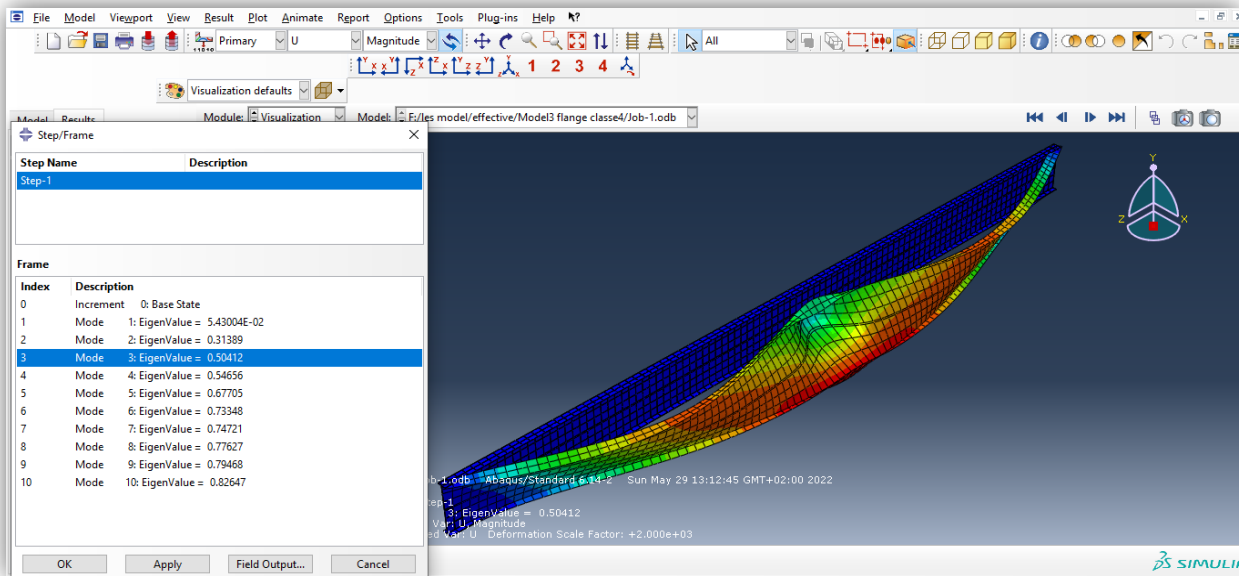Figure 5.21 Linear buckling analysis deformed shape mode 2

**Mode 3**



**Figure 5.22 Linear buckling analysis deformed shape mode3**

- **Results and discussion**

In this section, we calculate the effective critical lateral torsional buckling moment for unrestrained beam with different position of loads that is applied at the top flange, at the shear centre and at the bottom flange for all bi-symmetric sections.

**Table 5.21 Results of Section S1 ($t_f$ =20 mm)**

| Section | Position of load | $q_{el}$[KN] | $\mu_{cr}$ | $M_{cr}(KN.m)$ |
|---------|------------------|--------------|------------|----------------|
| 1 | Top | 619.447 | $8.21665*10^{-2}$ | 254.49 |
| 1 | Shear Centre | 619.447 | 0.11593 | 359.06 |
| 1 | Bottom | 619.447 | 0.17364 | 537.80 |

**Table 5.22 Results of Section S2 ($t_f$ =12 mm)**

| Section | Position of load | $q_{el}$[KN] | $\mu_{cr}$ | $M_{cr}(KN.m)$ |
|---------|------------------|--------------|------------|----------------|
| 2 | Top | 434.119 | $6.37449*10^{-2}$ | 138.36 |
| 2 | Shear Centre | 434.119 | $9.35867*10^{-2}$ | 203.13 |
| 2 | Bottom | 434.119 | 0.14240 | 309.09 |

In this section, we calculate the effective critical lateral torsional buckling moment for restrained beam with different position of loads that is applied at the top flange, at the shear centre and at the bottom flange for all mom-symmetric sections.

The overall results for the elastic linear analysis are shown in tables (5.21 to 5.24), and figure 5.23 depicts the variation of $M_{cr}$ in terms of flange's thickness. Similarly, with changing the geometrical properties from elastic to effective, the tendency of $M_{cr}$ is quite similar and the same remarks can be made as it was discussed in previous section. Once again, the impact of the investigated parameter showed their importance. In fact, one can notice from the above shown results that the values of the effective moment depend mainly on the slenderness of flange, that the position of the applied load. For each section as expected, $M_{cr}$ values depends on the load position with larger values in the bottom flange (tension zone).

### Table 5.23 Results of Section S3 ($t_f$ =10 mm)

| Section | Position of load | $q_{el}$[KN] | $\mu_{cr}$ | $M_{cr}(KN.m)$ |
|---|---|---|---|---|
| 3 | Top | 388.344 | $5.43004*10^{-2}$ | 105.44 |
| 3 | Shear Centre | 388.344 | $7.91957*10^{-2}$ | 153.77 |
| 3 | Bottom | 388.344 | 0.11879 | 230.66 |

### Table 5.24 Comparison of the whole considering the elastic properties

| ABAQUS POSITION OF LOAD | S1 | $M_{cr}$ | DIFFERENCE | S2 | $M_{cr}$ | DIFFERENCE | S3 | $M_{cr}$ | DIFFERENCE |
|---|---|---|---|---|---|---|---|---|---|
| TOP | | 254.49 | 0.708<1 | | 138.36 | 0.681<1 | | 105.44 | 0.685<1 |
| SHEAR CENTRE | | 359.06 | 1 | | 203.13 | 1 | | 153.77 | 1 |
| BOTTOM | | 537.80 | 1.497>1 | | 309.09 | 1.521>1 | | 230.66 | 1.500>1 |

These values decrease when P is applied at the shear centre and less values are found when the applied load is located at the top flange (compressive zone). However, the difference of the amount of Mcr varies from S1 to S3. In fact, the differences are being quasi- constant ranging from around 0.7 in the compressive flanges to 1.50 for tension flanges.
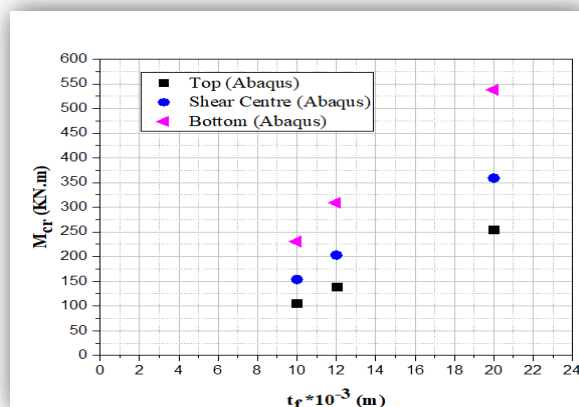


**Figure 5.23 Results as per ABAQUS of the Variation of $M_{cr}$ in terms of flange's thickness**

### 5.7 Overall comparison and conclusions of the linear elastic buckling analysis

In this chapter the results of linear elastic buckling analysis have been presented and individually discussed. It is worth to recall that three means have been used: EC3 analytical, LTBEAM and ABAQUS. The comparison of results reveals the importance and the impact of the investigated parameters on the carrying capacity of the cross-sections S1, S2 and S3.

Tables 5.25 To 5.27 show the obtained values from EC3, LTBEAM and ABAQUS for S1, S2 and S3 respectively using the elastic characteristics. These values of $M_{cr}$ are given in terms of load position: upper flange, at the shear centre and the lower flange.

As it can be easily noticed, values of $M_{cr}$, despite the mean by which is was determined are almost the same. Particularly for the finite element software where no sensitive difference has been detected.

**Table 5.25 Variation of $M_{cr}$ between EC3 LTBEAM and ABAQUS When P is applied the at the upper flange**

| POSITION OF LOAD | S1 | $M_{cr}$ | DIFFERENCE | S2 | $M_{cr}$ | DIFFERENCE | S3 | $M_{cr}$ | DIFFERENCE |
|---|---|---|---|---|---|---|---|---|---|
| TOP | | | | | | | | | |
| EC3 | | 254.49 | 1.038 | | 127.20 | 0.974 | | 106.09 | 0.974 |
| | | | 1.006 | | | 0.919 | | | 0.915 |
| LTBEAM | | 245.09 | 0.963 | | 130.52 | 1.026 | | 108.91 | 1.026 |
| | | | 1.019 | | | 0.943 | | | 0.940 |
| ABAQUS | | 240.43 | 0.944 | | 138.36 | 1.087 | | 115.85 | 1.091 |
| | | | 0.980 | | | 1.060 | | | 1.063 |

**Table 5.26 Variation of $M_{cr}$ between EC3 LTBEAM and ABAQUS when P is applied the at the SC**

| POSITION OF LOAD | S1 | $M_{cr}$ | DIFFERENCE | S2 | $M_{cr}$ | DIFFERENCE | S3 | $M_{cr}$ | DIFFERENCE |
|---|---|---|---|---|---|---|---|---|---|
| SHEAR CENTRE | | | | | | | | | |
| EC3 | | 358.25 | 0.999 | | 194.79 | 0.991 | | 162.27 | 0.990 |
| | | | 1.011 | | | 0.973 | | | 0.963 |
| LTBEAM | | 358.41 | 1.000 | | 196.51 | 1.008 | | 163.80 | 1.009 |
| | | | 1.012 | | | 0.982 | | | 0.972 |
| ABAQUS | | 354.02 | 0.988 | | 200.02 | 1.026 | | 168.45 | 1.038 |
| | | | 0.987 | | | 1.017 | | | 1.028 |

**Table 5.27 Variation of M_cr between EC3 LTBEAM and ABAQUS when P is applied the at the lower flange**

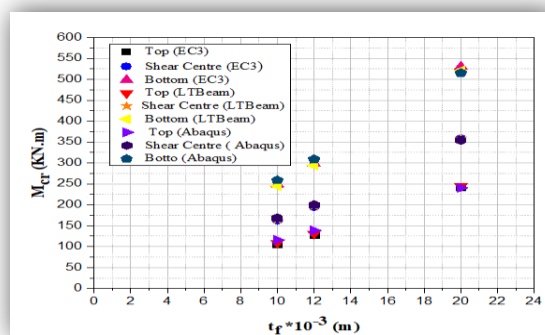| POSITION OF LOAD | S1 | $M_{cr}$ | DIFFERENCE | S2 | $M_{cr}$ | DIFFERENCE | S3 | $M_{cr}$ | DIFFERENCE |
|---|---|---|---|---|---|---|---|---|---|
| BOTTOM | | | | | | | | | |
| EC3 | | 530.38 | 1.018 | | 298.25 | 1.014 | | 248.41 | 1.014 |
| | | | 0.986 | | | 0.964 | | | 0.959 |
| LTBEAM | | 520.98 | 0.982 | | 294.02 | 0.985 | | 244.86 | 0.985 |
| | | | 0.968 | | | 0.951 | | | 0.945 |
| ABAQUS | | 537.80 | 1.013 | | 309.08 | 1.036 | | 258.85 | 1.054 |
| | | | 1.032 | | | 1.051 | | | 1.057 |



**Figure 5.24 Variation of M_cr between EC3 LTBEAM and ABAQUS When P is applied the at the upper flange, shear centre and lower flange**

### 5.8 COMPARISON EFFECTIVE (EC3, LTBEAM and ABAQUS)

Tables 5.28 To 5. 30 show the obtained values from EC3, LTBEAM and ABAQUS for S1, S2 and S3 respectively using the effective characteristics. These values of $M_{cr}$ are given in terms of load position: upper flange, at the shear centre and the lower flange.

As it can be easily noticed, values of $M_{cr}$, despite the mean by which is was determined are almost the same. Particularly for the finite element software where no sensitive difference has been detected.

**Table 5.28 Variation of M_cr between EC3 LTBEAM and ABAQUS when P is applied the at the upper flange**

| POSITION OF LOAD | S1 | $M_{cr}$ | DIFFERENCE | S2 | $M_{cr}$ | DIFFERENCE | S3 | $M_{cr}$ | DIFFERENCE |
|---|---|---|---|---|---|---|---|---|---|
| TOP | | | | | | | | | |
| EC3 | | 245.18 | 0.987 | | 129.45 | 0.974 | | 97.88 | 0.939 |
| | | | 0.963 | | | 0.935 | | | 0.928 |
| LTBEAM | | 248.40 | 1.013 | | 132.85 | 1.026 | | 104.16 | 1.064 |
| | | | 0.976 | | | 0.960 | | | 0.987 |
| ABAQUS | | 254.49 | 1.037 | | 138.36 | 1.068 | | 105.44 | 1.077 |
| | | | 1.024 | | | 1.041 | | | 1.012 |

### Table 5.29 Variation of M<sub>cr</sub> between EC3 LTBEAM and ABAQUS when P is applied the at the SC

| POSITION OF LOAD SHEAR CENTRE | S1 | $M_{cr}$ | DIFFERENCE | S2 | $M_{cr}$ | DIFFERENCE | S3 | $M_{cr}$ | DIFFERENCE |
|---|---|---|---|---|---|---|---|---|---|
| EC3 | | 363.40 | 0.999 | | 198.77 | 0.992 | | 149.42 | 0.954 |
| | | | 1.012 | | | 0.978 | | | 0.971 |
| LTBEAM | | 363.55 | 1.000 | | 200.28 | 1.007 | | 156.56 | 1.047 |
| | | | 1.012 | | | 0.985 | | | 1.018 |
| ABAQUS | | 359.06 | 0.988 | | 203.13 | 1.021 | | 153.77 | 1.029 |
| | | | 0.987 | | | 1.014 | | | 0.982 |

### Table 5.30 Variation of M<sub>cr</sub> between EC3 LTBEAM and ABAQUS when P is applied the at the lower flange

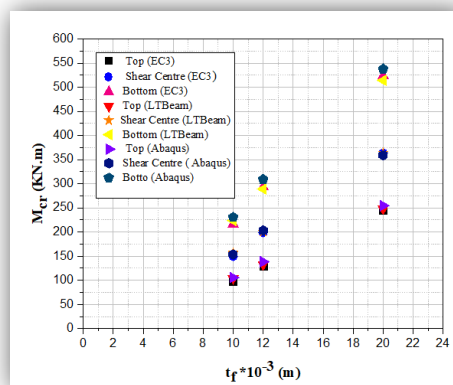| POSITION OF LOAD BOTTOM | S1 | $M_{cr}$ | DIFFERENCE | S2 | $M_{cr}$ | DIFFERENCE | S3 | $M_{cr}$ | DIFFERENCE |
|---|---|---|---|---|---|---|---|---|---|
| EC3 | | 523.37 | 1.017 | | 293.05 | 1.013 | | 216.09 | 0.966 |
| | | | 0.973 | | | 0.948 | | | 0.936 |
| LTBEAM | | 514.18 | 0.982 | | 289.01 | 0.935 | | 223.53 | 1.034 |
| | | | 0.956 | | | 0.935 | | | 0.969 |
| ABAQUS | | 537.80 | 0.027 | | 309.09 | 1.054 | | 230.66 | 1.067 |
| | | | 1.045 | | | 1.069 | | | 1.031 |



### Figure 5.25 Variation of M<sub>cr</sub> between EC3 LTBEAM and ABAQUS When P is applied the at the upper flange, shear centre and lower flange
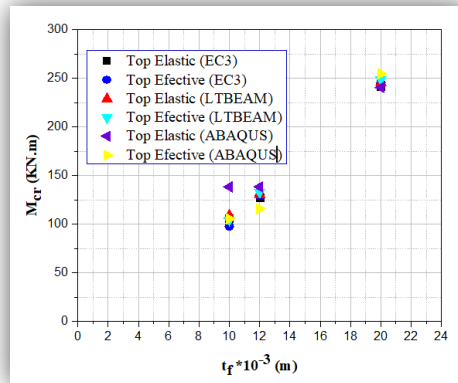
## 5.8 Comparison (ELASTIC and EFFECTIVE)



**Figure 5.26 Variation of $M_{cr}$ between EC3 LTBEAM and ABAQUS When P is applied the at the upper flange with elastic and effective characteristics**
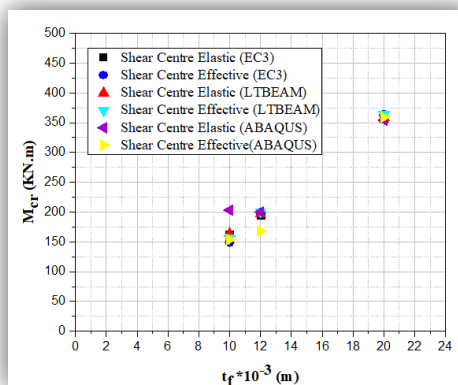


**Figure 5.27 Variation of $M_{cr}$ between EC3 LTBEAM and ABAQUS When P is applied the at the SC with elastic and effective characteristics**
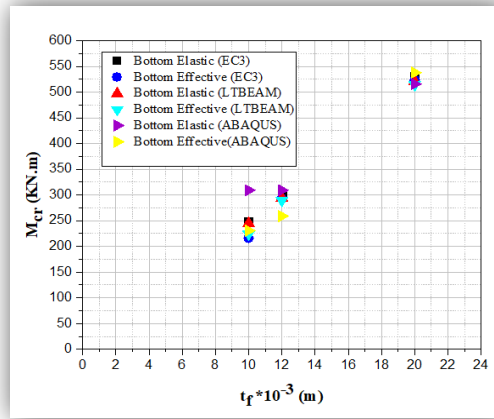
**Figure 5.28 Variation of M$_{cr}$ between EC3 LTBEAM and ABAQUS When P is applied the at the lower flange with elastic and effective characteristics**

**Table 5.31 Variation of M$_{cr}$ EC3 LTBEAM and ABAQUS when P is applied the at the upper flange considering elastic and effective characteristics**

| POSITION OF LOAD | ELASTIC | | EFFECTIVE | | DIFFERENCE | ELASTIC | | EFFECTIVE | | DIFFERENCE | ELASTIC | | EFFECTIVE | | DIFFERENCE |
|---|---|---|---|---|---|---|---|---|---|---|---|---|---|---|---|
| TOP | S1 | $M_{cr}$ | S1 | $M_{cr}$ | | S2 | $M_{cr}$ | S2 | $M_{cr}$ | | S3 | $M_{cr}$ | S3 | $M_{cr}$ | |
| EC3 | 241.98 | | 245.18 | | 0.986 | 127.20 | | 129.45 | | 0.982 | 106.09 | | 97.88 | | 1.083 |
| LTBEAM | 245.09 | | 248.40 | | 0.986 | 130.52 | | 132.85 | | 0.982 | 108.91 | | 104.16 | | 1.045 |
| ABAQUS | 254.49 | | 254.49 | | 1.000 | 138.36 | | 115.85 | | 1.194 | 138.36 | | 105.44 | | 1.312 |

**Table 5.32 Variation of M$_{cr}$ EC3 LTBEAM and ABAQUS when P is applied the at the SC considering elastic and effective characteristics**

| POSITION OF LOAD | ELASTIC | | EFFECTIVE | | DIFFERENCE | ELASTIC | | EFFECTIVE | | DIFFERENCE | ELASTIC | | EFFECTIVE | | DIFFERENCE |
|---|---|---|---|---|---|---|---|---|---|---|---|---|---|---|---|
| SHEAR CENTRE | S1 | $M_{cr}$ | S1 | $M_{cr}$ | | S2 | $M_{cr}$ | S2 | $M_{cr}$ | | S3 | $M_{cr}$ | S3 | $M_{cr}$ | |
| EC3 | 358.25 | | 363.40 | | 0.985 | 194.79 | | 198.77 | | 0.979 | 162.27 | | 149.42 | | 1.085 |
| LTBEAM | 358.41 | | 363.55 | | 0.985 | 196.51 | | 200.28 | | 0.981 | 163.80 | | 156.56 | | 1.046 |
| ABAQUS | 354.02 | | 359.06 | | 0.985 | 200.02 | | 168.45 | | 1.187 | 203.13 | | 153.77 | | 1.320 |

**Table 5.33 Variation of M$_{cr}$ EC3 LTBEAM and ABAQUS when P is applied the at the lower flange considering elastic and effective characteristics**

| POSITION OF LOAD | ELASTIC | | EFFECTIVE | | DIFFERENCE | ELASTIC | | EFFECTIVE | | DIFFERENCE | ELASTIC | | EFFECTIVE | | DIFFERENCE |
|---|---|---|---|---|---|---|---|---|---|---|---|---|---|---|---|
| BOTTOM | S1 | $M_{cr}$ | S1 | $M_{cr}$ | | S2 | $M_{cr}$ | S2 | $M_{cr}$ | | S3 | $M_{cr}$ | S3 | $M_{cr}$ | |
| EC3 | 530.38 | | 523.37 | | 1.013 | 298.25 | | 293.05 | | 1.017 | 248.41 | | 216.09 | | 1.149 |
| LTBEAM | 520.98 | | 514.18 | | 1.013 | 294.02 | | 289.01 | | 1.017 | 244.86 | | 223.53 | | 1.095 |
| ABAQUS | 537.80 | | 537.80 | | 1.000 | 309.08 | | 258.85 | | 1.194 | 309.09 | | 230.66 | | 1.340 |

### 5.9 Discussion and concluding remarks

As far as the elastic buckling analysis is concerned, it has been demonstrated trough the outcomes of this study the importance of each parameter. Some general conclusions can be made, namely:

-        What ever the mean used for determining the M$_{cr}$, similar values have been extracted.

-        The analytical equation given in EC3 does give accurate prediction, with less effort, of M$_{cr}$. Thus, EC3 can be used safely in the design process.

-        Finite element packages do not have the concept of classification recommended by EC3.

-        The class of the flange being of S1 and S2, no notable differences between the elastic and effective properties with bi-symmetric sections have been remarked. As if the class of flange does not influence the overall resistance to LTB of sections. However, for S3 where the flange class is 4, the cross-section is mono-symmetric   some differences can be noticed.

-        The position of the applied load has an important effect on the M$_{cr}$ value.

-        The eigen analysis performed by LTBEAM and ABAQUS give roughly the same values specially for the first buckling mode. This will give a more confidence to the ABAQUS model, as it will be used later on for more sophisticate analysis: inelastic buckling analysis taking into account the imperfection.

# $C$HAPTER 6:

# RESULTS AND DISCUSSION OF THE INELASTIC BUCKLING ANALYSIS OF SLENDER SECTIONS

### 6.1 Introduction

In this chapter, an introduction to the inelastic buckling analysis background is given. A full second order analysis takes into account the material non-linearity and geometric deformation. This second order analysis is essential when the buckling behaviour is influenced by the modified geometry of the structure under load. However, the axial strain in the arch members will cause the arch to flatten, which increases the axial forces and strains. The inelastic buckling models are built-up in Abaqus to investigate the impact of lateral torsional buckling on the carrying capacity of slender sections is provide and discussed.

### 6.2 Inelastic buckling analysis (GMNL)

When studying the behaviour of steel beam resistance to LTB instability, a geometrical and material non-linear imperfection analysis (GMNL) is carried out. To determine the lateral torsional buckling resistance of the beam as it considered to give most true lateral torsional buckling resistance of beam. Also, as explained in the previous section, the first order buckling analysis would only give eigenvectors for buckling modes related to the original geometry. The buckling instability, the load-displacement response shows a negative stiffness and the structure must release strain energy to remain in equilibrium( Figure 6.1). Therefore, it is important that a solution method is chosen that can predict the load-displacement response after lateral torsional buckling has occurred.
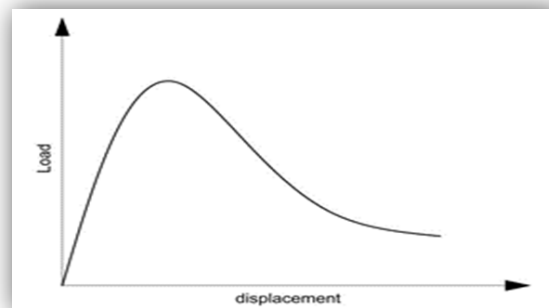


**Figure 6.1 Possible non-linear buckling load-displacement behaviour**

### 6.3 Modelling the nonlinear behaviour using ABAQUS

The theoretical background of such solution can be the modified Riks method or arc-length method. In ABAQUS, this is an algorithm which provides effective solutions for such cases. The modified Riks method uses a tangent line of a function to intersect with an arc, situated at the end of every step. From this point on, the curve will converge over the arc-length until it reaches an intersection of the arc with the function. At this point, the step is completed and the process will continue with the next step (Figure 6.2).
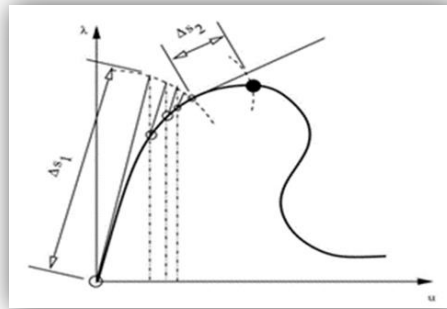
**Figure 6.2 Graphical example of the modified RIKS method**

In addition to the linear elastic model, the non-linear plastic model also includes the plastic material properties.

## 6.4 Material properties

(1) Material properties should be taken as characteristic values.

(2) Depending on the accuracy and the allowable strain required for the analysis the following assumptions for the material behaviour may be used, see (Figure 6.3):

a) elastic-plastic without strain hardening

b) elastic-plastic with a nominal plateau slope

c) elastic-plastic with linear strain hardening

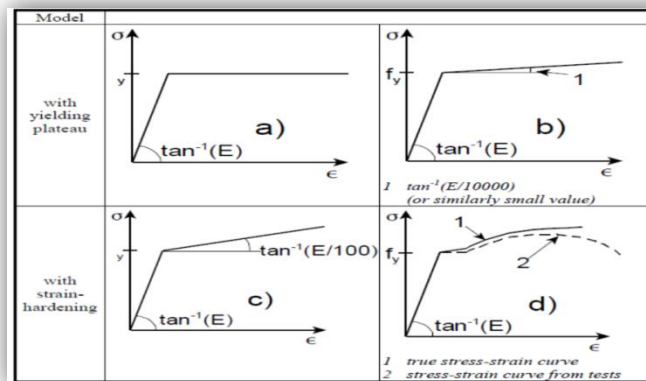d) true stress-strain curve modified from the test results as follows



**Figure 6.3 Modelling of material behaviour [Eurocode 3: Design of steel structures]**

$$\sigma_{true} = \sigma\,(1+\varepsilon)$$
$$\varepsilon_{true} = \ell n\,(1+\varepsilon)$$

## 6.5 Demonstration

In the following, a demonstration how to perform Riks approach implanted in ABAQUS.
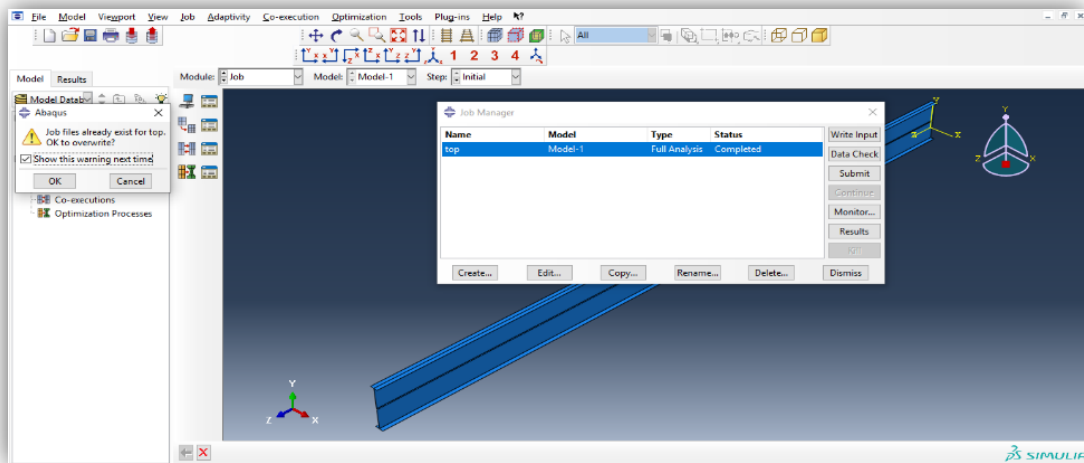
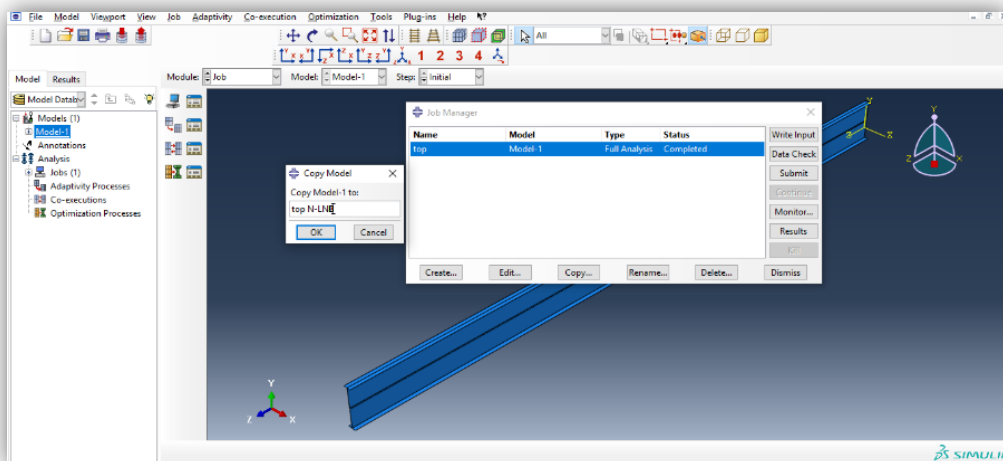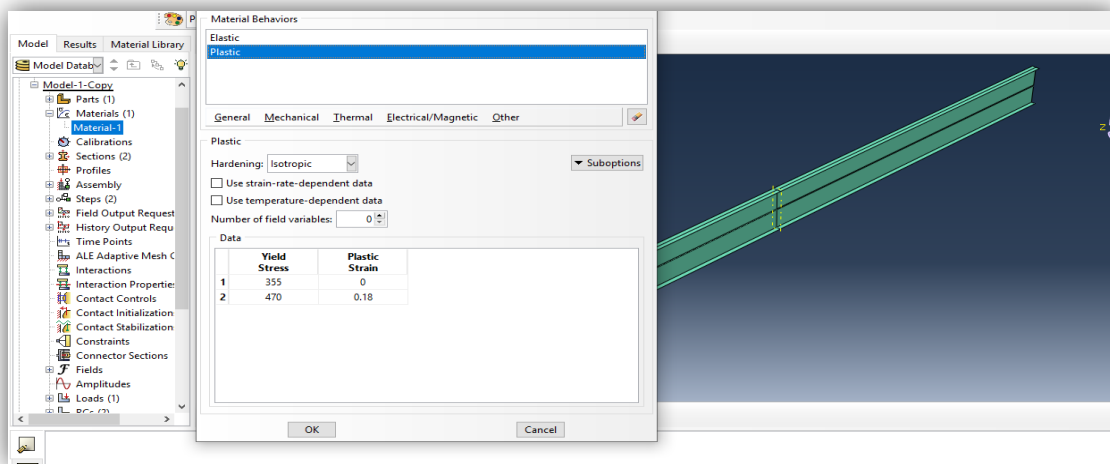**Figure 6.4 Executing the linear buckling analysis**



**Figure 6.5 Copy the model**
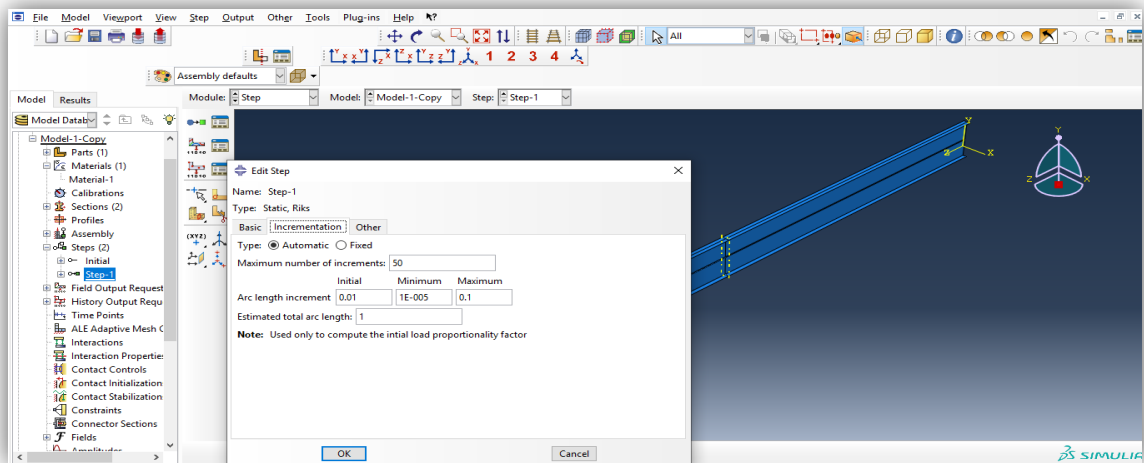


**Figure 6.6 Material properties**

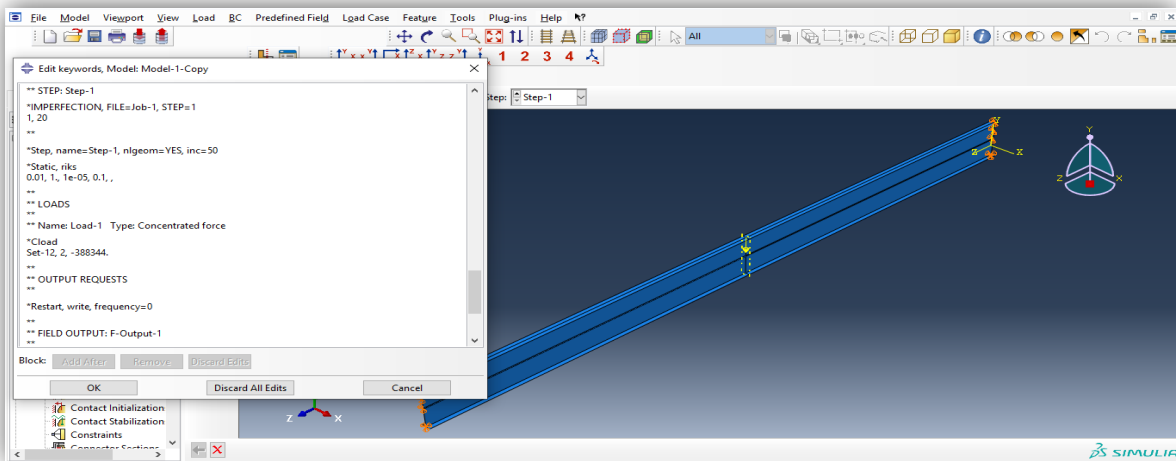**Figure 6.7 Performing RIKS analysis**



**Figure 6.8 Introducing the imperfection as per EC3 (1/1000)**
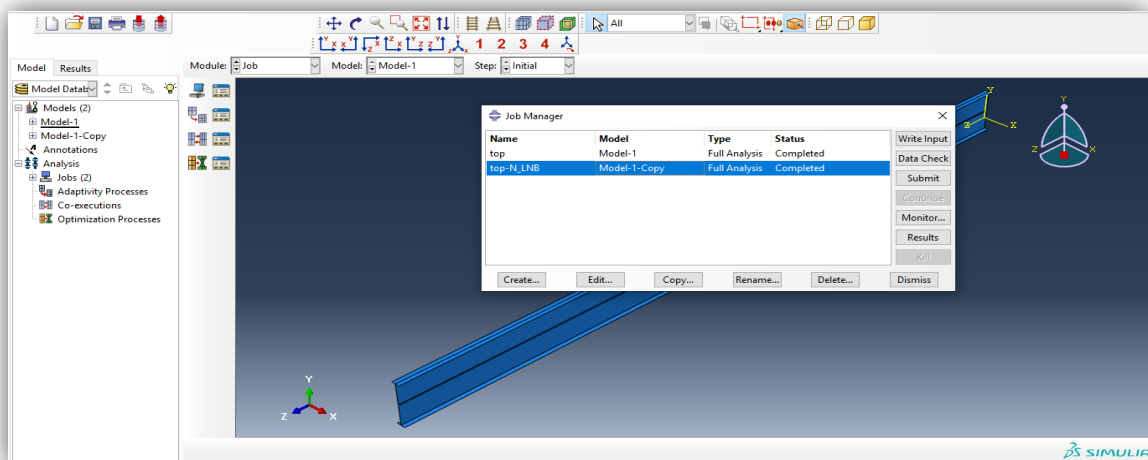


**Figure 6.9 Submitting the file**
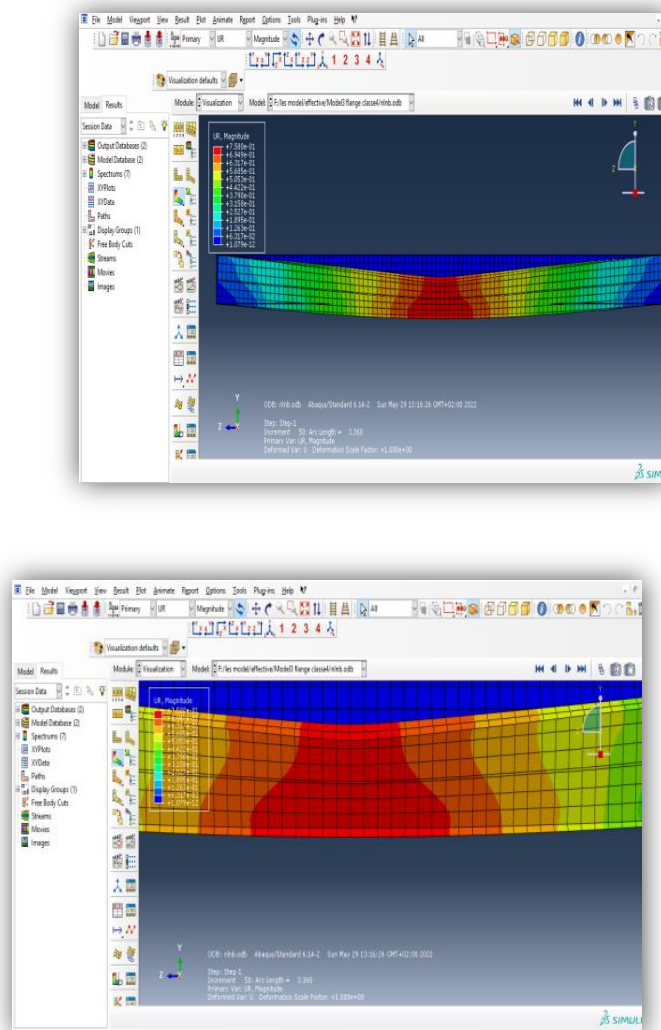
**Samples of results (Ur)**





**Figure 6.11 Deformed shape at ultimate increment**

### 6.6 Results and Discussion

The discussion will be held on the basis of the derived load-deflection curves from the modified RIKS analysis implanted in ABAQUS. Another discussion will be provided dealing with the ultimate of displacements. Hence, for each single step, the displacement and stiffness matrices are updated, with the inclusion of initial geometrical imperfection which is liable to generate torsion and/or lateral bending is obviously of concern, and normally with residual stresses (not considered in this study). Tables 6.

First of all, it should be noted that both load and boundary conditions have very important effects on the inelastic LTB failure mode results. The results from the modified RIKS method are given in terms of load proportionality factor $\lambda$ (LPF). In order to determine the actual critical load after

which the instability occurs, the applied load needs to be multiplied by the LPF λ. In Table, the load proportionality factor (LPF) and the actual critical load of unrestrained beam given.

Figures 6.12 and 6.13 show the outcomes during the whole loading history by considering three load positions with an elastic branch for elastic behaviour and then the beams behave nonlinearly due to the initial geometric imperfections and the nonlinear geometric and material.

Figures 6.12 (a), (b) and (c), for S1 to S3 respectively, retrace the Loads – Lateral deflections curves extracted from the modified RIKS results in terms of load application locations. taking into account the elastic geometrical properties. While Figures 6.13 (a), (b) and (c) represent the case of effective properties. Despite the fact that all considered sections are classified as class 4 to EC3, in the contrary to the linear buckling analysis discussed in the previous chapter, major differences in their behaviours can be seen as depicted in Figures 6.12 to 6.13 (a), (b) and (c). Independently of the used geometric properties, S1 shows quiet-different behaviour compared to S2 and S3 with flanges belonging to class 3 and 4 respectively.

For the particular cases of S2 and S3, it is evident from Figures 6.12 and 6.13 that linear load-deflection behaviour exists before inelastic lateral buckling starts to occur. It is obvious that varying flange slenderness, the member capacity is governed by the inelastic capacity, as mentioned in the previous section a soft decrease in stiffness in the post-buckling behaviour can be observed.

In fact, all considered sections show almost the same behaviour in the elastic range, with of course different value of $P_{cr}$ with larger values for S1 to S3 which can be attributed to the flange class. Thus, for sections loaded at the top flange, in the compressive zone, the values of $P_{cr}$ decrease from 50.89 kN to 27.67 and 23.19 kN for S1, S2 and S3 respectively. For sections loaded at the shear centre, the values of $P_{cr}$ decrease from 70.80 kN to 40 and 33.69 kN for S1, S2 and S3 respectively. Thus, for sections loaded at the bottom flange, in the tension zone, the values of $P_{cr}$ decrease from 107.55 kN to 61.81 and 51.76 kN for S1, S2 and S3 respectively.

Considering the obtained effective geometric properties, the same remarks can be made. With exception that in the case of S3 (i.e. web and flanges of class 4). In fact, for the cases of S1and S2 similar results have been found but with larger lateral displacements, the beam is weaker because of less lateral stiffness. For S3, $P_{cr}$ increases from 21.08 kN to 30.75 and 46.13 kN for load being localised in the top, at SC and at the bottom flange respectively. Compared to the above values, it can be seen that S3 with effective properties is weaker than it was with the elastic properties. In all considered cases, an almost the same behaviour in the elastic range, with of course different value of $P_{cr}$ with larger values for S1 to S3. For sections loaded at the shear centre, the values of $P_{cr}$ decrease from 70.80 kN to 40 and 33.69 kN for S1, S2 and S3 respectively. Thus, for sections loaded at the

bottom flange, in the tension zone, the values of $P_{cr}$ decrease from 107.55 kN to 61.81 and 51.76 kN for S1, S2 and S3 respectively. These values show the undeniable effects of the flange class and load location. In fact, with flange belonging to class 1 aids considerably the carrying capacity of the section to LTB. This strength decreases as the flanges slenderness's increase to about twice lesser for S3.

As can be easily seen, for the case of S2 and S3, two distinct branches curves characterized by linear pre-critical behaviour for the first branch and an inelastic post-buckling behaviour is recognised in the second branch. The second part of curves show a decrease in the stiffness of the beam. The load-lateral deflection curve starts to soften which means that the capability to resist LTB starts to degrade. The observed tendency of all studied I-beams subject to LTB to twist about their longitudinal axis and is suspected that such I-beams contain a form of negative rotational stiffness about their longitudinal axis.
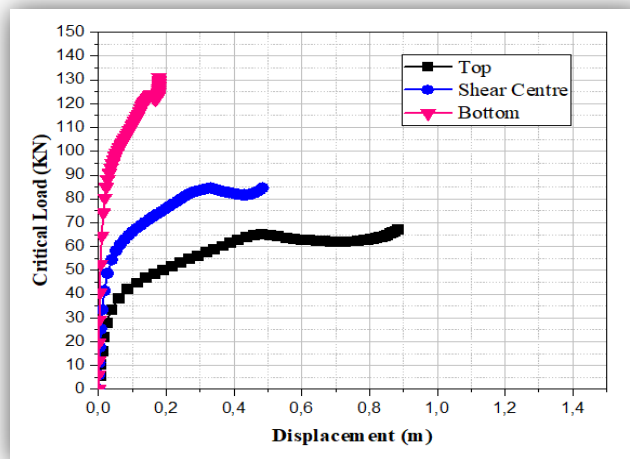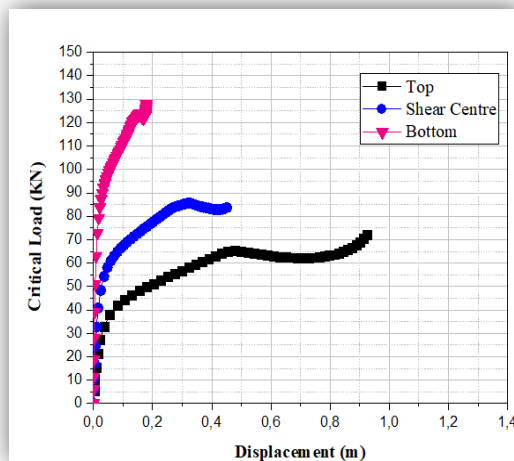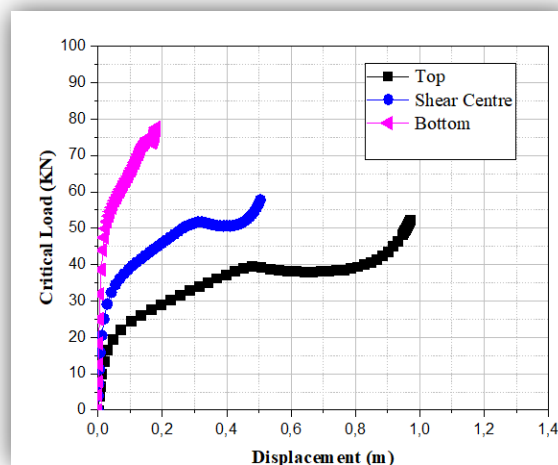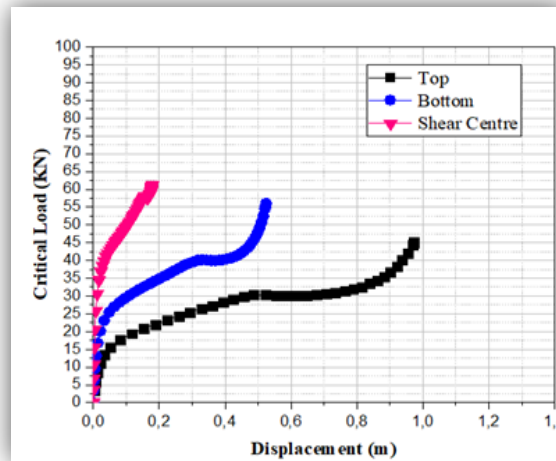


(a)
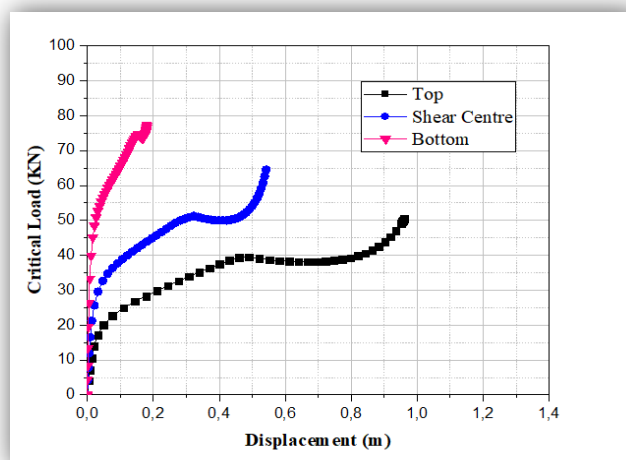


**(b)**
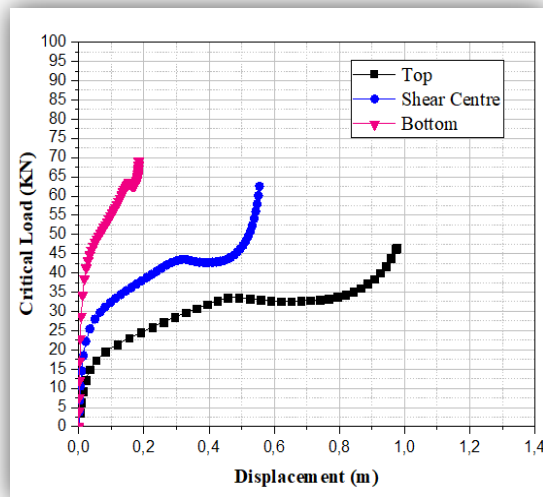
(c)

**Figure 6.12 Load- lateral displacement curves with a=S1, b=S2 and c=S3 to elastic properties**



**(a)**



**(b)**

**(c)**

**Figure 6.13 Figure 6.12 Load- lateral displacement curves with a=S1, b=S2 and c=S3 to effective properties**

## 6.7 Comparison

### 6.7.1 Comparison considering elastic characteristics

In the contrary of the conclusions made on the elastic buckling analysis in chapter 5, as the LTB is mainly bending behaviour, the class of flange plays an important role. In fact, as shown in Table 6.1 and Figure 6.14, providing flanges of class 1, the strength of the section, even class 4, has shown a full resistance to LTB. For sections S2 and S3, a decrease of the values of $P_{cr}$ to almost the half for upper flange loaded with similar behaviour in elastic range.

The same tendency can be remarked in Tables 6.2, Table 6.3 and Figures 6.15, 6.16 for section loaded in SG and at lower flange respectively.

**Table 6.1 Variation of $P_{cr}$ applied at the top for S1, S2 and S3**

| Position of load TOP | $P_{cr}$ | DIFFERENCE |
|---|---|---|
| S1 | 50.89 | 1.839 |
| | | 2.194 |
| S2 | 27.67 | 0.543 |
| | | 1.193 |
| S3 | 23.19 | 0.455 |
| | | 0.838 |
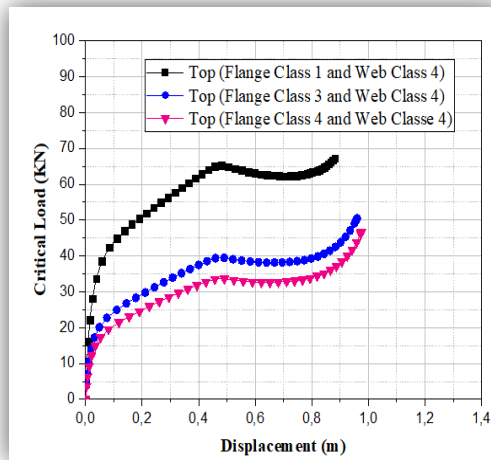
**Figure 6.14 Comparison of results with applied load at the top for S1, S2 and S3**

**Table 6.2 Variation of $P_{cr}$ applied at the SG for S1, S2 and S3**

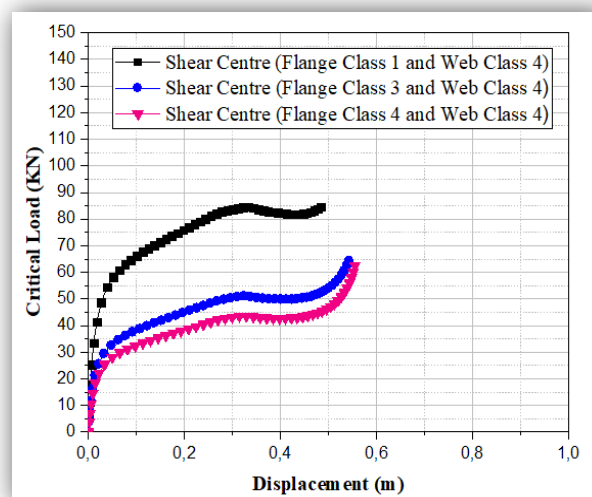| POSITION OF LOAD SHEAR CENTRE | $P_{cr}$ | DIFFERENCE |
|---|---|---|
| S1 | 70.80 | 1.77 |
| | | 2.101 |
| S2 | 40.00 | 0.564 |
| | | 1.187 |
| S3 | 33.69 | 0.475 |
| | | 0.842 |



**Figure 6.15 Figure 6.14 Comparison of results with applied load at SG for S1, S2 and S3**

### Table 6.3 Differences in $P_{cr}$ prediction of S1, S2 and S3 at the bottom

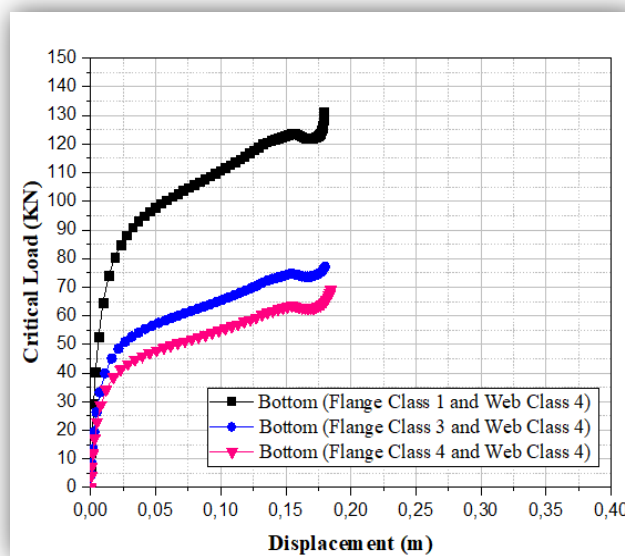| POSITION OF LOAD BOTTOM | $P_{cr}$ | DIFFERENCE |
|---|---|---|
| S1 | 107.55 | 1.740 |
|  |  | 2.077 |
| S2 | 61.81 | 0.574 |
|  |  | 1.194 |
| S3 | 51.76 | 0.481 |
|  |  | 0.837 |



**Figure 6.16 Figure 6.14 Comparison of results with applied load at the bottom for S1, S2 and S3**

### 6.7.2 Comparison considering the calculated effective characteristics

In models with effective properties, the same conclusions made be drawn as in the previous section with slightly different behaviour and values. Tables 6.4, 6.5 and 6.6, Figures 6.17, 6.18 and 6.19 give the general tendency of the elastic and inelastic LTB behaviour. Better performance of S1 can be noticed followed by S2 and at last S3 showed poorer behaviour with regard to LTB resistance.

### Table 6.4 Variation of $P_{cr}$ applied at the SC for S1, S2 and S3

| POSITION OF LOAD TOP | $P_{cr}$ | DIFFERENCE |
|---|---|---|
| S1 | 50.89 | 1.839 |
|  |  | 2.414 |
| S2 | 27.67 | 0.543 |
|  |  | 1.312 |
| S3 | 21.08 | 0.414 |
|  |  | 0.761 |

**Figure 6.17 Load- lateral displacement curves with a=S1, b=S2 and c=S3 to effective properties at top**

**Table 6.5 Variation of $P_{cr}$ applied at the SC for S1, S2 and S3**

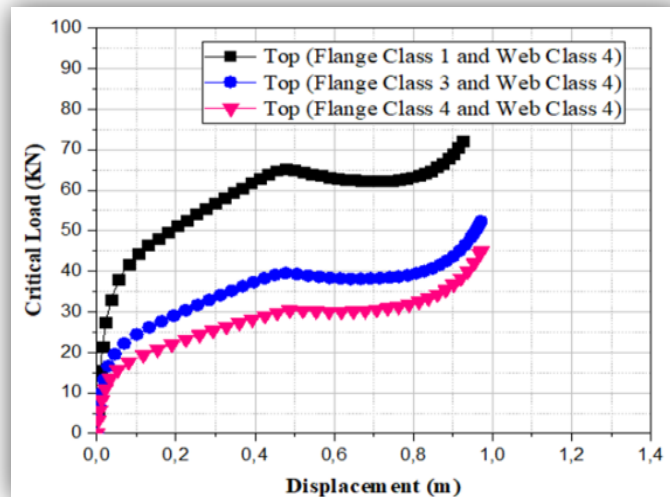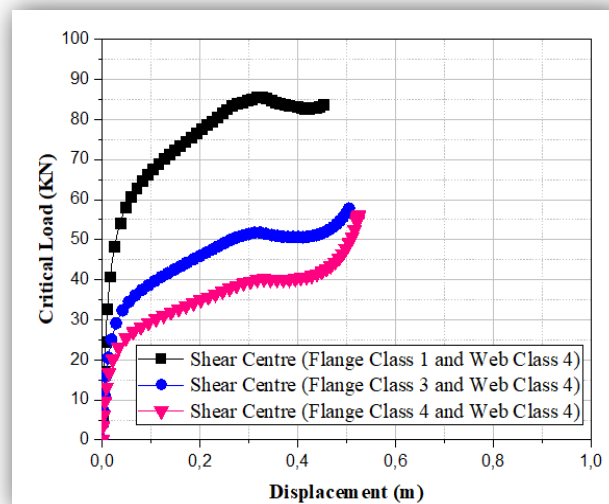| POSITION OF LOAD SHEAR CENTRE | $P_{cr}$ | DIFFERENCE |
|---|---|---|
| S1 | 71.81 | 1.767 |
| | | 2.335 |
| S2 | 40.62 | 0.565 |
| | | 1.320 |
| S3 | 30.75 | 0.428 |
| | | 0.757 |



**Figure 6.18 Load- lateral displacement curves with a=S1, b=S2 and c=S3 to effective properties at SC**

### Table 6.6 Variation of P$_{cr}$ applied at the bottom for S1, S2 and S3

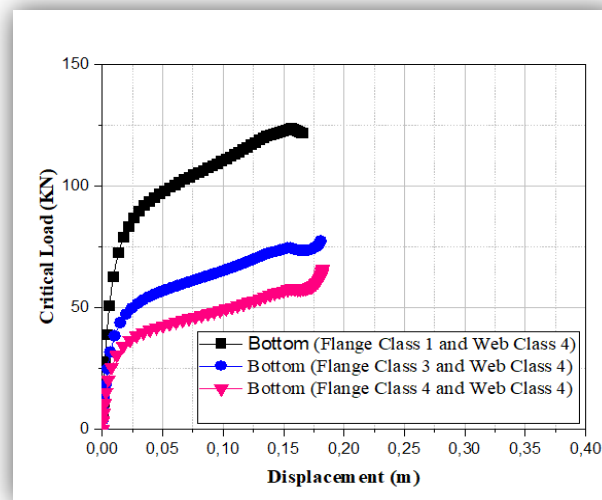| POSITION OF LOAD BOTTOM | P$_{cr}$ | DIFFERENCE |
|---|---|---|
| S1 | 107.56 | 1.740 |
|    |        | 2.331 |
| S2 | 61.81  | 0.574 |
|    |        | 1.339 |
| S3 | 46.13  | 0.428 |
|    |        | 0.746 |



**Figure 6.19 Load- lateral displacement curves with a=S1, b=S2 and c=S3 to effective properties at the bottom**

## 6.7.3 Comparison between results considering elastic and effective characteristics

Considering both properties, it can be seen from Tables 6.7 Figure 6.20 that values of P$_{cr}$ decrease with effective properties exclusively for S3, but not for S1 and S2 for the case of upper flange loaded. For Table 6.8 and Figure 6.21, all sections show a slight difference is noticed in P$_{cr}$ values when section are loaded at SG. Table 6.9 and Figure 6.23 show a notable decrease in P$_{cr}$ in S3 rather than the other sections.

### Table 6.7 Differences in P$_{cr}$ prediction (elastic and effective) of S1, S2 and S3 at the top

| POSITION OF LOAD TOP | ELASIC P$_{cr}$ | EFFECTIVE P$_{cr}$ | DIFFERENCE |
|---|---|---|---|
| S1 | 50.89 | 50.89 | 50.89=50.89 |
| S2 | 27.67 | 27.67 | 27.67=27.67 |
| S3 | 23.19 | 21.08 | 23.19>21.08 |
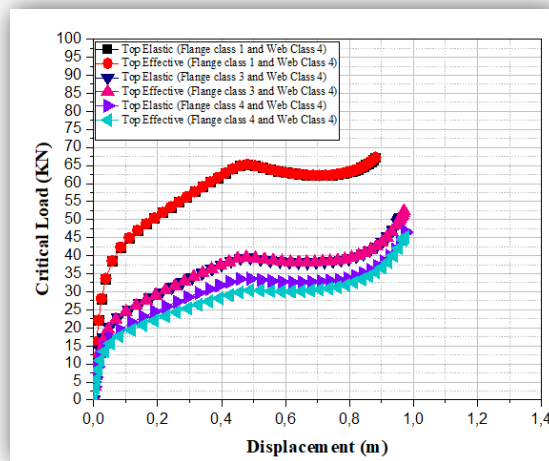
**Figure 6.20 Comparison of $P_{cr}$ (elastic and effective) for S1, S2 and S3 at the top**

**Table 6.8 Differences in $P_{cr}$ prediction (elastic and effective) of S1, S2 and S3 at the SC**

| POSITION OF LOAD SHEAR CENTRE | ELASIC $P_{cr}$ | EFFECTIVE $P_{cr}$ | DIFFERENCE |
|---|---|---|---|
| S1 | 70.80 | 71.81 | 70.80≤71.81 |
| S2 | 40.00 | 40.00 | 40.00≤40.62 |
| S3 | 33.69 | 30.75 | 33.69>30.75 |



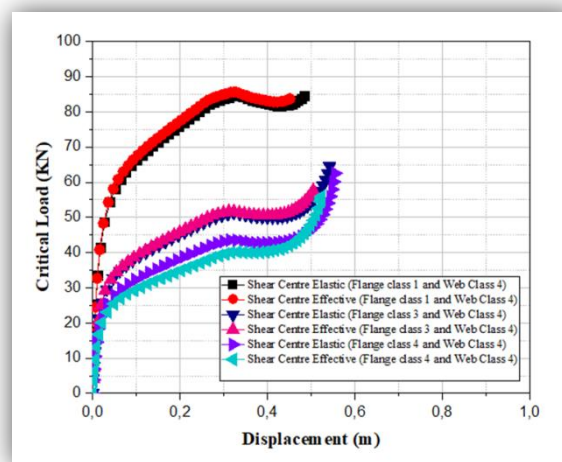**Figure 6.21 Differences in $P_{cr}$ prediction (elastic and effective) of S1, S2 and S3 at the SG**

**Table 6.9 Differences in $P_{cr}$ prediction (elastic and effective) of S1, S2 and S3 at the bottom**

| POSITION OF LOAD BOTTOM | ELASIC $P_{cr}$ | EFFECTIVE $P_{cr}$ | DIFFERENCE |
|---|---|---|---|
| S1 | 107.55 | 107.56 | 107.55=107.55 |
| S2 | 61.81 | 61.81 | 61.81=61.81 |
| S3 | 51.76 | 46.13 | 51.76>46.13 |
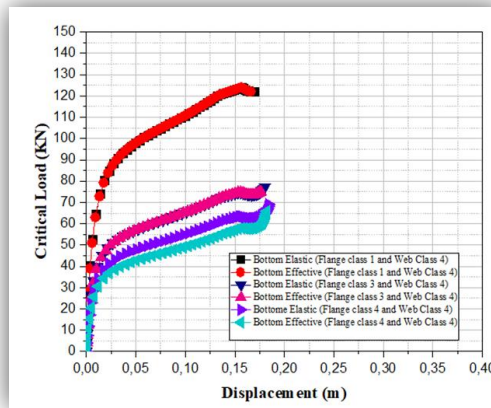
**Figure 6.22 Differences in $P_{cr}$ prediction (elastic and effective) of S1, S2 and S3 at the bottom**

## 6.8 Interpretation of deformed shaped beam

In the following, sample of results representing the last increment of section 3 are displayed. Figures depicted 6.23 To 6.25 shows the unreformed shape, for S3 exclusively with flange and web of class 4, at the ultimate loading increment. As can be seen, for three load positions, the occurrence of the local buckling instability phenomenon which exhibit local deformation of outstand flanges of I beam: upper, shear centre and lower flanges respectively. The general shape of the deformation looks like a continues thin plate in flexion which indicates that flanges undergoe local buckling. For flanges of class 1 and 2, the local buckling was not observed or, at least, not clearly for section S2.
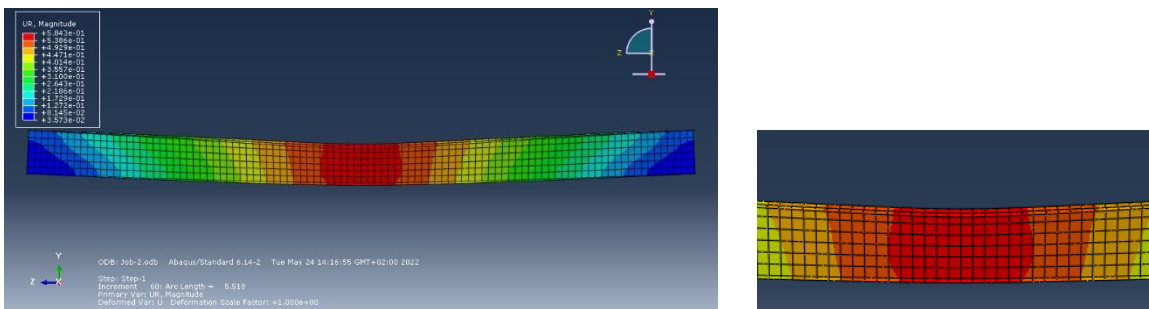


**Figure 6.23 Local buckling at the upper flange at ultimate increment with load applied at the upper flange of S3**
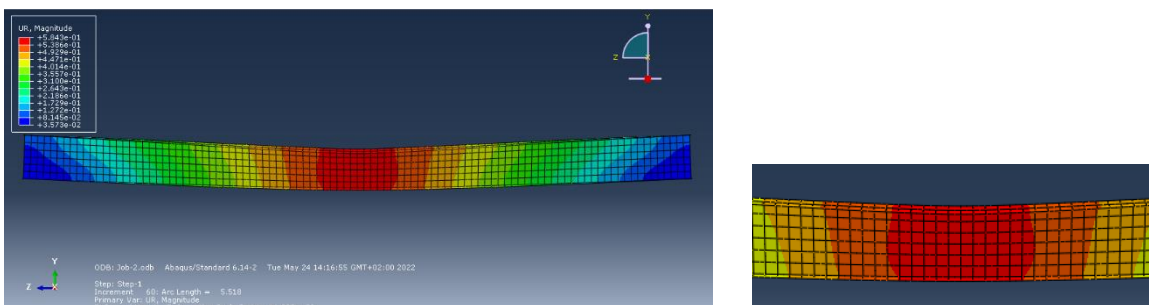


**Figure 6.24 Local buckling at the upper flange at ultimate increment with load applied at the SG flange of S3**
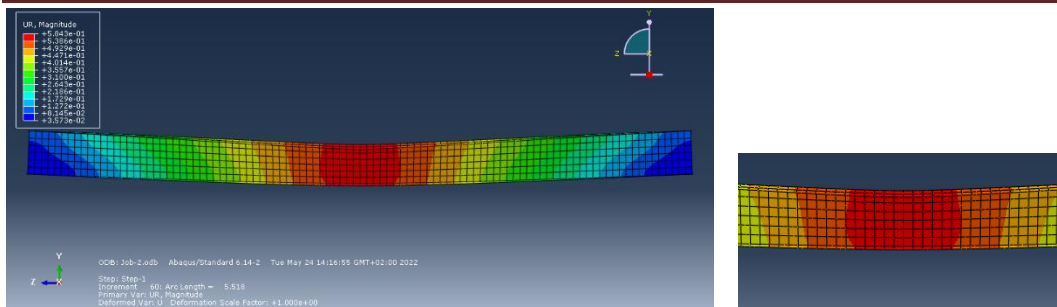
**Figure 6.25 Local buckling at the upper flange at ultimate increment with load applied at the lower flange of S3**

An interaction between the LB and LTB was observed in S3, with less significance in S2 but no interaction in S1. This prove, once more, that providing a flange of class 1 will transform in bending to some extent, the whole behaviour of class 2 even if it is declared to be class 4 as stated in EC3 as it envisages some exceptions to the general procedure for the classification. For cross sections with a class 4 web and class 1 or 2 flanges may be classified as class 2 cross sections with an effective web in accordance (clause 5.5.2(11)). For cross sections with a class 4 web and class 1 or 2 flanges may be classified as class 2 cross sections with an effective web in accordance (clause 5.5.2(11)).

# CONCLUSIONS AND SUGGESTIONS FOR FUTURE WORKS

## 1.    Conclusions

This present Master's dissertation aims to evaluate the impact of instability in elastic and inelastic behaviours on the carrying capacity of slender sections (of class 4). Despite the fact that their flanges class belong to class 1, 3 and 4 all studied sections are classified into class 4 because of web class 4. Some general conclusions can be made. As far as the elastic buckling analysis is concerned, applying the first order buckling analysis, it has been demonstrated throughout of the outcomes of this study the importance of each parameter., namely:

- Whatever the mean used for determining the $M_{cr}$, similar values have been extracted.

- The analytical equation given in EC3 does give accurate prediction of $M_{cr}$. Thus, EC3 can be used safely in the design process.

- Finite element numerical analysis gives very close values of $M_{cr}$ to those given by EC3 without considering the concept of classification recommended by EC3 with regard of different flange slenderness and location of load as explained in chapter 5.

- For S1 and S2, no notable differences have been remarked between the elastic and effective properties with bi-symmetric sections and hence, no significant effect of flange in the overall resistance to LTB of sections. However, for S3 where the flange class is 4, the cross-section is mono-symmetric some differences have been be noticed.

- The position of the applied load has an important effect on the $M_{cr}$ value, with as expected, the unfavourable case when the load is applied in the compressive flange.

- An important result is that the eigen buckling analysis performed by LTBEAM and ABAQUS software give roughly the same values specially in the first buckling mode. This gives a more confidence to the ABAQUS model, as it will be used later on for more sophisticate analysis: inelastic buckling analysis taking into account the imperfection.

As far as the inelastic buckling analysis, some interesting results have been found and discussed in chapter 6 3D models were implanted in ABAQUS software. The modified RIKS method uses a tangent line of a function to intersect with an arc, situated at the end of every step, the curve will converge over the arc-length until it reaches an intersection of the arc with the function. Figures in chapter 6 show the Loads.

Lateral deflections curves extracted from the modified RIKS results during the whole loading history by considering three load positions with an elastic branch for elastic behaviour and then the beams behave nonlinearly due to the initial geometric imperfections and the nonlinear geometric and material.

Summary of inelastic buckling results is given as follows:

- A validation of 3D linear model of ABAQUS with the LTBEAM was done. After, a parametric study using a second-order analysis carried out to investigate the same parameters.  Some interesting findings can be enumerated:

- Bearing in mind that torsional buckling is essentially flexural behaviour, the section of flanges is very important to equilibrated the bending moment.

- Despite the fact that all considered sections are classified as class 4 to EC3, in the contrary to the linear buckling analysis discussed in the previous chapter, major differences in their behaviours can be seen as depicted in relative Figures.

- All considered sections show almost the same behaviour in the elastic range, with of course different value of $P_{cr}$ with larger values for S1 to S3 which can be attributed to the flange class.

- Independently of the used geometric properties, S1 shows quiet-different behaviour compared to S2 and S3 with flanges belonging to class 3 and 4 respectively.

- Better performance of S1 can be noticed followed by S2 and at last S3 showed poorer behaviour with regard to LTB resistance.

- The class of flange plays an important and determinant role with high values of $P_{cr}$ despite the location of the applied load for S1 compared to other sections, i.e. S2 and S3.

- An interaction between the LB and LTB was observed in S3, with less significance in S2 but no interaction in S1. This prove, once more, that the global behaviour of cross section in flexure is governed by flange class section.

- It seems that providing a class 1 flange, the bending performance capacity is not greatly affected by web class 4.

- For all sections, the effective properties calculated seem to not have large influence for a beam mainly bent, even if some differences are being noticed for S3   with flange and web belonging to class 4.

- Some kind of interaction between the LB and LTB has been detected in upper flange of S3.

## 2.      Recommendations suggestions for future work:

It seems to be interesting to carry out a particular study in order:

- To assess the effect of steel grade: S235 ductile material on slender sections.

- To evaluate the effect other loading:  dynamic, cyclic and even seismic on slender section.

-  To explore the contribution of the web in high flexure loaded slender sections.

# BIBLIOGRAPHY

A.Labed,2019 — Cours de Chaprente Métalliques, Instability élastiques. Master Structures 2019. Université de Tébessa.

Erath.S, 2020 — Structural stability theory and practice: buckling of columns, beams, plates, and shells. (J. W. Sons, Éd.).

Silva et al, 2010 — E Silva, Deidre A, Brekenfeld, Caspar , Ebinger, Martin, hristensen, S{\o}ren, Barber, P Alan, Butcher, Kenneth S, et al. (2010). he benefits of intravenous thrombolysis relate to the site of baseline arterial occlusion in the Echoplanar Imaging Thrombolytic Evaluation Trial (EPITHET). (A. H. Assoc, Éd.) Stroke, 41(02), 295--299.

EN 1993-1-1:2005 — Design of steel structures – part 1-1: General rules and rules for buildings.

De Gardner et al, 2010 — Gardner, Leroy, & Nethercot, David A. (2011). Designers' Guide to (I. publishing, Éd.).

De Beg, Darko et al ,2012 — Beg, Darko, Kuhlmann, Ulrike, Davaine, Laurence, & Braun, Benjamin. (2012). Design of plated structures: Eurocode 3: Design of steel structures, part 1-5: Design of plated structures. (J. W. Sons, Éd.).

Abutair.Baker Wael,2017 — Parametric Investigation Of The Elastic And Inelastic Resistance Of I Slender Welded Steel Beam To Lateral Torsional Buckling. Master dissertation Department of Civil Engineering University of Tebessa, 2017.

A. Galea — CTICM, [online]. Available: http://www.cticm.com/content/Ltbeam-version-1011.

Khennane. A, 2013 — Introduction to finite element analysis using MATLAB{\textregistered} and abaqus. (C. Press, Éd.).

ABAQUS — Standard analysis user's manual 5ersion 6.14-, 2018.

Marwa Boudjadja ,2019 — 3D Numerical Investigation Of The Linear And Non-Linear Performance Of Steel Structures Having Web Openings Under Different Loading Conditions. Master dissertation Department of Civil Engineering University of Tebessa, 2019.

Taras A and Greiner R ,2010 — New design curves for lateral-torsional buckling – proposal based on a

consistent derivation. Journal of Constructional Steel Research 66(5): 648–663.

| | |
|---|---|
| Couto C, Ferreira J, Vila Real P. et al, 2015 | Numerical investigation on lateral torsional buckling of steel beams with class 4 cross-section – comparison with existing design formulae. In: Eighth international conference on advances in steel structures Lisbon, Lisbon, 22–24 July. |
| J. Ferreira P. Vila Real C. Couto,2017 | Comparison of the General Method with the Overall Method for the out-of-plane stability of members with lateral restraints. Engineering Structures Volume 151, 15 November 2017, Pages 153-172. |
| C. Lee and S.P Chiew, 2019 | A Review of Class 4 Slender Section Properties Calculation For Thin-Walled Steel Sections According To Ec3. Advanced Steel Construction – Vol. 15 No. 3 (2019) 259–266 |
| C. Couto and P.Vila Real ,2019 | A proposal based on the effective section factor for the lateral-torsional buckling of beams with slender I-shaped welded sections. Thin-Walled Structures Volume 145, December 106389. |
| N. Seres and K.Fejes,2020 | Lateral-torsional buckling of girders with class 4 web: Investigation of coupled instability in EC3-based design approach. Advances in Structural Engineering 1–16 The Author(s) 2020 Article reuse guidelines |
| EN1993-1-6 (2006) Eurocode 3 | Design of steel structures – part 1-6: Strength and stability of shell structures. |
| EN1993-1-5 (2006) Eurocode 3 | Design of steel structures –part 1-5: Plated structural elements. |